The Stochastic Geometry of non-Gaussian Fields

Beuman, T.H.

THE STOCHASTIC GEOMETRY OF NON-GAUSSIAN FIELDS

PROEFSCHRIFT

ter verkrijging van
de graad van Doctor aan de Universiteit Leiden,
op gezag van Rector Magnificus prof.mr. C.J.J.M. Stolker,
volgens besluit van het College voor Promoties
te verdedigen op dinsdag 8 december 2015
klokke 12:30 uur

door

THOMAS HUBERTUS BEUMAN

geboren te Baarn
in 1985

Promotor:	Prof.dr. V. Vitelli
Co-promotor:	Dr. J. Paulose
Promotiecommissie:	Prof.dr. M.R. Dennis (University of Bristol, UK)
	Prof.dr. C.W.J. Beenakker
	Prof.dr. E.R. Eliel
	Dr. L. Giomi
	Prof.dr. K.E. Schalm

Casimir PhD series, Delft-Leiden 2015-33
ISBN 978-90-8593-239-0
An electronic version of this thesis can be found at
https://openaccess.leidenuniv.nl

The cover shows lines of principal curvature, which indicate the direction along which the curvature of a given surface is maximal (or minimal). At some points the curvature is the same in all directions, so that this direction is not defined. These topological defects are called umbilical points (see chapters 1 and 3). The image on the back represents a Gaussian field.
The design is an adaptation from an image originally published in PNAS 109: 19943-19948 (2012).

CONTENTS

GAUSSIAN FIELDS AND GEOMETRY

Before discussing non-Gaussian fields, we first cover the relevance, definition and characteristics of Gaussian fields. This first part also treats the critical points and umbilical points that will feature in the later chapters. The definitions and notations introduced here will be important for the non-Gaussian fields to follow.

1

INTRODUCTION

Many processes, not only in physics but also elsewhere, are stochastic in nature. Some of these, such as radioactive decay, are intrinsically random. Others can be treated stochastically by virtue of their complexity, such as an ideal gas: It is practically impossible to know, let alone keep track of, the locations and velocities of all the particles, due to the vast number of them in any meaningful amount of gas. The hugeness of this number is however at the same time a blessing, since we can translate our ignorance into a probability distribution and calculate expectation values. The law of large numbers ensures that the typical amount by which a measured value, obtained from a real system, deviates from such a theoretical value scales with the inverse of the square root of the number of independent elements involved. The fact that this number is typically gargantuan ensures the reliability of statistical physics.

When dealing with large numbers, probability theory provides another helping hand: the central limit theorem. For almost any probability distribution, the average (or sum) of a large number of independent identically distributed variables is Gaussian distributed, in the limit that the number goes to infinity. This makes the Gaussian distribution the archetype of all distributions and a natural first-order approximation for a lot of random processes, especially those that represent the sum of a lot of parts.

Consider for instance the amount of rain that will fall on a certain day on a certain spot somewhere in The Netherlands. On some days there is no rain at all, on others it rains a lot. The relatively large probability of no rain at all compared to just a tiny bit, as well as the impossibility of a negative amount, means that the corresponding distribution is far from a Gaussian one. If we were however to consider a whole year rather than just one day, adding together the contributions of lots of different rain clouds, we would find a distribution with a bell-shaped curve.

This principle can be extended to multiple dimensions as well. Suppose we are not considering one (zero-dimensional) variable ψ, but a two-dimensional stochastic field $\psi(x, y)$. If this field is the result of a summation of a lot of random fields, we may be assured that it acquires Gaussian characteristics. What this means is that, if we consider any fixed point (x_0, y_0), the corresponding value $\psi(x_0, y_0)$ serves as a Gaussian variable.

As a simple example, let us return to the rain and consider the amount of downfall in a year in lots of spots all over the country. In the continuum limit, when the spots correspond to infinitesimal areas, we have a random field, obtained by adding together the contributions of all the individual rain clouds.

One added complication when considering a field instead of a single variable is that there are also spatial correlations to consider. Whereas a single Gaussian variable is completely specified by its expected value μ and standard deviation σ, a Gaussian field additionally requires this correlation function. As will be demonstrated later in this chapter, this correlation function is closely related to the *spectrum* of the Gaussian field.

It should come as no surprise that Gaussian random fields can be found in a wide variety of areas in physics. They are for instance often used to model laser speckle patterns [8, 20], which may arise from a laser beam scattered from a rough surface. They also make a good approximation for the projected gravitational potential of the universe, since this is the product of accumulating all mass along each line of sight [29], thereby stepping into the domain of the central limit theorem. As another well-known example, the temperature of the cosmic microwave background radiation, or CMB, is not the same in all directions, but shows tiny deviations from the mean value of 2.725 K [13, 37]. It is known to be very close to Gaussian [41], but there is specific interest in detecting non-Gaussianities [22, 24] since this may offer a window on the specifics of inflation, the period from which the radiation originates. Other examples include medical images of brain activity [47] and surface roughness [32].

Likewise, geometry and topology are of increasing interest in physics. As a mathematical enterprise, topology is the study of spacial structures, in particular properties that do not change under continuous deformations such as bending and stretching. Topological defects are locations where a certain function defined on some manifold (a structure in space) is not well-defined. Consider for instance the cardinal directions: If you draw a little arrow representing north everywhere on the globe, you will see that they are parallel everywhere except at the poles. On those places north is not

properly defined. Topology tells us that is in fact impossible to draw any set of arrows such that they align everywhere on a sphere; you will always get one or more defects. Not only that, defects can be classified by their *topological index* and for this example the total index of all defects will always be +2. For the cardinal directions the two poles both have index +1.

The robustness of defects and the relative ease with which they can typically be found makes them an attractive target of study in physics [21, 30, 38]. When energy is involved for instance, defects are typically places of high buildups of energy [36]. In optics, there is interest in L lines where the polarization is linear. Similarly, there are C points (or C lines, depending on the number of dimensions of the field in question) where the polarization is circular [3, 42, 43]. These and other topological entities, such as phase singularities, have been the subject of several studies involving the aforementioned speckle fields [2, 11, 15, 18, 46]. The CMB is another common (near-)Gaussian target [12, 28, 44]. Other examples showing the use of geometry and topology in fields can be found in weak gravitational lensing [45], nematics [14, 27], random energy surfaces [6] and superfluids near criticality [23, 33].

For a given field we can readily study its geometric features, such as the locations of its local maxima and minima. A random field does not have a geometry as such, since it is not fixed, but we can consider its *stochastic geometry*. That is to say, we can make statements about the expected number of maxima and minima per unit area, for instance. The relations between such quantities and the spectrum of a Gaussian field, as well as other stochastic properties, have already been the subject of several studies [4, 10, 11, 16, 17, 19, 34, 35, 46]. The properties that are relevant to this thesis will be reviewed at the end of this chapter.

We shall begin by formally defining Gaussian fields and explore some of their properties. This is followed by an introduction to the geometric entities that are featured in this thesis. The concept of maxima and minima will most likely be very familiar, but a rigorous exploration of their defining characteristics will help to more easily grasp the mathematics to follow in the subsequent chapters. It may also help when the probably less familiar umbilical points are covered.

1.1 GAUSSIAN FIELDS

The Gaussian distribution is the archetype of a continuous probability density. It is given by

$$p(x) = \frac{1}{\sqrt{2\pi}\sigma} \exp\left(-\tfrac{1}{2}\left(\frac{x-\mu}{\sigma}\right)^2\right), \tag{1.1}$$

where μ and σ are the expectation value and standard deviation of the stochastic variable respectively. One of its special properties is that the sum of two independent stochastic variables, that adhere to this distribution, is itself also a Gaussian variable, albeit of course with $\mu = \mu_1 + \mu_2$ and $\sigma^2 = \sigma_1^2 + \sigma_2^2$. This property can be considered to be one of the components of the proof of the central limit theorem, which states that (under some very general conditions) the sum (or average) of a large number of independent stochastic variables acquires a Gaussian distribution, in the limit that the number goes to infinity [31]. Because of this, many random processes can be well approximated using a Gaussian distribution, e.g. the number of times a (fair) coin comes up heads when it is flipped a (large) number of times, or the amount of rain that falls at a certain spot during a year.

A Gaussian random field is an extension of this principle to two dimensions. Formally, it is a stochastic function $H(\boldsymbol{r})$. The minimum requirement for a Gaussian field is that the probability distribution of $H(\boldsymbol{r_0})$ at any point $\boldsymbol{r_0}$ has to be described by a Gaussian. More generally, if we consider the values that the field attains at any number of points, $\xi_1 = H(\boldsymbol{r_1})$, $\xi_2 = H(\boldsymbol{r_2})$, $\ldots$, $\xi_n = H(\boldsymbol{r_n})$, the joint probability distribution has to be of the form

$$p(\xi_1, \ldots, \xi_n) \propto \exp\left(-\tfrac{1}{2}\sum_{i,j} A_{ij}\xi_i\xi_j\right), \tag{1.2}$$

where A_{ij} are constants. These constants give information about the relative values at different points (which would be useful for example if we wanted to know the distribution of the derivative of the field).

Any well-behaved Gaussian field can be decomposed into Fourier modes, resulting in the sum of an infinite number of wave functions

$$H(\boldsymbol{r}) = H_0 + \sum_{\boldsymbol{k}} A(\boldsymbol{k}) \cos(\boldsymbol{k}\cdot\boldsymbol{r} + \phi_{\boldsymbol{k}}). \tag{1.3}$$

This shows how much of the fluctuations occur at each wavelength; for example, a surface of water might fluctuate with some random waves. If

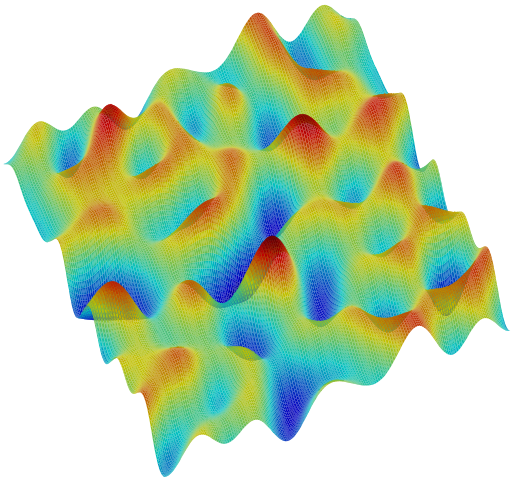

Figure 1.1: A realization of a Gaussian field with periodic boundary conditions.

that is due to some external sound at a certain frequency, the Fourier transform will be strongest at the corresponding wavelength.

This procedure may also be turned around: A Gaussian field may be generated by adding together a large number of Fourier modes. We will now discuss a field that is generated in this way and try to understand how the statistics of the phase factors $\phi_{\boldsymbol{k}}$ reflect properties of the field, such as Gaussianity and translational invariance.

The defining characteristic of a Gaussian field is that the phases $\phi_{\boldsymbol{k}}$ are random and completely uncorrelated to each other. Already, by translational invariance, second-order correlations between ϕ_k and $\phi_{k'}$ are ruled out. If the phases are *completely* independent, then at each individual point $\boldsymbol{r}$, $H(\boldsymbol{r})$ is the sum of an infinite number of independent random numbers between -1 and 1 (as a result of the cosine in eq. (1.3)), each weighted by a factor $A(\boldsymbol{k})$. Thus, by the central limit theorem, $H(\boldsymbol{r})$ is a Gaussian random variable. In contrast, in a non-Gaussian field the phases *are* correlated, i.e. the phases of different modes depend on each other. This mechanism is often called *mode coupling*.

So far no statements have been made about the function $A(\boldsymbol{k})$: It has no influence on the Gaussianity (nor on the homogeneity) of H. Indeed, this function is a free parameter, called the *amplitude spectrum*. While all Gaussian fields share some general properties, other more specific properties (such as the density of critical points, as we shall see) depend on this amplitude spectrum. For example, when $A(\boldsymbol{k})$ is large for vectors $\boldsymbol{k}$ with

a small norm, the field H is dominated by these waves with small wave vectors and hence large wave lengths, resulting in a more slowly varying H as compared to a Gaussian field that is dominated by large wave vectors.

There is one more condition that we will pose: Next to being homogeneous, we will also only consider fields that are *isotropic*, i.e. have rotational symmetry. This is achieved by requiring that $A(\boldsymbol{k})$ depends on the magnitude of $\boldsymbol{k}$ only, i.e. $A(\boldsymbol{k}) = A(k)$.

In order to make a clear distinction between Gaussian and non-Gaussian, throughout this thesis H will be used to indicate an (isotropic) Gaussian field and ψ any (homogeneous and isotropic) field. Later we will also use h, to indicate a perturbed Gaussian field.

1.1.1 *Spectra and moments*

Let us start by calculating the mean and standard deviation of a Gaussian field H, the equivalents of μ and σ of a Gaussian variable. This involves expectation values, which are obtained by integrating over all possible values of all random variables, which in this case, are the uniformly distributed phases:

$$\langle \dots \rangle \equiv \left(\prod_{\boldsymbol{k}} \int \frac{\mathrm{d}\phi_{\boldsymbol{k}}}{2\pi} \right) \dots \tag{1.4}$$

The mean is then simply

$$\begin{aligned} \langle H(\boldsymbol{r}) \rangle &= \left\langle H_0 + \sum_{\boldsymbol{k}} A(k) \cos(\boldsymbol{k} \cdot \boldsymbol{r} + \phi_{\boldsymbol{k}}) \right\rangle \\ &= H_0 + \sum_{\boldsymbol{k}} A(k) \left\langle \cos(\boldsymbol{k} \cdot \boldsymbol{r} + \phi_{\boldsymbol{k}}) \right\rangle \\ &= H_0 + \sum_{\boldsymbol{k}} A(k) \int \frac{\mathrm{d}\phi_{\boldsymbol{k}}}{2\pi} \cos(\boldsymbol{k} \cdot \boldsymbol{r} + \phi_{\boldsymbol{k}}) \\ &= H_0. \end{aligned} \tag{1.5}$$

For the variance (standard deviation squared) we find

$$\begin{aligned} &\langle (H - \langle H \rangle)^2 \rangle \\ &\quad = \left\langle \left(\sum_{\boldsymbol{k}} A(k) \cos(\boldsymbol{k} \cdot \boldsymbol{r} + \phi_{\boldsymbol{k}}) \right)^2 \right\rangle \\ &\quad = \sum_{\boldsymbol{k}\boldsymbol{k}'} A(k) A(k') \left\langle \cos(\boldsymbol{k} \cdot \boldsymbol{r} + \phi_{\boldsymbol{k}}) \cos(\boldsymbol{k}' \cdot \boldsymbol{r} + \phi_{\boldsymbol{k}'}) \right\rangle. \end{aligned} \tag{1.6}$$

Since the phases are uncorrelated, for $\boldsymbol{k} \neq \boldsymbol{k'}$ we find

$$\begin{aligned}&\Big\langle \cos(\boldsymbol{k}\cdot\boldsymbol{r}+\phi_{\boldsymbol{k}})\cos(\boldsymbol{k'}\cdot\boldsymbol{r}+\phi_{\boldsymbol{k'}})\Big\rangle \\ &\qquad = \Big\langle \cos(\boldsymbol{k}\cdot\boldsymbol{r}+\phi_{\boldsymbol{k}})\Big\rangle\Big\langle \cos(\boldsymbol{k'}\cdot\boldsymbol{r}+\phi_{\boldsymbol{k'}})\Big\rangle = 0. \end{aligned} \tag{1.7}$$

Hence the term in the double sum can only be nonzero for $\boldsymbol{k} = \boldsymbol{k'}$. As a result we get

$$\langle (H - \langle H\rangle)^2\rangle = \sum_{\boldsymbol{k}} A(k)^2 \Big\langle \cos^2(\boldsymbol{k}\cdot\boldsymbol{r}+\phi_{\boldsymbol{k}})\Big\rangle = \sum_{\boldsymbol{k}} \tfrac{1}{2}A(k)^2. \tag{1.8}$$

When we have a Gaussian variable x with a certain μ and σ, we can make a transformation to $\tilde{x} = \frac{x-\mu}{\sigma}$, which is then a *standard* Gaussian variable, having $\tilde{\mu} = 0$ and $\tilde{\sigma} = 1$. This translation and rescaling has no effect on the overall properties of x and is typically introduced for convenience. We will apply a similar transformation, by setting $\langle H\rangle = 0$ and $\langle H^2\rangle = 1$. This translates to the conditions $H_0 = 0$ and $\sum_{\boldsymbol{k}} \frac{1}{2}A(k)^2 = 1$. This normalization is for the purpose of simplicity only and has no impact on any analysis to follow. Our working definition of a Gaussian field thus becomes

$$H(\boldsymbol{r}) = \sum_{\boldsymbol{k}} A(k)\cos(\boldsymbol{k}\cdot\boldsymbol{r}+\phi_{\boldsymbol{k}}). \tag{1.9}$$

While the vectors $\boldsymbol{k}$ in eq. (1.9) form a discrete set, usually they are sufficiently finely spaced so that we can treat the amplitude spectrum $A(k)$ as a continuous function defined over the positive reals. If we take our normalization condition, and replace the sum with an integral, we get

$$\begin{aligned}1 &= \sum_{\boldsymbol{k}} \tfrac{1}{2}A(k)^2 = \int \mathrm{d}\boldsymbol{k}\, \tfrac{1}{2}a(k)^2 = \int_0^{2\pi}\int_0^{\infty} k\,\mathrm{d}k\mathrm{d}\theta\, \tfrac{1}{2}a(k)^2 \\ &= \int_0^{\infty} \mathrm{d}k\,\pi k a(k)^2 = \int_0^{\infty} \mathrm{d}k\,\Pi(k). \end{aligned} \tag{1.10}$$

Here $a(k)$ indicates the continuous spectrum equivalent to the discrete amplitudes $A(k)$. The newly introduced function $\Pi(k) \equiv \pi k a(k)^2$ is the *power spectrum* of H.

Some properties of a Gaussian field depend on the amplitude spectrum. In many cases this dependence can be expressed in terms of the *moments* of the spectrum

$$K_n \equiv \sum_{\boldsymbol{k}} \tfrac{1}{2}A(k)^2 k^n = \int_0^{\infty} \mathrm{d}k\,\Pi(k)k^n. \tag{1.11}$$

The normalization condition can be translated as $K_0 = 1$.

1.1.2 *Two-point correlation function*

Correlation functions are often used to probe the Gaussianity of a given random field. This is because for Gaussian fields, they obey certain relations, as reviewed below. We will first calculate the two-point correlation function.

The two-point correlation function $C(\boldsymbol{r_1}, \boldsymbol{r_2})$ of a field ψ is defined as

$$C(\boldsymbol{r_1}, \boldsymbol{r_2}) = \langle \psi(\boldsymbol{r_1}) \psi(\boldsymbol{r_2}) \rangle. \tag{1.12}$$

When ψ is homogeneous and isotropic, C depends only on the distance between $\boldsymbol{r_1}$ and $\boldsymbol{r_2}$

$$C(R) = \langle \psi(\boldsymbol{r}) \psi(\boldsymbol{r} + \boldsymbol{R}) \rangle, \tag{1.13}$$

where $\boldsymbol{r}$ is any point and $\boldsymbol{R}$ is any vector of length R. For a Gaussian field H we find (if we set $\boldsymbol{r} = 0$ for convenience, which we are free to do)

$$\begin{aligned} C(R) &= \langle H(0) H(\boldsymbol{R}) \rangle \\ &= \left\langle \left(\sum_{\boldsymbol{k}} A(k) \cos(\phi_{\boldsymbol{k}}) \right) \left(\sum_{\boldsymbol{k}} A(k) \cos(\boldsymbol{k} \cdot \boldsymbol{R} + \phi_{\boldsymbol{k}}) \right) \right\rangle \\ &= \sum_{\boldsymbol{k}\boldsymbol{k'}} A(k) A(k') \Big\langle \cos(\phi_{\boldsymbol{k}}) \cos(\boldsymbol{k'} \cdot \boldsymbol{R} + \phi_{\boldsymbol{k'}}) \Big\rangle. \end{aligned} \tag{1.14}$$

Since the phases $\phi_{\boldsymbol{k}}$ are uncorrelated, the correlation is automatically zero when $\boldsymbol{k} \neq \boldsymbol{k'}$, hence

$$\begin{aligned} C(R) &= \sum_{\boldsymbol{k}} A(k)^2 \Big\langle \cos(\phi_{\boldsymbol{k}}) \cos(\boldsymbol{k} \cdot \boldsymbol{R} + \phi_{\boldsymbol{k}}) \Big\rangle \\ &= \sum_{\boldsymbol{k}} A(k)^2 \Big\langle \tfrac{1}{2} \cos(\boldsymbol{k} \cdot \boldsymbol{R} + 2\phi_{\boldsymbol{k}}) + \tfrac{1}{2} \cos(\boldsymbol{k} \cdot \boldsymbol{R}) \Big\rangle. \end{aligned} \tag{1.15}$$

Since $\phi_{\boldsymbol{k}}$ is uniformly distributed, the expectation value of the first cosine is zero, and we are left with

$$C(R) = \sum_{\boldsymbol{k}} \tfrac{1}{2} A(k)^2 \cos(\boldsymbol{k} \cdot \boldsymbol{R}) = \int \mathrm{d}\boldsymbol{k}\, \tfrac{1}{2} a(k)^2 \cos(\boldsymbol{k} \cdot \boldsymbol{R}). \tag{1.16}$$

We thus find that the two-point correlation function of a Gaussian field is the Fourier transform of its (two-dimensional) power spectrum. Therefore, in essence, the correlation function is as much a complete description of a Gaussian field as the power spectrum is. Also, by determining the correlation function and taking the inverse Fourier transform, one obtains the spectrum.

The moments, defined before in terms of the power spectrum, can be related to the derivatives of the correlation function at $R = 0$. Because of symmetry, we must have $C(R) = C(-R)$, hence $C(R)$ is an even function and all its odd derivatives at zero vanish. To obtain the even derivatives, we must first eliminate the vector $\boldsymbol{R}$ in the equation above. We are free to choose its direction, so let us take $\boldsymbol{R} = R\hat{x}$. We then get

$$\begin{aligned} C^{(2n)}(R) &= \left(\frac{\mathrm{d}}{\mathrm{d}R}\right)^{2n} \int \mathrm{d}\boldsymbol{k}\, \tfrac{1}{2} a(k)^2 \cos(k_x R) \\ &= \int \mathrm{d}\boldsymbol{k}\, \tfrac{1}{2} a(k)^2 (-1)^n k_x^{2n} \cos(k_x R), \qquad (1.17) \\ C^{(2n)}(0) &= (-1)^n \int \mathrm{d}\boldsymbol{k}\, \tfrac{1}{2} a(k)^2 k_x^{2n} \\ &= (-1)^n \int_0^{2\pi} \int_0^{\infty} k\, \mathrm{d}k \mathrm{d}\theta\, \tfrac{1}{2} a(k)^2 k^{2n} \cos^{2n}\theta \\ &= (-1)^n K_{2n} \frac{1}{2\pi} \int_0^{2\pi} \mathrm{d}\theta\, \cos^{2n}\theta \\ &= (-1)^n \frac{(2n-1)!!}{2^n n!} K_{2n}. \qquad (1.18) \end{aligned}$$

We thus find a one-to-one relation between the moments and the derivatives of the correlation function. The derivative of the correlation function $C^{(2n)}(0)$ is related to roughness in the field itself. In fact, $C^{(2n)}(0)$ is equal to $(-1)^n \langle (H^{(n)}(x))^2 \rangle$, the fluctuations of the n-th derivative (apart from a sign).

1.1.3 *Higher-order correlation functions*

In general, the n-point correlation function is defined as the expectation value $\langle \psi(\boldsymbol{r_1}) \psi(\boldsymbol{r_2}) \dots \psi(\boldsymbol{r_n}) \rangle$, as a function of $\boldsymbol{r_1}$ through $\boldsymbol{r_n}$. For a Gaussian field, this correlation function can be expressed in terms of two-point correlation functions, analogous to Wick's theorem. As a result, a non-Gaussian field can be recognized by checking whether this relation holds. In practice, this test can be applied to a single Gaussian field if it is homogeneous. In that case, the correlation function depends only on separations of the points $\boldsymbol{r_2} - \boldsymbol{r_1}$ through $\boldsymbol{r_n} - \boldsymbol{r_1}$. From a given homogeneous field ψ, one obtains (a good approximation of) this correlation function by averaging over all (or a lot of) configurations with fixed spacings but translated to different $\boldsymbol{r_1}$'s.

The simplest case of the relationship is

$$\langle H_1H_2H_3H_4\rangle = \langle H_1H_2\rangle\langle H_3H_4\rangle + \langle H_1H_3\rangle\langle H_2H_4\rangle + \langle H_1H_4\rangle\langle H_2H_3\rangle, \tag{1.19}$$

where we introduced the notation $H_i \equiv H(\boldsymbol{r_i})$ for shortness. In general, correlations between an even number of variables with $n > 2$ can be reduced to the two-point correlations, while correlations between an odd number of variables always vanish. These properties follow from the definition of the Gaussian field: The n variables $H(r_i)$ are described by a correlated Gaussian distribution, and hence their correlation functions can be calculated explicitly from Gaussian integrals.

We shall now show how this characteristic relation comes about for our Fourier superposition. When we calculate the four-point correlation in the same way as we did for the two-point correlation, we bring the brackets inside the (quadruple) sum, which gives us the term

$$\Big\langle \cos(\boldsymbol{k_1}\cdot\boldsymbol{r_1}+\phi_{\boldsymbol{k_1}})\cos(\boldsymbol{k_2}\cdot\boldsymbol{r_2}+\phi_{\boldsymbol{k_2}}) \times \cos(\boldsymbol{k_3}\cdot\boldsymbol{r_3}+\phi_{\boldsymbol{k_3}})\cos(\boldsymbol{k_4}\cdot\boldsymbol{r_4}+\phi_{\boldsymbol{k_4}})\Big\rangle, \tag{1.20}$$

which is summed for all combinations of $\boldsymbol{k_1}$ through $\boldsymbol{k_4}$. The first thing to note is that, whenever e.g. $\boldsymbol{k_1}$ is not equal to any of the other $\boldsymbol{k_i}$, the correlation is automatically zero; this is because $\cos(\boldsymbol{k_1}\cdot\boldsymbol{r_1}+\phi_{\boldsymbol{k_1}})$ is then independent of all other factors, can therefore be separated, and gives zero. Hence the correlation can only be nonzero if each $\boldsymbol{k_i}$ is equal to (at least) one other $\boldsymbol{k_i}$. We can distinguish the cases $\boldsymbol{k_1} = \boldsymbol{k_2}, \boldsymbol{k_3} = \boldsymbol{k_4}$ and $\boldsymbol{k_1} = \boldsymbol{k_3}, \boldsymbol{k_2} = \boldsymbol{k_4}$ and $\boldsymbol{k_1} = \boldsymbol{k_4}, \boldsymbol{k_2} = \boldsymbol{k_3}$. Let us focus on the first case; the sum of all these correlations gives

$$\sum_{\boldsymbol{k_1},\boldsymbol{k_3}} A(k_1)^2A(k_3)^2\Big\langle \cos(\boldsymbol{k_1}\cdot\boldsymbol{r_1}+\phi_{\boldsymbol{k_1}})\cos(\boldsymbol{k_1}\cdot\boldsymbol{r_2}+\phi_{\boldsymbol{k_1}}) \times \cos(\boldsymbol{k_3}\cdot\boldsymbol{r_3}+\phi_{\boldsymbol{k_3}})\cos(\boldsymbol{k_3}\cdot\boldsymbol{r_4}+\phi_{\boldsymbol{k_3}})\Big\rangle. \tag{1.21}$$

This can be split into

$$\sum_{\boldsymbol{k_1}} A(k_1)^2\Big\langle \cos(\boldsymbol{k_1}\cdot\boldsymbol{r_1}+\phi_{\boldsymbol{k_1}})\cos(\boldsymbol{k_1}\cdot\boldsymbol{r_2}+\phi_{\boldsymbol{k_1}})\Big\rangle \times \sum_{\boldsymbol{k_3}} A(k_3)^2\Big\langle \cos(\boldsymbol{k_3}\cdot\boldsymbol{r_3}+\phi_{\boldsymbol{k_3}})\cos(\boldsymbol{k_3}\cdot\boldsymbol{r_4}+\phi_{\boldsymbol{k_3}})\Big\rangle = \langle H(\boldsymbol{r_1})H(\boldsymbol{r_2})\rangle\langle H(\boldsymbol{r_3})H(\boldsymbol{r_4})\rangle. \tag{1.22}$$

Applying the same to the other cases and adding them together precisely gives eq. (1.19).

One may note that the case $\boldsymbol{k_1} = \boldsymbol{k_2} = \boldsymbol{k_3} = \boldsymbol{k_4}$ was not treated correctly. However, since $\boldsymbol{k_i}$ can take on an infinite number of values, and this case only provides one degree of freedom instead of the two we had for the other cases, these correlations only have a vanishing contribution.

From this example, it is not hard to see that in general, an n-point correlation function can be factorized, i.e. written as the sum of products of two-point correlations, where the sum features all possible ways in which the n variables can be paired up.

1.2 STOCHASTIC GEOMETRY

1.2.1 *Critical points*

A critical point $\boldsymbol{r_0} = (x_0, y_0)$ on a surface $f(x, y)$ is a point where the derivative along both the x and the y direction is zero:

$$f_x(x_0, y_0) = f_y(x_0, y_0) = 0. \tag{1.23}$$

The derivative is then in fact zero along all directions.

Critical points can be divided into two categories: extrema and saddle points. An extremum is a local maximum or minimum, while a saddle point is a maximum along some directions but a minimum along others. An example of a saddle point is the function $f(x, y) = x^2 - y^2$ at the origin, which increases for changes in x but decreases for changes in y. The classification of a critical point (x_0, y_0) can be expressed in terms of the second derivatives of f. Let us define $f_\theta(r)$ as $f(x, y)$ along a line through (x_0, y_0) at the angle θ:

$$f_\theta(r) = f(x_0 + r\cos\theta, y_0 + r\sin\theta). \tag{1.24}$$

In one dimension, a critical point is a maximum (minimum) if the second derivative is negative (positive):

$$\begin{aligned} f''_\theta(0) &= \left.\frac{\mathrm{d}^2 f_\theta}{\mathrm{d}r^2}\right|_{r=0} \\ &= f_{xx}(x_0, y_0)\cos^2\theta + f_{yy}(x_0, y_0)\sin^2\theta + 2f_{xy}(x_0, y_0)\sin\theta\cos\theta \\ &= (\tfrac{1}{2} + \tfrac{1}{2}\cos 2\theta) f_{xx} + (\tfrac{1}{2} - \tfrac{1}{2}\cos 2\theta) f_{yy} + \sin 2\theta f_{xy} \\ &= \tfrac{1}{2}(f_{xx} + f_{yy}) + \tfrac{1}{2}(f_{xx} - f_{yy})\cos 2\theta + f_{xy}\sin 2\theta. \end{aligned} \tag{1.25}$$

This value of the second derivative at (x, y) along the direction θ is called the *curvature* along this direction at this point.

More insight is gained by applying the transformation

$$\begin{aligned} \tfrac{1}{2}(f_{xx} - f_{yy}) &= R\cos\alpha, & R &= \tfrac{1}{2}\sqrt{(f_{xx} - f_{yy})^2 + 4f_{xy}^2}, \\ f_{xy} &= R\sin\alpha, & \tan\alpha &= \frac{2f_{xy}}{f_{xx} - f_{yy}}. \end{aligned} \tag{1.26}$$

With this we find:

$$\begin{aligned} f''_\theta(0) &= \tfrac{1}{2}(f_{xx} + f_{yy}) + R(\cos\alpha\cos 2\theta + \sin\alpha\sin 2\theta) \\ &= \tfrac{1}{2}(f_{xx} + f_{yy}) + \tfrac{1}{2}\sqrt{(f_{xx} - f_{yy})^2 + 4f_{xy}^2}\cos(2\theta - \alpha). \end{aligned} \tag{1.27}$$

We have an extremum if and only if the curvature $f''_\theta(0)$ is either exclusively positive or exclusively negative over the entire θ range, which we can easily see is the case when

$$|f_{xx} + f_{yy}| > \sqrt{(f_{xx} - f_{yy})^2 + 4f_{xy}^2} \quad \Leftrightarrow \quad f_{xx}f_{yy} - f_{xy}^2 > 0. \tag{1.28}$$

The type of extremum (maximum or minimum) is then determined by the sign of f_{xx} and f_{yy}.

In summary, we have:

<table>
<tr><td colspan="3">Critical point</td></tr>
<tr><td colspan="2">Extremum</td><td rowspan="2">Saddle point</td></tr>
<tr><td>Maximum</td><td>Minimum</td></tr>
<tr><td colspan="2">$f_{xx}f_{yy} - f_{xy}^2 > 0$</td><td rowspan="2">$f_{xx}f_{yy} - f_{xy}^2 < 0$</td></tr>
<tr><td>$f_{xx}, f_{yy} < 0$</td><td>$f_{xx}, f_{yy} > 0$</td></tr>
</table>

Another way of identifying critical points is to look at the gradient of the field. The critical points appear as shown in fig. 1.2. For an extremum, all gradient lines either point toward or away from the point, whereas for a saddle point there are exactly four lines connected to it: two incoming and two outgoing, which are perpendicular to each other.

Another defining characteristic is the *topological index*, or charge, or *Poincaré index* of the points. Formally, this is defined as

$$n = \frac{1}{2\pi}\oint \nabla\theta \cdot \mathrm{d}l, \tag{1.29}$$

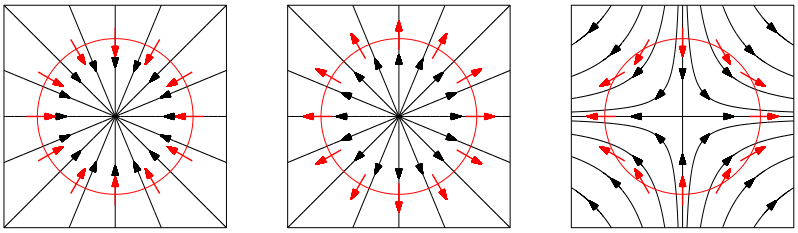

(a) (b) (c)

Figure 1.2: The gradient field (black) around (a) a maximum, (b) a minimum and (c) a saddle point. The red circle and arrows show how the gradient rotates around the critical point.

where the path-integral is taken over a (small) counterclockwise loop around this defect only. In words, it counts the number of revolutions the gradient direction makes when traversing this closed loop. For both types of extrema, in a full counterclockwise loop the gradient goes through a full counterclockwise cycle; these points thus have index $n = +1$. Contrarily, in a counterclockwise loop around a saddle point the gradient rotates clockwise; its topological index is therefore $n = -1$ (the minus sign reflects that it rotates in the opposite direction with respect to the direction the loop is traversed in).

The topological index can be deduced from the second derivatives. For a point $\boldsymbol{r}$ near a critical point $\boldsymbol{r_0}$, the gradient is given by

$$\nabla f = \begin{pmatrix} f_{xx} & f_{xy} \\ f_{xy} & f_{yy} \end{pmatrix} \begin{pmatrix} x - x_0 \\ y - y_0 \end{pmatrix} = \mathsf{A}(\boldsymbol{r} - \boldsymbol{r_0}). \tag{1.30}$$

If A were the identity matrix, then a counterclockwise loop around $\boldsymbol{r_0}$ would obviously result in a rotation by 2π, giving index $+1$. In general, A may stretch and rotate $\boldsymbol{r}$, neither of which would have an effect on the index. However, if A includes a reflection, the gradient would rotate in the opposite direction and the index becomes -1. Whether A describes a reflection is encoded in the sign of its determinant

$$\det \mathsf{A} = f_{xx} f_{yy} - f_{xy}^2. \tag{1.31}$$

Hence we find the same criterion separating extrema from saddle points as before.

1.2.2 *Umbilical points*

Umbilical points are points on a surface where the curvature of the surface is the same along all directions. At an umbilical point the surface is thus locally spherical (or flat).

We return to the curvature as defined in eq. (1.27), repeated here for convenience:

$$f''_\theta(0) = \tfrac{1}{2}(f_{xx} + f_{yy}) + \tfrac{1}{2}\sqrt{(f_{xx} - f_{yy})^2 + 4f_{xy}^2}\cos(2\theta - \alpha). \qquad (1.32)$$

The two *principal directions* are the directions along which the curvature is maximal or minimal. The corresponding curvatures are known as the *principal curvatures*. We can easily see that these two directions are given by $2\theta - \alpha = k\pi$ and hence perpendicular to each other.

As noted before, at an umbilical point the curvature is the same along all directions. In other words, the two principal curvatures are the same, and the principal directions cannot be defined. From eq. (1.32), the definition of an umbilical point is easily seen to be

$$f_{xx} = f_{yy} \qquad \text{and} \qquad f_{xy} = 0. \qquad (1.33)$$

Umbilical points can be classified into three types. The distinction can be clearly made when one looks at the *curvature lines*. These are curves which are always tangent to a principal direction, either the one corresponding to the maximal curvature or the minimum one. These two sets of curvature lines intersect at right angles, since as noted before, the principal directions are always perpendicular to each other.

At an umbilical point, no principal direction can be defined, giving one of the three patterns shown in fig. 1.3. There are three types: *lemons*, *monstars* and *stars* [4, 9].

These umbilical points too are topological defects, with an index. When we follow a closed counterclockwise loop around them, we see from fig. 1.3 that, for the point labeled *star*, the direction makes half a clockwise rotation, which means a topological index of $-1/2$. The other two umbilical points have index $+1/2$.

Another characteristic separating the three is the number of curvature lines that terminate at the umbilical point. For a *lemon*, this is one, whereas for the other two it is three. We see that the third type of umbilical point shares properties with both others: It has topological index $+1/2$, as does a lemon, and three curvature lines terminating at it, like a star. This in-between nature of the point is reflected in its name: *monstar*.

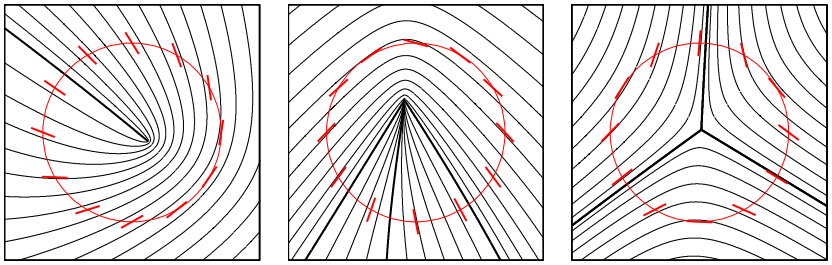

(a) (b) (c)

Figure 1.3: One set of curvature lines (black) around (a) a lemon, (b) a monstar and (c) a star. The other set shows the same pattern in all cases. The red circle and line segments show how the principal direction rotates around the umbilical point.

The three types of umbilical point can also be distinguished using the third derivatives, much like the various types of critical points can be identified from the second derivatives. From eqs. (1.26) and (1.32) we see that the two principal directions, for which the curvature is maximal or minimal, are given by

$$\tan 2\theta = \tan \alpha = \frac{2f_{xy}}{f_{xx} - f_{yy}}. \tag{1.34}$$

Note that the directions are given by angles modulo π, so this equation has two solutions: the two principal directions. The angle 2θ can be pictured as the argument of the vector $\boldsymbol{v} = \binom{f_{xx}-f_{yy}}{2f_{xy}}$. At an umbilical point, both vector components are zero (hence the angle / principal direction is not defined). In order to determine the topological index, we need to know what the principal directions are in close proximity to this point, in order to evaluate the infinitesimal loop in eq. (1.29). We can expand $\boldsymbol{v}$ using the third derivatives. For a point $\boldsymbol{r}$ near an umbilical point $\boldsymbol{r_0}$ we have

$$\boldsymbol{v} = \begin{pmatrix} f_{xxx} - f_{yyx} & f_{xxy} - f_{yyy} \\ 2f_{xyx} & 2f_{xyy} \end{pmatrix} \begin{pmatrix} x - x_0 \\ y - y_0 \end{pmatrix} = \mathsf{A}(\boldsymbol{r} - \boldsymbol{r_0}). \tag{1.35}$$

As before, the sign of the index depends on the sign of the determinant of A:

$$\tfrac{1}{2} \det \mathsf{A} = (f_{xxx} - f_{xyy}) f_{xyy} + (f_{yyy} - f_{xxy}) f_{xxy}. \tag{1.36}$$

Introducing $\alpha = f_{xxx}, \beta = f_{xxy}, \gamma = f_{xyy}, \delta = f_{yyy}$, we thus find (see also [4])

$$\alpha\gamma - \gamma^2 + \beta\delta - \beta^2 \begin{cases} > 0 & \text{for L, M} \\ < 0 & \text{for S} \end{cases} \tag{1.37}$$

As mentioned before, the criterion separating the lemons from the monstars (and stars), is the number of (locally straight) lines ending at the umbilical point: one for lemons, three for (mon)stars (that is one/three for each principal direction). This can also be expressed in terms of α, β, γ and δ. Consider again a point $\boldsymbol{r}$ near $\boldsymbol{r_0}$. The principal directions are given by θ modulo $\frac{1}{2}\pi$, hence one of the two is directed toward the umbilical point when the argument ϕ of $\boldsymbol{r} - \boldsymbol{r_0}$ is equal to θ at $\boldsymbol{r}$, modulo $\frac{1}{2}\pi$.

To find an algebraic statement of this condition, we double both sides: $2\phi \equiv 2\theta \pmod{\pi}$. The right-hand side is the argument of $\boldsymbol{v}$ by eq. (1.34). We can also find a vector whose argument is given by the left-hand side: Let $\binom{x}{y} = \boldsymbol{r} - \boldsymbol{r_0}$; then 2ϕ is the argument of the vector $\binom{x^2-y^2}{2xy}$. This is easily seen by mapping $\binom{x}{y}$ to the complex number $x + iy$ and taking its square, which doubles the argument, and then mapping back. The condition for $\boldsymbol{r}$ being on a terminating curvature line is that the arguments of these two vectors must match modulo π, which translates to $\binom{x^2-y^2}{2xy}$ and $\mathsf{A}\binom{x}{y}$ being parallel to each other. This condition can be mathematically expressed as

$$\begin{aligned} 0 &= \tfrac{1}{2}\begin{pmatrix} -2xy & x^2 - y^2 \end{pmatrix} \mathsf{A} \begin{pmatrix} x \\ y \end{pmatrix} \\ &= \tfrac{1}{2}\begin{pmatrix} -2xy & x^2 - y^2 \end{pmatrix} \begin{pmatrix} (\alpha - \gamma)x - (\delta - \beta)y \\ 2\beta x + 2\gamma y \end{pmatrix} \\ &= \beta x^3 - (\alpha - 2\gamma)x^2 y + (\delta - 2\beta)xy^2 - \gamma y^3. \end{aligned} \tag{1.38}$$

The superfluous factor $\frac{1}{2}$ at the beginning was introduced to remove a redundant factor of 2 at the end. Note that this equation describes lines passing through $\boldsymbol{r_0}$, whereas the curvature lines actually terminate on the defect. On one side of $\boldsymbol{r_0}$, such a passing line corresponds to the line of maximal curvature, on the other side to minimal curvature. This is easily seen from eq. (1.25), if one notes that the second derivatives change sign when passing through $\boldsymbol{r_0}$.

The number of straight lines passing through $\boldsymbol{r_0}$ is thus equal to the number of (real) roots of this cubic equation (that is, by interpreting this

as an equation in x/y). This is captured by the discriminant: If it is positive, then there are three roots; if it is negative, there is only one. This results in (see also [4])

$$\begin{aligned} &4\Big(3\gamma(\alpha-2\gamma)-(\delta-2\beta)^2\Big)\\ &\times\Big(3\beta(\delta-2\beta)-(\alpha-2\gamma)^2\Big)\\ &-\Big((\delta-2\beta)(\alpha-2\gamma)-9\beta\gamma\Big)^2 \end{aligned} \quad \begin{cases} >0 & \text{for M, S} \\ <0 & \text{for L} \end{cases} \tag{1.39}$$

In summary:

Umbilical point		
Index $+\frac{1}{2}$		Index $-\frac{1}{2}$
Lemon	Monstar	Star
eq. (1.37) >0		eq. (1.37) <0
eq. (1.39) <0	eq. (1.39) >0	

1.2.3 *Critical and umbilical point densities*

The density of critical points on a Gaussian field naturally depends on the power spectrum of the field. In fact, it only depends on the moments K_2 and K_4 [34]:

$$n_{\text{crit}} = \frac{K_4}{2\sqrt{3}\pi K_2}. \tag{1.40}$$

We will derive this as an intermediate result in chapter 2.

It may not come as a surprise that the density of umbilical points also only depends on two moments [4]:

$$n_{\text{umb}} = \frac{K_6}{4\pi K_4}. \tag{1.41}$$

There are also some statements that can be made about the densities of the various types of critical (umbilical) points, relative to each other. The Poincaré-Hopf theorem states that the total index of a vector field (i.e. the sum of the indices of all topological defects) is equal to the Euler

characteristic of the underlying manifold, which for the 2D-plane is simply zero. For the critical points this means that the densities of extrema (index $+1$) and saddle points (index -1) is equal.

A sketchy proof (a proper proof can be found in most books on differential topology, e.g. [40]) of this theorem applied to the present case is given in [35] and is roughly as follows: For any closed loop, the gradient makes a counterclockwise cycle for every extremum that is enclosed by the loop, and a clockwise cycle for every saddle point (cycles of both type cancel each other out). In other words:

$$\#(\text{counterclockwise cycles}) = \\ \#(\text{extrema}) - \#(\text{saddle points}). \tag{1.42}$$

Consider now loops of increasing size L on a (random) surface. The number of cycles traversed by the gradient along the loop is at most proportional to the size of the loop L, but the number of critical points enclosed scales as the area, L^2. The only way in which the above formula can continue to hold for large L is if both sides go to zero.

For Gaussian fields, the set of extrema consists of maxima and minima in equal densities. This can be seen easily from the fact that $-H$ is as much a Gaussian as H is (this sign change can be brought about by adding π to all phases $\phi_{\boldsymbol{k}}$). The maxima of H are the minima of $-H$ and vice versa. Upon averaging, we thus find that their numbers are balanced. In summary:

$$\alpha_{\text{saddle}} = \tfrac{1}{2}, \qquad \alpha_{\text{min}} = \alpha_{\text{max}} = \tfrac{1}{4}, \tag{1.43}$$

where α stands for the density fraction with respect to the total density.

Similarly, for the umbilics, the Poincaré-Hopf theorem means that the density of stars (with index $+1/2$) equals the combined density of lemons and monstars (with index $-1/2$). In other words, the star *fraction*, that is the density of stars divided by the total density of umbilical points, is always $1/2$. Although there is no such universal constraint on the lemon and monstar fractions, it has been shown that, for isotropic Gaussian random fields, these are fixed as well [4, 11]:

$$\alpha_{\text{S}} = \tfrac{1}{2}, \qquad \alpha_{\text{M}} = \tfrac{1}{2} - \alpha_{\text{L}} = \frac{1}{2} - \frac{1}{\sqrt{5}} = 0.053. \tag{1.44}$$

Note in particular that it does not depend on the spectrum of the field. The number 0.053 we will see again in chapter 3.

NON-GAUSSIAN FIELDS

Now we take a Gaussian field and apply a perturbation to it, so that it becomes non-Gaussian. We then investigate the effects this has on the stochastic geometry. Chapters 2 and 3 deal with local perturbations and the effect that they have on extrema and umbilical points respectively. Chapter 4 covers nonlocal perturbations and finally chapter 5 deals with coarse-graining.

2

CRITICAL POINTS OF A NON-GAUSSIAN RANDOM FIELD

2.1 NON-GAUSSIAN FIELDS

As explained in the introduction, a Gaussian distribution is usually a good approximation to use for a random process, especially one that can be considered to be a sum or average of a large number of independent sub-processes. It is however the deviation from Gaussianity that is usually of special interest.

If we go back to the example of the amount of rain that falls throughout the country in a year, we might be interested to see if there are certain areas where there is more (or less) downfall than in others. The complication is that this is automatically the case, simply because of random fluctuations. If we want to see what the influence is of, say, the geographical structure of the landscape, we would like to filter out these random fluctuations and focus on the non-Gaussian contribution to the random field.

Detecting non-Gaussianity can be accomplished by testing the field to see whether it has the properties that Gaussian fields are known to have, such as the ones outlined in chapter 1.

The goal of this thesis is to take this one step further, by determining how the stochastic geometric properties change *quantitatively* in relation to the non-Gaussianity. This could then in turn be used to identify the type of non-Gaussianity and/or its size.

This chapter is devoted to studying the effects of non-Gaussianity on the statistics of maxima and minima, specifically the difference between the two. For a Gaussian field, the densities of maxima and minima is obviously the same due to symmetry. For a non-Gaussian field this may no longer be the case.

We will first consider a field of the form $h(\boldsymbol{r}) = F_{NL}(H(\boldsymbol{r}))$, where H is a Gaussian field and F_{NL} is any (nonlinear) function (e.g. the identity plus a perturbation), which depends only on $H(\boldsymbol{r})$, i.e. the original (unperturbed) value of the field at that same point. This scheme we will refer to as a *local perturbation*. The more generic case of a nonlocal perturbation will be the subject of chapter 4.

The outline of this chapter is as follows. We demonstrate how the imbalance between maxima and minima can be calculated in section 2.2. Section 2.3 is devoted to determining the key ingredient, namely the probability distribution for the values of minima in a Gaussian field. In section 2.4 we arrive at the final result, compare it with results from computer generated fields and point out the main features. Finally, section 2.5 provides an overview of our findings and their implications.

2.2 MAXIMA VERSUS MINIMA

Transforming the field with F_{NL} does not cause the maxima and minima to move around, but they may switch type, depending on the sign of $F'_{NL} = \mathrm{d}F_{NL}/\mathrm{d}H$ at the point in question. To see this, recall that maxima and minima, together with saddle points, are *critical points*. The critical points of h are given by

$$0 = \boldsymbol{\nabla} h(\boldsymbol{r}) = \frac{\mathrm{d}h}{\mathrm{d}H}\boldsymbol{\nabla} H(\boldsymbol{r}) = F'_{NL}(H)\boldsymbol{\nabla} H(\boldsymbol{r}). \tag{2.1}$$

We see that the critical points of H and h are the same points; however, the prefactor $F'_{NL}(H)$ may influence the type of critical point. The three types can be distinguished by considering the second derivatives: Saddle points have $h_{xx}h_{yy} - h_{xy}^2 < 0$, whereas for maxima and minima (extrema) this is positive. For maxima, unlike minima, we have $h_{xx} < 0$ (and $h_{yy} < 0$).

Consider a critical point $\boldsymbol{r_0}$ and let $z = H(\boldsymbol{r_0})$. The second derivatives of h at $\boldsymbol{r_0}$ simply have an extra factor $F'_{NL}(z)$ as compared to the second derivatives of H. This has no influence on the sign of $h_{xx}h_{yy} - h_{xy}^2$. Therefore, the saddle points (extrema) of H are also saddle points (extrema) of h. However, a maximum (minimum) of H is a minimum (maximum) of h when $F'_{NL}(z) < 0$. In order to determine how many extrema will undergo such a transformation, we need to know how often $F'_{NL}(z) < 0$ at such a point.

Let $g(z)$ be the probability density that a certain minimum $\boldsymbol{r_0}$ of H has the value $H(\boldsymbol{r_0}) = z$. The probability P that a minimum of H becomes a maximum of h is then

$$P = \int_{z:F'_{NL}(z)<0} \mathrm{d}z\, g(z). \tag{2.2}$$

For example, if we consider a square perturbation $h = H + \varepsilon H^2$, for which $F'_{NL}(z) = 1 + 2\varepsilon z$, we have

$$P = \int_{-\infty}^{-\frac{1}{2\varepsilon}} \mathrm{d}z\, g(z). \tag{2.3}$$

Because of the symmetry of H, the maxima are distributed according to $g(-z)$. With that, we can similarly define a probability Q that a maximum becomes a minimum going from H to h.

Let n_0 be the density of minima (or maxima) of H. The density of minima (maxima) of H which are maxima (minima) of h is then Pn_0 (Qn_0). We can quantify the resulting imbalance in maxima and minima in the dimensionless parameter

$$\begin{aligned}\Delta n \equiv \frac{n_{\max} - n_{\min}}{n_{\max} + n_{\min}} &= \frac{(1+P-Q)n_0 - (1-P+Q)n_0}{2n_0} \\ &= P - Q = \int_{z:F'_{NL}(z)<0} \mathrm{d}z \Big(g(z) - g(-z)\Big).\end{aligned} \tag{2.4}$$

Thus, if we can determine $g(z)$, we can calculate the exact imbalance between the maxima and minima of h.

2.3 DISTRIBUTION OF MINIMUM VALUES

2.3.1 *One dimension*

Let us first consider the probability distribution for minimum values of a Gaussian function on a line. We will then generalize to two dimensions, and afterward, discuss how these distributions depend on the power spectrum.

We start with

$$H(x) = \sum_k A(k) \cos(kx + \phi_k). \tag{2.5}$$

The minima are given by $H_x(x_0) = 0$ and $H_{xx}(x_0) > 0$. We would thus like to know the probability density that $H(x_0) = z$, given that $H_x(x_0) = 0$ and $H_{xx}(x_0) > 0$:

$$\begin{aligned} g(z) &= p(H(x_{\min}) = z) \\ &= \frac{1}{n}\, p(H(x_0) = z \wedge H_x(x_0) = 0 \wedge H_{xx}(x_0) > 0). \end{aligned} \tag{2.6}$$

Here $n \equiv p(H_x(x_0) = 0 \wedge H_{xx}(x_0) > 0)$ can be identified as the density of the minima.

Finding $g(z)$ thus requires us to determine the joint probability distribution $p(H(x_0), H_x(x_0), H_{xx}(x_0))$. Since H is homogeneous, p does not depend on x_0.

Let us take a closer look at the first derivative

$$\begin{aligned} H_x(x_0) &= \sum_k A(k)(-k)\sin(kx_0 + \phi_k) \\ &= \sum_k kA(k)\cos(kx_0 + \phi_k + \tfrac{1}{2}\pi). \end{aligned} \tag{2.7}$$

We see that the expression for H_x still describes a Gaussian: The phases are simply increased by $\frac{1}{2}\pi$ (modulo 2π) and the spectrum has picked up a factor of k. The bottom line is that $H_x(x_0)$ is a Gaussian variable, and it is easy to confirm that the same goes for $H_{xx}(x_0)$ (or any derivative).

We thus have three Gaussian variables. The joint probability distribution of a set of (correlated) Gaussian random variables is given by (see e.g. [35]; compare eq. (1.2))

$$p(\xi_1, \ldots, \xi_n) = \frac{1}{(2\pi)^{n/2}\sqrt{\det C}} \exp\left(-\tfrac{1}{2}\sum_{i,j}(C^{-1})_{ij}\xi_i\xi_j\right), \tag{2.8}$$

where C is the matrix of correlations

$$C_{ij} = \langle \xi_i \xi_j \rangle. \tag{2.9}$$

Let us calculate $\langle H(x_0)H_{xx}(x_0)\rangle$ as an example. Again, homogeneity allows us to set $x_0 = 0$ for convenience. We then find

$$\begin{aligned}\langle H(x_0)H_{xx}(x_0)\rangle &= \langle H(0)H_{xx}(0)\rangle \\ &= \left\langle \sum_k A(k)\cos\phi_k \sum_{k'} A(k')(-k'^2)\cos\phi_{k'} \right\rangle \\ &= \sum_{kk'} A(k)A(k')(-k'^2)\Big\langle \cos\phi_k \cos\phi_{k'} \Big\rangle \\ &= \sum_{kk'} A(k)A(k')(-k'^2)\tfrac{1}{2}\delta_{kk'} \\ &= \sum_k -\tfrac{1}{2}A(k)^2k^2 = -K_2. \end{aligned} \tag{2.10}$$

Here we made use of the moment K_2 defined in eq. (1.11).

An even and an odd derivative of H are always uncorrelated, e.g.

$$\begin{aligned}\langle H(0)H_x(0)\rangle &= \sum_{kk'} A(k)A(k')(-k')\Big\langle \cos\phi_k \sin\phi_{k'} \Big\rangle \\ &= \sum_{kk'} A(k)^2(-k)\Big\langle \cos\phi_k \sin\phi_k \Big\rangle \delta_{kk'} = 0. \end{aligned} \tag{2.11}$$

This is because an even derivative features cosines while an odd derivative has sines, and their product averages to zero, as above.

The final result is that for H, H_x and H_{xx} the correlations are

$$C = \begin{pmatrix} 1 & 0 & -K_2 \\ 0 & K_2 & 0 \\ -K_2 & 0 & K_4 \end{pmatrix}. \tag{2.12}$$

The determinant of C is $K_2(K_4 - K_2^2)$ and its inverse is

$$C^{-1} = \frac{1}{K_2(K_4 - K_2^2)} \begin{pmatrix} K_2K_4 & 0 & K_2^2 \\ 0 & K_4 - K_2^2 & 0 \\ K_2^2 & 0 & K_2 \end{pmatrix}. \tag{2.13}$$

This gives

$$\begin{aligned} p(H, H_x, H_{xx}) = &\frac{1}{(2\pi)^{3/2}\sqrt{K_2(K_4 - K_2^2)}} \\ &\times \exp\left(\frac{H_x^2}{2K_2} - \frac{K_4H^2 + 2K_2HH_{xx} + H_{xx}^2}{2(K_4 - K_2^2)} \right). \end{aligned} \tag{2.14}$$

The plan is now to set $H = z$ and $H_x = 0$ and integrate p over H_{xx}. However, one important factor still needs to be added. The probability we have calculated is actually a probability density (since the probability that $H'(x_0) = 0$ and $H(x_0) = z$ exactly is zero), and it is not defined with respect to the variables we need. It is defined by fixing a point x_0 and determining the probability that H_x vanishes within a certain tolerance at that point, as in

$$\frac{P(H(x_0) \in [z, z + \mathrm{d}z] \wedge H_x(x_0) \in [0, \mathrm{d}H'])}{\mathrm{d}z\,\mathrm{d}H'}. \tag{2.15}$$

Instead, we actually want the probability that there is an *exact* critical point within a certain distance of x_0:

$$\frac{P\begin{pmatrix} \exists\, x_m \in [x_0, x_0 + \mathrm{d}x] : \\ H(x_m) \in [z, z + \mathrm{d}z] \wedge H_x(x_m) = 0 \end{pmatrix}}{\mathrm{d}x\,\mathrm{d}z}. \tag{2.16}$$

Over the range $\mathrm{d}x$, $\mathrm{d}H'$ varies by

$$\mathrm{d}H' = \left|\frac{\partial H_x}{\partial x}\right| \mathrm{d}x = |H_{xx}|\mathrm{d}x. \tag{2.17}$$

In order to get the desired probability density with respect to x, we need to multiply our current probability density by $|H_{xx}|$.

The probability distribution for the minima is thus given by (see eq. (2.6))

$$g(z) = \frac{1}{n}\int_0^\infty \mathrm{d}H_{xx}\, p(H = z, H_x = 0, H_{xx})\, |H_{xx}|. \tag{2.18}$$

The prefactor, featuring the density of minima n, can be regarded as a normalization constant and is found by integrating $g(z)$ over the entire z-range. This is easily accomplished by taking the expression above and first integrating over z, and only then over H_{xx}. The result is

$$\int_{-\infty}^{\infty} \mathrm{d}z\, g(z) = 1 \quad \Rightarrow \quad n = \frac{1}{2\pi}\sqrt{K_4/K_2}. \tag{2.19}$$

The integrand in eq. (2.18) is also Gaussian, but it is only integrated over for positive H_{xx}, resulting in

$$\begin{aligned} g(z) = &\sqrt{\frac{1-\lambda}{2\pi}} \exp\left(-\frac{1}{2(1-\lambda)}\, z^2\right) \\ &- \tfrac{1}{2}\sqrt{\lambda}\, z \exp\left(-\tfrac{1}{2}z^2\right) \operatorname{erfc}\left(\sqrt{\frac{\lambda}{2(1-\lambda)}}\, z\right). \end{aligned} \tag{2.20}$$

Here erfc is the complementary error function

$$\operatorname{erfc}(x) \equiv \frac{2}{\sqrt{\pi}} \int_x^\infty \mathrm{d}t\, e^{-t^2}, \tag{2.21}$$

which converges to 1 as x goes to $-\infty$. The two parameters K_2 and K_4 have been merged into a single dimensionless parameter

$$\lambda \equiv \frac{K_2^2}{K_4} \qquad (0 \le \lambda \le 1). \tag{2.22}$$

Note that we set $K_0 \equiv \langle H^2 \rangle = 1$ for convenience. In the generic case $K_0 \neq 1$, we have $\lambda = K_2^2/(K_0 K_4)$. A proof that $\lambda \le 1$ is derived explicitly in the next section.

2.3.2 *Two dimensions*

In two dimensions, the procedure to calculate the distribution of the minima is similar. The minima are defined by the conditions $H_x = H_y = 0$ (defining critical points), $H_{xx}H_{yy} - H_{xy}^2 > 0$ (separating extrema from saddle points) and $H_{xx}, H_{yy} > 0$ (distinguishing minima from maxima). We thus need to find $p(H, H_x, H_y, H_{xx}, H_{yy}, H_{xy})$. This is still a Gaussian joint distribution function.

We start again by determining the correlations, for example (again setting $\boldsymbol{r} = 0$ for convenience)

$$\begin{aligned}
\langle H_{xx}H_{yy} \rangle &= \sum_{\boldsymbol{k}\boldsymbol{k}'} A(k)A(k')k_x^2 k_y'^2 \left\langle \cos\phi_{\boldsymbol{k}} \cos\phi_{\boldsymbol{k}'} \right\rangle \\
&= \sum_{\boldsymbol{k}\boldsymbol{k}'} A(k)A(k')k_x^2 k_y'^2 \tfrac{1}{2}\delta_{\boldsymbol{k}\boldsymbol{k}'} = \sum_{\boldsymbol{k}} \tfrac{1}{2} A(k)^2 k_x^2 k_y^2 \\
&= \frac{1}{2\pi} \int_0^{2\pi} \int_0^\infty \mathrm{d}k \mathrm{d}\theta\, \Pi(k) k^4 \cos^2\theta \sin^2\theta \\
&= \tfrac{1}{8} \int_0^\infty \mathrm{d}k\, \Pi(k) k^4 = \tfrac{1}{8} K_4.
\end{aligned} \tag{2.23}$$

In the third line we replaced the sum by an integral and performed it using polar coordinates.

Remember from the one-dimensional case that the correlation of an even and an odd derivative is always zero, because in the calculation we encounter a product of a cosine and a sine, which integrated over the (random) phase yields zero. Based on the calculation method demonstrated

above, we can make a more general statement: When the combined number of x-derivatives (y-derivatives) is odd, the integral over θ (as above) features a cosine (sine) with an odd exponent; the integral over θ then gives zero. If we apply this rule to our six variables, we see that H_x, H_y and H_{xy} all have no "compatible match" in this respect; therefore, they are uncorrelated to all other variables. This allows us to factorize the joint probability distribution

$$\begin{aligned} &p(H, H_x, H_y, H_{xx}, H_{yy}, H_{xy}) \\ &\quad = p(H_x)\, p(H_y)\, p(H_{xy})\, p(H, H_{xx}, H_{yy}). \end{aligned} \tag{2.24}$$

The probability densities of the individual variables are straightforward,

$$p(H_x) = \frac{1}{\sqrt{\pi K_2}} \exp\left(-\frac{1}{K_2} H_x^2\right), \tag{2.25a}$$

$$p(H_y) = \frac{1}{\sqrt{\pi K_2}} \exp\left(-\frac{1}{K_2} H_y^2\right), \tag{2.25b}$$

$$p(H_{xy}) = \frac{2}{\sqrt{\pi K_4}} \exp\left(-\frac{4}{K_4} H_{xy}^2\right). \tag{2.25c}$$

For H, H_{xx} and H_{yy}, we determine the correlation matrix

$$C = \begin{pmatrix} 1 & -\frac{1}{2}K_2 & -\frac{1}{2}K_2 \\ -\frac{1}{2}K_2 & \frac{3}{8}K_4 & \frac{1}{8}K_4 \\ -\frac{1}{2}K_2 & \frac{1}{8}K_4 & \frac{3}{8}K_4 \end{pmatrix}. \tag{2.26}$$

The determinant of C is $\frac{1}{8}K_4(K_4 - K_2^2)$ and its inverse is

$$C^{-1} = \frac{1}{K_4(K_4 - K_2^2)} \begin{pmatrix} K_4^2 & K_2 K_4 & K_2 K_4 \\ K_2 K_4 & 3K_4 - 2K_2^2 & 2K_2^2 - K_4 \\ K_2 K_4 & 2K_2^2 - K_4 & 3K_4 - 2K_2^2 \end{pmatrix}. \tag{2.27}$$

After some rearranging, eq. (2.8) gives

$$\begin{aligned} p(H, H_{xx}, H_{yy}) = {} & \frac{1}{\pi^{3/2}\sqrt{K_4(K_4 - K_2^2)}} \\ & \times \exp\left(-\frac{(K_4 H + K_2 H_{xx} + K_2 H_{yy})^2}{2K_4(K_4 - K_2^2)}\right. \\ & \left. - \frac{(H_{xx} - H_{yy})^2}{2K_4} - \frac{H_{xx}^2 + H_{yy}^2}{K_4}\right). \end{aligned} \tag{2.28}$$

As in the one-dimensional case, we now have a probability density with respect to H_x and H_y, which we need to convert to one with respect to x and y. For that we need to multiply p by the Jacobian determinant

$$\left|\frac{\partial(H_x, H_y)}{\partial(x, y)}\right| = |H_{xx}H_{yy} - H_{xy}^2|. \tag{2.29}$$

The probability distribution for the minima is thus given by

$$\begin{aligned} g(z) &= \frac{1}{n}\, p(H_x = 0)\, p(H_y = 0) \\ &\quad \times \iiint \mathrm{d}H_{xx}\mathrm{d}H_{yy}\mathrm{d}H_{xy} \Big(p(H = z, H_{xx}, H_{yy}) \\ &\qquad \times p(H_{xy})\, |H_{xx}H_{yy} - H_{xy}^2|\Big) \\ &= \frac{1}{n\pi K_2} \iiint \mathrm{d}H_{xx}\mathrm{d}H_{yy}\mathrm{d}H_{xy} \Big(p(z, H_{xx}, H_{yy}) \\ &\qquad \times p(H_{xy})\, |H_{xx}H_{yy} - H_{xy}^2|\Big). \end{aligned} \tag{2.30}$$

The integrals must be taken over the volume for which $H_{xx}H_{yy} - H_{xy}^2 > 0$ and $H_{xx}, H_{yy} > 0$, which forms the domain of the minima. These constraints and the integration can be simplified by making the following change of variables,

$$r\cos\theta = \tfrac{1}{2}(H_{xx} - H_{yy}), \tag{2.31a}$$

$$r\sin\theta = H_{xy}, \tag{2.31b}$$

$$s = \tfrac{1}{2}(H_{xx} + H_{yy}), \tag{2.31c}$$

$$\mathrm{d}H_{xx}\mathrm{d}H_{yy}\mathrm{d}H_{xy} = 2r\,\mathrm{d}r\mathrm{d}s\mathrm{d}\theta. \tag{2.32}$$

In terms of these new variables, we have $H_{xx}H_{yy} - H_{xy}^2 = s^2 - r^2$ and the constraints of the volume are given by $0 < r < s$. We get

$$\begin{aligned} g(z) &= \frac{1}{n\pi K_2} \int_0^{2\pi}\int_0^{\infty}\int_0^{s} \mathrm{d}r\mathrm{d}s\mathrm{d}\theta\, \frac{4r(s^2 - r^2)}{\pi^2 K_4\sqrt{K_4 - K_2^2}} \\ &\quad \times \exp\left(-\frac{K_4 z^2 + 4K_2 s z + 4s^2}{2(K_4 - K_2^2)} - \frac{4r^2}{K_4}\right). \end{aligned} \tag{2.33}$$

The density of the minima n can again readily be obtained by integrating over z:

$$\int_{-\infty}^{\infty} \mathrm{d}z\, g(z) = 1 \quad \Rightarrow \quad n = \frac{K_4}{8\sqrt{3}\pi K_2}. \tag{2.34}$$

Note that this result matches eq. (1.40) (remember that minima comprise one fourth of all critical points).

After evaluating the double integral (taking care to integrate over r first), we obtain

$$\begin{aligned} g(z) = & \\ & \sqrt{\frac{3}{2\pi(3-2\lambda)}} \exp\left(-\frac{3}{2(3-2\lambda)}\, z^2\right) \operatorname{erfc}\left(\sqrt{\frac{\lambda}{2(1-\lambda)(3-2\lambda)}}\, z\right) \\ & - \sqrt{\frac{3}{2\pi}} \lambda (1-z^2) \exp\left(-\tfrac{1}{2} z^2\right) \operatorname{erfc}\left(\sqrt{\frac{\lambda}{2(1-\lambda)}}\, z\right) \\ & - \frac{1}{\pi} \sqrt{3\lambda(1-\lambda)}\, z \exp\left(-\frac{1}{2(1-\lambda)}\, z^2\right). \end{aligned} \tag{2.35}$$

The two parameters K_2 and K_4 have been merged into one as before,

$$\lambda \equiv \frac{K_2^2}{K_4} \qquad (0 \le \lambda \le 1). \tag{2.36}$$

Again, when we set $K_0 = \langle H^2 \rangle \neq 1$, we get $\lambda = K_2^2/(K_0 K_4)$.

Let us prove that $\lambda \le 1$. After some rearranging, we see that this is equivalent to $K_0 K_4 - K_2^2 \ge 0$. We find

$$K_0 K_4 - K_2^2 = \iint \mathrm{d}k \mathrm{d}k' \, \Pi(k) \Pi(k') (k'^4 - k^2 k'^2). \tag{2.37}$$

Note that we could just as well replace k'^4 with k^4 (because everything else is symmetric in k and k'), and hence also with $\frac{1}{2}(k^4 + k'^4)$. If we do the latter, we can rewrite

$$\tfrac{1}{2}(k^4 + k'^4) - k^2 k'^2 = \tfrac{1}{2}(k - k')^2. \tag{2.38}$$

We see that this is positive, together with $\Pi(k)$ and $\Pi(k')$, hence the integrand is positive and the integral too, which concludes the proof.

We have compared eq. (2.35) with distributions obtained from computer-generated Gaussian fields. Details about these numerical simulations and how the minima were identified can be found in appendix A. As can be seen in fig. 2.1, the agreement between eq. (2.35) and the numeric results is excellent.

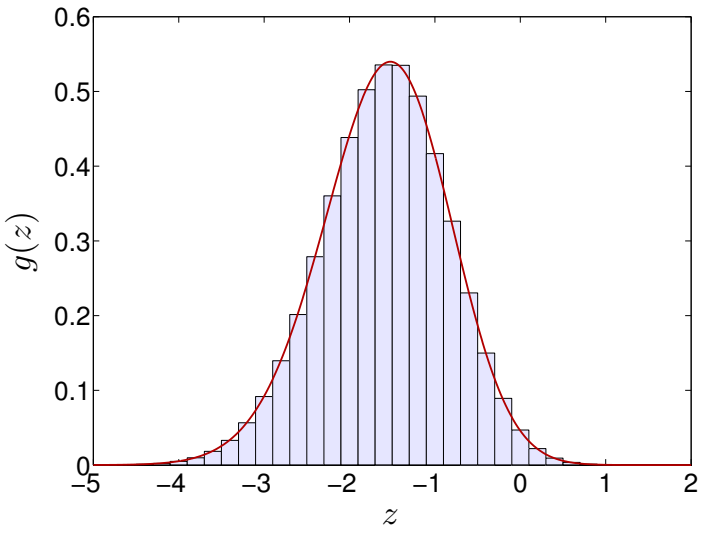

(a)

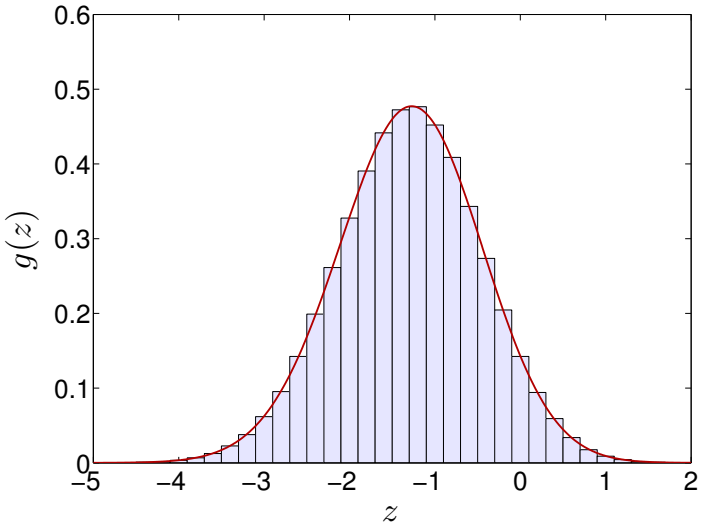

(b)

Figure 2.1: Histograms of the values of 10^6 minima obtained from simulations, together with the distribution given by eq. (2.35), for (a) a disk spectrum ($\lambda = \frac{3}{4}$); (b) a Gaussian spectrum ($\lambda = \frac{1}{2}$).

Let us take a closer look at eq. (2.35). The two limits of λ give results with interesting physical interpretations:

$$\lim_{\lambda\to 0} g(z) = \frac{1}{\sqrt{2\pi}} e^{-\frac{1}{2}z^2} - \sqrt{\lambda}\frac{4}{\sqrt{3\pi}} z e^{-\frac{1}{2}z^2} + O(\lambda), \tag{2.39a}$$

$$\lim_{\lambda\to 1} g(z) = (1-\operatorname{sgn} z)\sqrt{\frac{3}{2\pi}}\left(e^{-z^2} - 1 + z^2\right)e^{-\frac{1}{2}z^2}. \tag{2.39b}$$

The case $\lambda = 0$ occurs when K_4 is unbounded (e.g. when $\Pi(k)$ scales as k^{-6}). We see that the distribution is then an elementary Gaussian. A rough intuitive explanation for this is as follows: The key feature of this limit is that the maxima and minima arise from very rapid oscillations that are superimposed on top of a slowly-varying field. In fact, if K_4 is extremely large, the waves with a short wavelength (large $|\boldsymbol{k}|$) have an amplitude that is small, but not negligible. They therefore create large fluctuations in the gradient of the field and hence a lot of extrema; a fact that can also be seen from eq. (2.34). Meanwhile, the height of the surface at any point (including the abundant minima) is dominated by the waves with a large amplitude, which have long wavelengths (small $|\boldsymbol{k}|$). The location of the minima and the height of the surface are thus roughly *independent*. Therefore, the distribution of the value of H at a minimum is the same as for any other point, namely Gaussian.

Now we consider $\lambda = 1$. From our proof that $\lambda \leq 1$, it is not hard to see that this can only occur when $\Pi(k) = \delta(k - k_0)$ for some constant k_0. This is called a ring spectrum, since the only occurring wave vectors are the ones with $|\boldsymbol{k}| = k_0$, which describes a circle in $\boldsymbol{k}$-space. Inspecting eq. (2.39b) we see that, due to the factor $(1 - \operatorname{sgn} z)$, all minima have a negative value of H, as the simulations also show (see fig. 2.2). The explanation is that height fields with a ring spectrum necessarily satisfy $\nabla^2 H = -k_0^2 H$. Therefore, if H is positive, the mean curvature $H_{xx} + H_{yy} < 0$, so the point cannot be a minimum. In other words, such Gaussian fields are random solutions to Helmholtz's equation; they could represent the height field of a large membrane resonating at a certain frequency, but with some randomness preventing a particular mode among the many at that frequency from stabilizing.

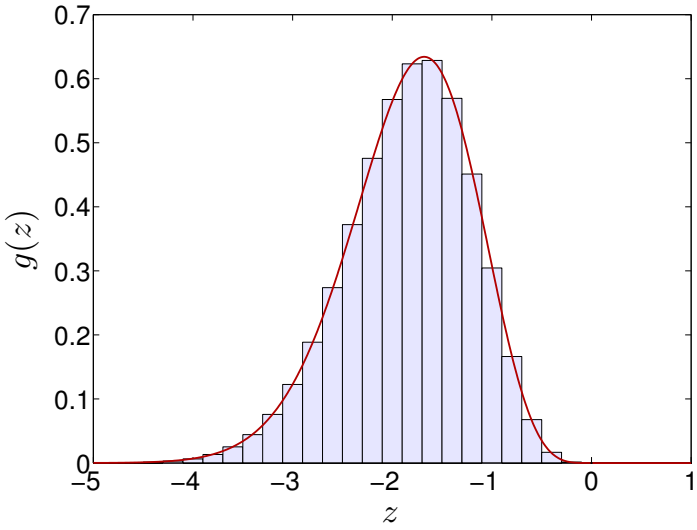

Figure 2.2: Histogram of the values of 10^6 minima obtained from simulations, together with the distribution given by eq. (2.35), for a ring spectrum ($\lambda = 1$). No minima with a positive value of H were found.

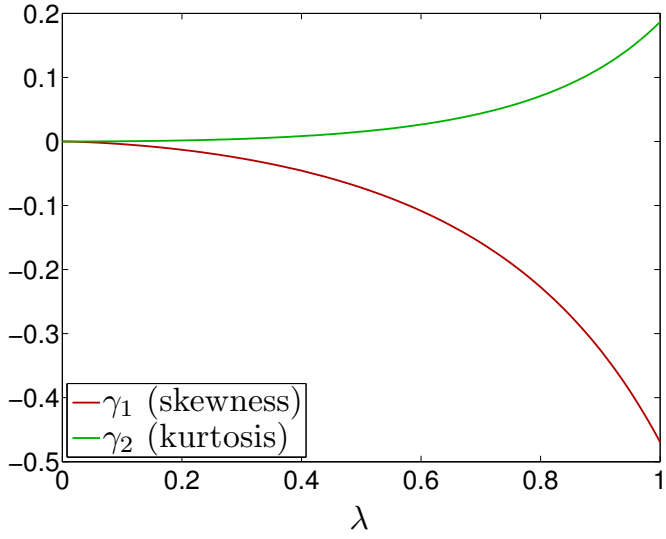

Figure 2.3: The skewness (γ_1) and kurtosis (γ_2) of the distribution (eq. (2.35)) as a function of λ (see eqs. (2.41a) and (2.41b)).

While eq. (2.35) appears quite complex, some of its parameters have more transparent forms. The expectation value μ and standard deviation σ for example are

$$\mu = -4\sqrt{\frac{2}{3\pi}\lambda}, \tag{2.40a}$$

$$\sigma = \sqrt{1 - \frac{32 - (6\sqrt{3} - 2)\pi}{3\pi}\lambda}. \tag{2.40b}$$

When looking at fig. 2.1, it appears that the distribution is itself almost Gaussian. This can be captured in the skewness γ_1 and kurtosis γ_2,

$$\begin{aligned}\gamma_1 \equiv \frac{\mu_3}{\sigma^3} &= -\frac{4\sqrt{2}\Big(64 - (18\sqrt{3} - 11)\pi\Big)}{\Big(3\pi\lambda^{-1} - (32 - (6\sqrt{3} - 2)\pi)\Big)^{3/2}} \\ &= -\frac{3.46}{(9.42\lambda^{-1} - 5.63)^{3/2}},\end{aligned} \tag{2.41a}$$

$$\begin{aligned}\gamma_2 \equiv \frac{\mu_4}{\sigma^4} - 3 &= \frac{4\Big(-1536 + 32(18\sqrt{3} - 11)\pi + 9(2\sqrt{3} - 9)\pi^2\Big)}{\Big(3\pi\lambda^{-1} - (32 - (6\sqrt{3} - 2)\pi)\Big)^2} \\ &= \frac{2.68}{(9.42\lambda^{-1} - 5.63)^2}.\end{aligned} \tag{2.41b}$$

Here μ_n is the n-th moment about the mean: $\mu_n \equiv \langle(\xi - \langle\xi\rangle)^n\rangle$. The skewness is a measure of the symmetry of a distribution around the mean, while the kurtosis gives an indication of its "peakiness". For a Gaussian distribution, both the skewness and the kurtosis are zero. They can therefore be considered as a measure of the Gaussianity of a distribution; note however that a distribution is not necessarily Gaussian if both parameters are zero. The two parameters are shown in fig. 2.3. Naturally, they both go to zero for $\lambda \to 0$.

2.4 MAXIMA AND MINIMA IMBALANCE

Now that we have obtained $g(z)$, we can calculate the relative imbalance between the densities of maxima and minima of $h = F_{NL}(H)$, in accordance with eq. (2.4):

$$\Delta n \equiv \frac{n_{\max} - n_{\min}}{n_{\max} + n_{\min}} = \int_{z:F'_{NL}(z)<0} \mathrm{d}z \Big(g(z) - g(-z)\Big). \tag{2.42}$$

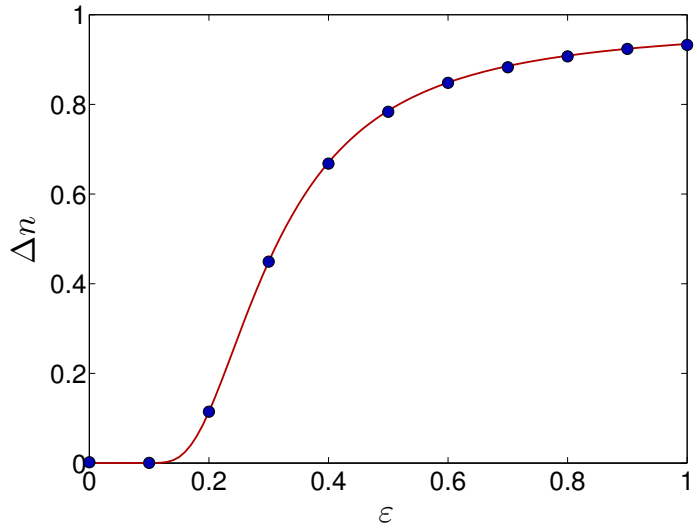

(a)

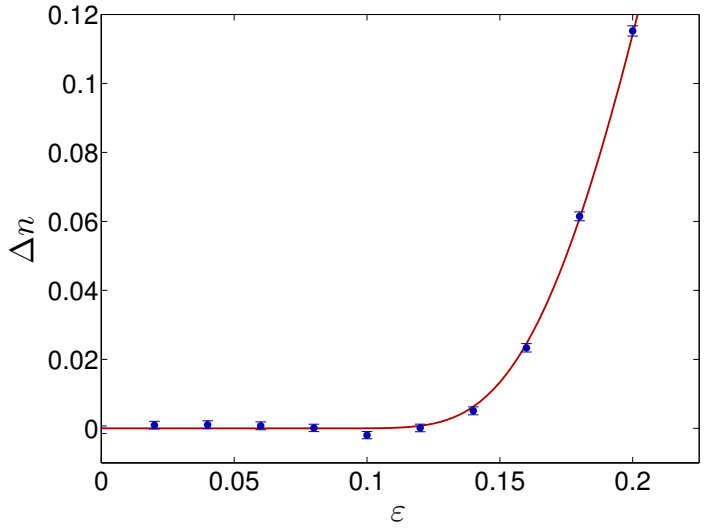

(b)

Figure 2.4: Δn for $h = H + \varepsilon H^2$ as a function of ε, where H has a disk spectrum ($\lambda = \frac{3}{4}$). The data points stem from simulations, the solid curve is eq. (2.42). The two graphs are for different ranges of ε.

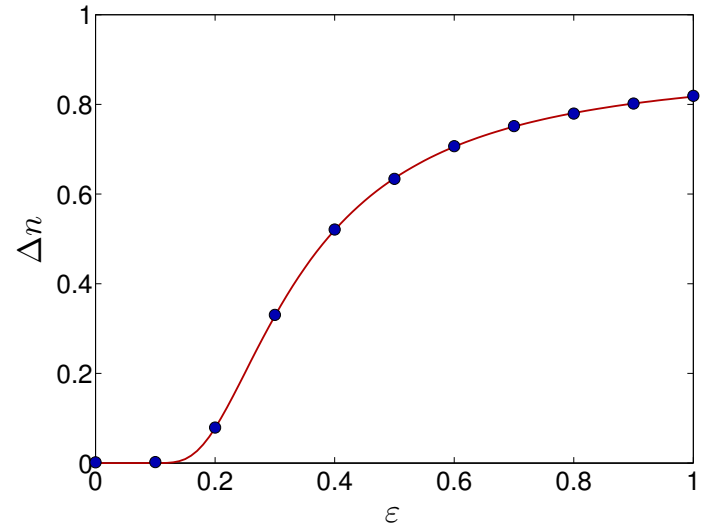

(a)

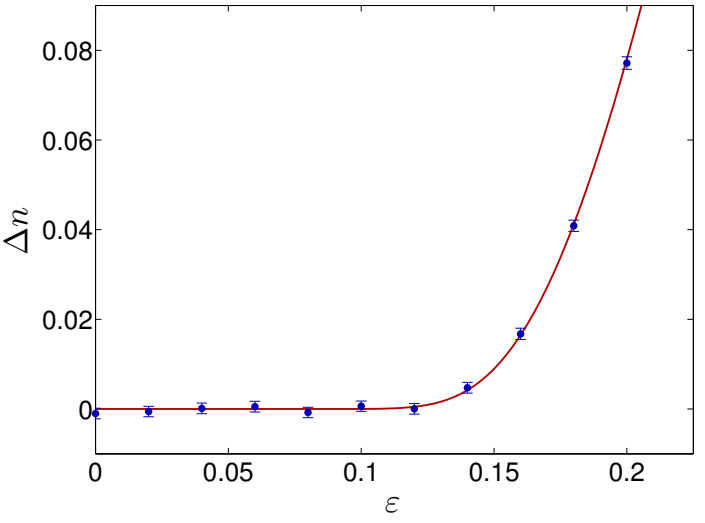

(b)

Figure 2.5: Δn for $h = H + \varepsilon H^2$ as a function of ε, where H has a Gaussian spectrum ($\lambda = \frac{1}{2}$). The data points stem from simulations, the solid curve is eq. (2.42). The two graphs are for different ranges of ε.

The most basic example of a perturbed Gaussian for which we may expect $\Delta n \neq 0$ is $h = H + \varepsilon H^2$. In this case, the domain of integration is $(-\infty, -\frac{1}{2\varepsilon}]$. We have compared eq. (2.42) with results from computer-generated fields, for two different spectra: In fig. 2.4 a so-called disk spectrum was used:

$$A(k)^2 \sim \theta(k_0 - k), \qquad K_{2n} = \frac{k_0^{2n}}{n+1}, \qquad \lambda = \frac{3}{4}. \tag{2.43}$$

Fig. 2.5 features results for a Gaussian spectrum:

$$A(k)^2 \sim \exp(-k^2/2k_0^2), \qquad K_{2n} = 2^n n! k_0^{2n}, \qquad \lambda = \frac{1}{2}. \tag{2.44}$$

In both cases, we see an excellent agreement between the results from the simulations and our theoretical formula.

In both graphs, we see that Δn increases dramatically starting $\varepsilon \approx 0.15$. This can be explained intuitively as follows: The balance in densities of maxima and minima is disturbed by extrema located below $H = -\frac{1}{2\varepsilon}$. Since H is a standard Gaussian, such low values (i.e. large negative values) of H are exponentially rare. It is only when $-\frac{1}{2\varepsilon}$ is in the order of -1 that a significant Δn can be expected. To get a rough estimate for the number of these extrema, we can just look at the density of points with $H = -\frac{1}{2\varepsilon}$ (ignoring the requirement that they be minima does not change the exponential dependence). This is $e^{-1/(8\varepsilon^2)}$. A more careful approximation (see appendix B) gives $\Delta n \sim \sqrt{\frac{3}{2\pi}}\frac{\lambda}{\varepsilon} e^{-1/(8\varepsilon^2)}$.

This argument also applies to the generic case $h = H + \varepsilon f_{NL}(H)$, where f_{NL} designates a perturbation and ε is a parameter controlling the size of the perturbation. Now $\varepsilon f'_{NL}(H)$ needs to be in the order of 1 for Δn to be significantly nonzero. Thus measuring the imbalance between maxima and minima does not give a very sensitive test of the type of non-Gaussianity that we have considered here, in the limit of small ε. However, eq. (2.42) is a nonperturbative result that also holds for large ε.

2.5 CONCLUSIONS

For a random field given by $h(\boldsymbol{r}) = F_{NL}(H(\boldsymbol{r}))$, where H is a Gaussian field and F_{NL} any (nonlinear) function, we find that the densities of maxima and minima of h may differ. We have shown what the imbalance is as a function of the transformation F_{NL} and the power spectrum of H. Our result is exact, and does not rely on perturbation theory, a nice feature since

F_{NL} does not have to be small for our result to apply. This is confirmed by our simulations. On the other hand, the imbalance between maxima and minima is exponentially small when ε is small. Directly measuring the skewness at a given point, for example is much more sensitive to ε when $\varepsilon \ll 1$.

The simple reason is that, when H is of order one, h is a monotonic function of H, and hence it has the same numbers of maxima and minima. Only very large fluctuations in H can lead to an imbalance. Other types of non-Gaussian fields are more likely to have appreciable imbalances between maxima and minima. For example, the nonlinear evolution of a field, such as the height of a surface on which particles are accumulating, could give rise to an imbalance between maxima and minima. The diffusion of the particles for instance might preferentially smooth out maxima.

3

UMBILICAL POINTS OF A NON-GAUSSIAN RANDOM FIELD

In this chapter we stick with local perturbations, but look at the umbilical points instead. As covered in chapter 1, umbilical points come in three types: lemons, monstars and stars. For topological reasons, half of all umbilical points are lemons, for any field. There is no such general constraint for monstars and lemons, but as stated in eq. (1.44), for isotropic Gaussian fields these ratios are fixed as well; they do not depend on the spectrum [4, 11]. Therefore, should, for a given field, the relative density of monstars differ from the requisite 5.3%, one may immediately conclude that the field in question is not an isotropic Gaussian one.

Crucially such a test requires only that the line field corresponding to the principal curvature directions is measurable; the statistics of the scalar height field from which the curvature directions are derived can be probed without being directly observed.

To give an example of a case where the near-Gaussian field of interest is not directly observable, consider the phenomenon of weak gravitational lensing [25]. As stipulated by the theory of general relativity, matter bends spacetime, which also affects light rays. The light from a distant galaxy for instance, does not come to us in a straight line, due to the presence of matter between that galaxy and us. As a result, we see a distorted image of the galaxy. In general, a circular object will look like an ellipse. While most of the matter in the universe is believed to be made up of dark matter which we cannot (yet) detect, the shear field *can* be detected. The near-Gaussian field in this case is obtained by projecting the mass onto the sky, along the lines of sight. This is called the *projected gravitational potential*. On large scales, this field is approximately Gaussian by virtue of the central limit theorem, since the projection involves summing over a lot of regions which are randomly distributed. On smaller scales however,

interactions can give rise to non-Gaussian contributions. If we interpret the projected gravitational potential as a (near-Gaussian) surface, then the shear direction corresponds to the principal direction of this surface [45]. In terms of the shear field, the umbilical points correspond to points in the sky where a circular light source still appears circular.

Another example of a physical process in which umbilical points can prove their usefulness is in the context of optical speckle fields. These fields arise for example when a coherent beam of light scatters from a rough surface. Since the many reflected waves become superimposed, this produces a random pattern of intensity with approximately Gaussian statistics. In this case, it is the points of circular polarization that can be identified as umbilical points. The relative densities of the various types of umbilical points have been found to match the theoretical predictions in experiments [15]. Other contexts in which umbilical points can offer a window for non-Gaussianity include polarization singularities in the cosmic microwave background [12, 28, 41, 44], topological defects in a nematic [14, 27] and a superfluid near criticality [23, 33].

Here, we will again study by how much the monstar fraction changes, in relation to the applied perturbation. Unlike the previous chapter, the locality of the perturbation does not keep the umbilical points in place, so a method similar to the one presented there is not available. Instead, we assume the perturbation to be small and determine the changes in the monstar fraction up to first order.

The outline of this chapter is as follows. In sections 3.1 through 3.4 the various steps and concepts that are needed for this calculation are explained, before the final result is arrived at in section 3.5. The theoretical result is then compared to results from computer simulations in section 3.6. Finally, section 3.7 provides a summary and conclusions.

3.1 THE GENERATING FUNCTION

We consider a field of the form $h(\boldsymbol{r}) = H(\boldsymbol{r}) + f(H(\boldsymbol{r}))$, where $H(\boldsymbol{r})$ is a Gaussian field and f a small nonlinear function of $H(\boldsymbol{r})$ only. As we have seen in eqs. (1.33), (1.37) and (1.39), the monstars can be defined using the second and third derivatives of the field h with respect to x and y. Determining the monstar fraction thus boils down to determining how likely it is that at a specific point $\boldsymbol{r}$ the third derivatives $\alpha = h_{xxx}(\boldsymbol{r})$, $\beta = h_{xxy}(\boldsymbol{r})$, $\gamma = h_{xyy}(\boldsymbol{r})$ and $\delta = h_{yyy}(\boldsymbol{r})$ are such that eqs. (1.37) and

(1.39) prescribe a monstar, given that the second derivatives obey $h_{xx}(\boldsymbol{r}) = h_{yy}(\boldsymbol{r})$ and $h_{xy}(\boldsymbol{r}) = 0$.

In order to determine this, we require the joint probability distribution of these seven stochastic variables. When we have this, we can set $h_{xx} = h_{yy}$ and $h_{xy} = 0$ and integrate α, β, γ and δ over the appropriate ranges to get the density of monstars and all umbilical points respectively. The ratio of these then gives the monstar fraction.

We shall arrive at the desired probability distribution by determining the corresponding generating function, which is defined as the Fourier transform of the probability distribution [31]. For a set of n correlated variables $\{h_i\}$ this is

$$\begin{aligned}\chi(\lambda_1, \ldots, \lambda_n) &= \int \mathrm{d}h_1 \ldots \mathrm{d}h_n \, p(h_1, \ldots, h_n) e^{i(h_1\lambda_1 + \ldots + h_n\lambda_n)} \\ &= 1 + i\sum_j \langle h_j \rangle \lambda_j + \frac{i^2}{2!} \sum_{j_1, j_2} \langle h_{j_1} h_{j_2} \rangle \lambda_{j_1} \lambda_{j_2} \\ &\quad + \frac{i^3}{3!} \sum_{j_1, j_2, j_3} \langle h_{j_1} h_{j_2} h_{j_3} \rangle \lambda_{j_1} \lambda_{j_2} \lambda_{j_3} + \ldots \end{aligned} \tag{3.1}$$

Here, the coefficients $\langle \ldots \rangle$ are the *moments*, or multivariable correlations defined by

$$\langle h_{j_1} \ldots h_{j_k} \rangle \equiv \int \mathrm{d}h_1 \ldots \mathrm{d}h_n \, p(h_1, \ldots, h_n) h_{j_1} \ldots h_{j_k}. \tag{3.2}$$

Eq. (3.1) is proved by expanding the exponential term by term.

Upon taking the logarithm of χ and expanding, the quantities known as the *cumulants* are revealed:

$$\begin{aligned}\log \chi &= i\sum_j C_1(h_j)\lambda_j + \frac{i^2}{2!} \sum_{j_1, j_2} C_2(h_{j_1}, h_{j_2}) \lambda_{j_1} \lambda_{j_2} \\ &\quad + \frac{i^3}{3!} \sum_{j_1, j_2, j_3} C_3(h_{j_1}, h_{j_2}, h_{j_3}) \lambda_{j_1} \lambda_{j_2} \lambda_{j_3} + \ldots \end{aligned} \tag{3.3}$$

The cumulants can be written in terms of the moments, as can be seen by taking the logarithm of eq. (3.1) and expanding it. For example,

$$\begin{aligned}C(h_1, h_2, h_3) &= \langle h_1 h_2 h_3 \rangle - \langle h_1 \rangle \langle h_2 h_3 \rangle - \langle h_2 \rangle \langle h_3 h_1 \rangle \\ &\quad - \langle h_3 \rangle \langle h_1 h_2 \rangle + 2\langle h_1 \rangle \langle h_2 \rangle \langle h_3 \rangle. \end{aligned} \tag{3.4}$$

In reverse, the moments can be written in terms of the cumulants, e.g.

$$\begin{aligned}\langle h_1 h_2 h_3\rangle = {} & C(h_1,h_2,h_3) + C(h_1)C(h_2,h_3) + C(h_2)C(h_3,h_1) \\ & + C(h_3)C(h_1,h_2) + C(h_1)C(h_2)C(h_3). \end{aligned} \tag{3.5}$$

If all the moments or all the cumulants are known, we can construct the generating function and perform an inverse Fourier transformation to obtain the probability distribution.

The defining characteristic of Gaussian random variables H_i is that all cumulants are zero, with the exception of the second-order ones $C_2(H_i, H_j) = \langle H_i H_j\rangle$. In this case, the generating function is thus

$$\chi(\lambda_1,\ldots,\lambda_n) = \exp\left(-\tfrac{1}{2}\sum_{ij} C_2(H_i,H_j)\lambda_i\lambda_j\right). \tag{3.6}$$

The inverse Fourier transformation yields the standard distribution for correlated Gaussian random variables,

$$p(H_1,\ldots,H_n) = \frac{1}{(2\pi)^{n/2}\sqrt{\det\sigma}} \exp\left(-\tfrac{1}{2}\sum_{i,j}(\sigma^{-1})_{ij} H_i H_j\right), \tag{3.7}$$

where σ is the matrix of correlations, $\sigma_{ij} = \langle H_i H_j\rangle$. This we already encountered in eq. (2.8).

For a Gaussian field H, the derivatives are themselves also Gaussian fields; the above formula therefore gives their joint distribution (see section 2.3). For the non-Gaussian field h, there are some small corrections to this distribution. To find these corrections to first order, we need to determine the cumulants to first order in $f(H)$. We will see that only a small number of cumulants are nonzero up to this order. Before we proceed to derive them, we switch to a complex coordinate system which allows for optimal usage of translational and rotational symmetry, which h has inherited from H for the type of perturbations under consideration.

3.2 COMPLEX COORDINATES REPRESENTATION

To find the distribution of umbilical points, we now have to find the joint distribution of the seven second and third derivatives of h. All these variables can be combined into a more compact form by using complex coordinates. These will make it easier to evaluate the integral that determines the monstar density, and will help us to work out the probability distribution with the help of symmetry.

The complex coordinates are given by

$$\begin{aligned} z &= x + iy, \qquad & x &= \tfrac{1}{2}(z + z^*), \\ z^* &= x - iy, \qquad & y &= \tfrac{1}{2}i(z^* - z). \end{aligned} \tag{3.8}$$

Of course, as complex numbers, z and z^* are not independent; however we can formally define partial derivatives with respect to each of them, using the chain rule, just like we could if this transformation involved a real number instead of i.

The derivatives with respect to z and z^* are given by

$$\frac{\partial}{\partial z} = \tfrac{1}{2}\frac{\partial}{\partial x} - \tfrac{1}{2}i\frac{\partial}{\partial y}, \qquad \frac{\partial}{\partial z^*} = \tfrac{1}{2}\frac{\partial}{\partial x} + \tfrac{1}{2}i\frac{\partial}{\partial y}. \tag{3.9}$$

We see that the derivatives with respect to z and z^* are each other's conjugate, but again, we consider both to be linear transformations of ∂_x and ∂_y.

The usefulness of using z and z^* can be immediately seen from h_{zz}:

$$h_{zz} = \partial_z^2 h = \tfrac{1}{4}(\partial_x - i\partial_y)^2 h = \tfrac{1}{4}(h_{xx} - h_{yy} + 2ih_{xy}). \tag{3.10}$$

We see that the definition of an umbilical point can be captured in one equation: $h_{zz} = 0$.

The various types of umbilical points were defined in eqs. (1.37) and (1.39) using the "normal" third derivatives $h_{xxx} = \alpha$, $h_{xxy} = \beta$, $h_{xyy} = \gamma$ and $h_{yyy} = \delta$. In terms of h_{zzz}, h_{zzz^*}, $h_{zz^*z^*}$ and $h_{z^*z^*z^*}$ the two conditions for a monstar become

$$|h_{zzz^*}|^2 - |h_{zzz}|^2 > 0, \tag{3.11a}$$

$$\begin{aligned} 27|h_{zzz}|^4 - |h_{zzz^*}|^4 - 18|h_{zzz}|^2|h_{zzz^*}|^2 \\ - 4(h_{zzz}h_{zz^*z^*}^3 + h_{z^*z^*z^*}h_{zzz^*}^3) > 0. \end{aligned} \tag{3.11b}$$

Here $|h_{zzz}|^2$ and $|h_{zzz^*}|^2$ represent $h_{zzz}h_{z^*z^*z^*}$ and $h_{zzz^*}h_{zz^*z^*}$ respectively.

The density of monstars will be given by integrating the probability distribution $p(h_{zz} = 0, h_{zzz}, h_{zzz^*})$ over the range defined by these conditions. This probability distribution is determined by the cumulants of combinations of the three variables. Rotational and translational symmetry however imply that only a small number of these combinations yield a nonzero cumulant.

First, consider the consequences of the isotropy (rotational symmetry) of the field $h(\boldsymbol{r})$ for a moment like $\langle h_{z^*}(\boldsymbol{r})h_{zz}(\boldsymbol{r})\rangle$. Note that, due to homogeneity (translational symmetry), this moment does not depend on r; it will

often be dropped from now on. Isotropy implies that this moment should not change if we rotate the field around $\boldsymbol{r}$, over any angle α. In terms of z and z^*, this results in the transformation

$$\begin{aligned} z' &= e^{i\alpha} z, & \partial_{z'} &= e^{-i\alpha} \partial_z, \\ z'^* &= e^{-i\alpha} z^*, & \partial_{z'^*} &= e^{i\alpha} \partial_{z^*}. \end{aligned} \tag{3.12}$$

As a result, we get $\langle h_{z'} h_{z'^* z'^*} \rangle = e^{i\alpha} \langle h_z h_{z^* z^*} \rangle$. Since we argued that the two expectation values must be equal, for any α, we must have $\langle h_{z^*} h_{zz} \rangle = 0$.

In general, following a rotation, expectation values pick up a factor $e^{ik\alpha}$, where k is the number of z^* derivatives inside the bracket minus the number of z derivatives. By the above argument, the expectation value is zero when $k \neq 0$. Therefore, an expectation value can only be nonzero if the numbers of z and z^* derivatives inside the bracket are equal. Since a cumulant is a sum of products of expectation values, featuring every variable once in every product (compare eq. (3.4)), the same property applies to cumulants.

The homogeneity (translational symmetry) of the fields under consideration provides another useful trick that relates different cumulants to one another. As already stated, a moment like $\langle h_1(\boldsymbol{r}) \dots h_n(\boldsymbol{r}) \rangle$ does not depend on $\boldsymbol{r}$. Hence the derivative of this with respect to z or z^* is zero. Applying the product rule gives

$$\begin{aligned} 0 &= \partial_z \langle h_1 \dots h_n \rangle \\ &= \langle (\partial_z h_1) h_2 \dots h_n \rangle + \dots + \langle h_1 h_2 \dots (\partial_z h_n) \rangle. \end{aligned} \tag{3.13}$$

For $n = 2$, this gives the useful relation

$$\langle (\partial_z h_1) h_2 \rangle = -\langle h_1 (\partial_z h_2) \rangle. \tag{3.14}$$

In essence, for a two-point correlation it is possible to "transfer" a z derivative from the one term to the other at the cost of an overall minus sign (reminiscent of integration by parts when the boundary term is zero). The same applies of course to a z^* derivative. For example, we find the relation $\langle h_{zz} h_{z^* z^*} \rangle = -\langle h_z h_{zz^* z^*} \rangle$.

Together, these two symmetries put constraints on the probability distribution $p(h_{zz}, h_{zzz}, h_{zzz^*})$. In particular, they explain why the monstar fraction is always the same for any Gaussian distribution [4]: A Gaussian distribution does not have many degrees of freedom to start with; only the two-point correlations between the variables are adjustable. In this case, the two-point correlations between any two of these variables is zero, by

rotational symmetry, while the variances of h_{zzz} and h_{zzz^*} are equal by translational symmetry. Hence (after setting $h_{zz} = 0$ to identify the umbilical points), the distribution $p(h_{zz} = 0, h_{zzz}, h_{zzz^*})$ is always the same apart from a scale, and that determines the monstar fraction. This argument can be generalized to singularities in the polarization field of light (even though the field might not be derived from a scalar field h), and so Gaussian polarization fields have the same monstar fraction as well, as shown in [11].

On the other hand, when h has non-Gaussian contributions, there are many more cumulants, and symmetry is not enough to constrain them anymore. For the field $h = H + f(H)$ we are studying, we proceed to calculate the cumulants explicitly.

3.3 THE CUMULANTS

Although the problem is now cast in terms of complex derivatives, the recipe outlined in section 3.1 still applies. The task is to determine the cumulants of h_{zz}, h_{zzz}, h_{zzz^*} and their conjugates up to first order in the perturbation f.

These cumulants have the general form $C_n(D_1 h, \dots, D_n h)$, where each D_j represents a number of z and z^* derivatives. For the moment, let us consider each $D_j h$ to be at a different point $\boldsymbol{r_j}$, i.e. $C_n(D_1 h(\boldsymbol{r_1}), \dots, D_n h(\boldsymbol{r_n}))$. Later we will set all points equal again. For convenience, we shall drop the vector notation, i.e. $r_i = \boldsymbol{r_i}$. Since now each derivative D_j acts only at a specific point, we can bring them outside the cumulant:

$$\begin{aligned} &C_n(D_1 h, \dots, D_n h) \\ &\quad = D_1 \dots D_n C_n(h(r_1), \dots, h(r_n))\Big|_{r_1 = \dots = r_n}. \end{aligned} \tag{3.15}$$

Let us write $h(r_j) = h_j$ for shortness, and focus on $C_n(h_1, \dots, h_n)$. Inserting $h_j = H_j + f(H_j)$, expanding the cumulant and keeping only terms up to first order in f yields

$$\begin{aligned} C_n(h_1, \dots, h_n) = C_n(&H_1, \dots, H_n) \\ &+ C_n(f(H_1), H_2, \dots, H_n) \\ &+ C_n(H_1, f(H_2), \dots, H_n) \\ &+ \dots + C_n(H_1, H_2, \dots, f(H_n)). \end{aligned} \tag{3.16}$$

The first term on the right-hand side is now simply the cumulant of a set of Gaussian random variables, which, as discussed before, is zero for $n > 2$. The other terms can be evaluated perturbatively and are equivalent to each other. Consider the second term as an example. For a cumulant involving Gaussian variables and one function of a Gaussian we have (see appendix C)

$$\begin{aligned} &C_n(f(H_1), H_2, \ldots, H_n) \\ &\quad = \langle f^{(n-1)}(H_1)\rangle \langle H_1 H_2\rangle \langle H_1 H_3\rangle \ldots \langle H_1 H_n\rangle. \end{aligned} \tag{3.17}$$

When we reinsert the derivatives D_2 through D_n from eq. (3.15) and set $r_2 = \ldots = r_n = r$ we get

$$\begin{aligned} &D_1 \ldots D_n C_n(f(H(r_1)), \ldots, H(r_n))\Big|_{r_1=\ldots=r_n} \\ &\quad = D_1 \langle f^{(n-1)}(H_1)\rangle \langle H_1 D_2 H\rangle \ldots \langle H_1 D_n H\rangle\Big|_{r_1=r}. \end{aligned} \tag{3.18}$$

Now we can reinsert D_1 and then set $r_1 = r$, as prescribed by eq. (3.15). Remember that D_1 only acts on H_1. Due to the product rule, we have to consider all possible ways in which the derivatives in D_1 can be distributed over all H_1's. Recall from section 3.2 that, after setting $r_1 = r$, each expectation value can only be nonzero if the number of z and z^* derivatives inside are equal. Note also that $\langle f^{(n-1)}(H_1)\rangle$ does not depend on r_1, hence any derivative of it is zero. Therefore, the only nonzero contributions stemming from the product rule are those distributions that make the number of z and z^* derivatives equal inside each bracket.

We consider the cumulant $C_3(h_{zz}, h_{zz^*z^*}, h_{zz^*z^*})$ as an example to demonstrate the procedure. First, we find

$$\begin{aligned} &C_3(h_{zz}, h_{zz^*z^*}, h_{zz^*z^*}) \\ &\quad = C_3(H_{zz}, H_{zz^*z^*}, H_{zz^*z^*}) \\ &\qquad + \partial_{z_1 z_1}(\langle f''(H)\rangle \langle H_1 H_{zz^*z^*}\rangle \langle H_1 H_{zz^*z^*}\rangle) \\ &\qquad + 2\partial_{z_2 z_2^* z_2^*}(\langle f''(H)\rangle \langle H_2 H_{zz}\rangle \langle H_2 H_{zz^*z^*}\rangle). \end{aligned} \tag{3.19}$$

The first term is zero, since all cumulants of Gaussian variables are zero beyond second order. For the second term, we need to consider how to distribute the two ∂_{z_1} derivatives to make all expectation values nonzero. The only possibility is to put one ∂_{z_1} in front of each H_1. Note however that

this term appears twice in the product rule, because there are two ways of distributing the two derivatives. After setting $r_1 = r$ we thus have

$$\begin{aligned}&\partial_{z_1 z_1}(\langle f''(H)\rangle\langle H_1 H_{zz^*z^*}\rangle\langle H_1 H_{zz^*z^*}\rangle)\\&\quad = 2\langle f''(H)\rangle\langle H_z H_{zz^*z^*}\rangle^2.\end{aligned} \tag{3.20}$$

In the third term on the right-hand side of eq. (3.19) we have one ∂_z and two ∂_{z^*}'s to distribute. The first H_2 needs $\partial_{z^*z^*}$ to balance the derivatives and the other takes the ∂_z derivative. There are no multiple ways to distribute these derivatives in this case and therefore

$$\begin{aligned}&\partial_{z_2 z_2^* z_2^*}(\langle f''(H)\rangle\langle H_2 H_{zz}\rangle\langle H_2 H_{zz^*z^*}\rangle)\\&\quad = \langle f''(H)\rangle\langle H_{z^*z^*} H_{zz}\rangle\langle H_z H_{zz^*z^*}\rangle.\end{aligned} \tag{3.21}$$

Combining everything together results in

$$\begin{aligned}&C_3(h_{zz}, h_{zz^*z^*}, h_{zz^*z^*})\\&\quad = 2\langle f''(H)\rangle\langle H_z H_{zz^*z^*}\rangle(\langle H_z H_{zz^*z^*}\rangle + \langle H_{z^*z^*} H_{zz}\rangle).\end{aligned} \tag{3.22}$$

Finally, due to translational symmetry, we have

$$\langle H_z H_{zz^*z^*}\rangle + \langle H_{z^*z^*} H_{zz}\rangle = \partial_z\langle H_z H_{z^*z^*}\rangle = 0. \tag{3.23}$$

We thus find that $C_3(h_{zz}, h_{zz^*z^*}, h_{zz^*z^*}) = 0$.

Now we will show that there are only a finite number of nonzero cumulants (up to first order in f). In fact, there are none beyond the fourth order. Consider eq. (3.16) with $n > 4$. The first term (zero order) is zero because it is the cumulant of more than two Gaussian variables. For the other ones we apply the recipe of eq. (3.18). We have $n-1$ brackets in which the z and z^* derivatives need to be matched. Since we are only considering the variables h_{zz}, h_{zzz}, h_{zzz^*} and their conjugates, each one has a mismatch to begin with. However, since D_1 has only three derivatives at most, it is not possible to balance the derivatives in all $n-1$ brackets.

This "lack of derivatives" also kills a lot of cumulants of lower order, especially fourth order. For example, in $C_4(h_{zz}, h_{z^*z^*}, h_{zzz^*}, h_{zz^*z^*})$ the first two variables require two derivatives to balance the derivatives and the other two require one. Therefore, no matter from which variable the derivatives are distributed, there is always a shortage.

These are all the nonzero cumulants (the two asymmetric ones have a conjugate twin in which all z's and z^*'s are interchanged):

$$\begin{aligned}
C_2(h_{zz}, h_{z^*z^*}) &= \sigma(1 + 2\langle f'(H)\rangle), && \text{(3.24a)}\\
C_2(h_{zzz}, h_{z^*z^*z^*}) &= \tau(1 + 2\langle f'(H)\rangle), && \text{(3.24b)}\\
C_2(h_{zzz^*}, h_{zz^*z^*}) &= \tau(1 + 2\langle f'(H)\rangle), && \text{(3.24c)}\\
C_3(h_{zz}, h_{zzz^*}, h_{z^*z^*z^*}) + conj. &= -3\sigma^2\langle f''(H)\rangle, && \text{(3.24d)}\\
C_4(h_{zzz^*}, h_{zzz^*}, h_{zz^*z^*}, h_{zz^*z^*}) &= -8\sigma^3\langle f'''(H)\rangle, && \text{(3.24e)}\\
C_4(h_{zzz}, h_{zz^*z^*}, h_{zz^*z^*}, h_{zz^*z^*}) + conj. &= -6\sigma^3\langle f'''(H)\rangle, && \text{(3.24f)}
\end{aligned}$$

where

$$\begin{aligned}
\sigma &\equiv \langle H_{zz}H_{z^*z^*}\rangle = -\langle H_z H_{zz^*z^*}\rangle, && \text{(3.25a)}\\
\tau &\equiv \langle H_{zzz}H_{z^*z^*z^*}\rangle = \langle H_{zzz^*}H_{zz^*z^*}\rangle. && \text{(3.25b)}
\end{aligned}$$

Note that the trick based on translational symmetry was used to equate the expectation values. In the second equation, it was used twice (transferring a ∂_z one way and a ∂_{z^*} the other way).

The parameters σ and τ are related to the moments K_n of H. This is most easily seen by writing H in complex variables:

$$\begin{aligned}
H &= \sum_{\boldsymbol{k}} A(k)\cos(\boldsymbol{k}\cdot\boldsymbol{r} + \phi_{\boldsymbol{k}})\\
&= \sum_{k} A(|k|)\cos\left(\tfrac{1}{2}(k^*z + kz^*) + \phi_k\right). && \text{(3.26)}
\end{aligned}$$

Here $k = k_x + ik_y$ is the complex analogue of $\boldsymbol{k} = \binom{k_x}{k_y}$. With this we find

$$\begin{aligned}
H_{zzz} &= \sum_{k} A(k)\tfrac{1}{8}(k^*)^3\sin\left(\tfrac{1}{2}(k^*z + kz^*) + \phi_k\right), && \text{(3.27a)}\\
H_{z^*z^*z^*} &= \sum_{k} A(k)\tfrac{1}{8}k^3\sin\left(\tfrac{1}{2}(k^*z + kz^*) + \phi_k\right). && \text{(3.27b)}
\end{aligned}$$

Hence:

$$\tau = \langle H_{zzz}H_{z^*z^*z^*}\rangle = \langle \tfrac{1}{8}(k^*)^3\tfrac{1}{8}k^3\rangle = \tfrac{1}{64}K_6. \qquad \text{(3.28)}$$

Similarly, we have $\sigma = \frac{1}{16}K_4$.

3.4 PROBABILITY DISTRIBUTION

With the aid of the cumulants we can build the logarithm of the generating function (see eq. (3.3)), provided that we identify the appropriate variables in Fourier space. Consider h_{zz} and $h_{z^*z^*}$ for example. These complex variables represent two real variables ξ_x and ξ_y, the real and imaginary part of h_{zz}. Let λ_x and λ_y be their Fourier counterparts. The generating function is

$$\begin{aligned}\chi(\lambda_x, \lambda_y, \ldots) &= \int \mathrm{d}\xi_x \mathrm{d}\xi_y \ldots \, p(\xi_x, \xi_y, \ldots) e^{i(\xi_x\lambda_x + \xi_y\lambda_y + \ldots)} \\ &= \langle e^{i(\xi_x\lambda_x + \xi_y\lambda_y + \ldots)} \rangle. \end{aligned} \tag{3.29}$$

The exponent can be written in terms of the complex variables,

$$\xi_x\lambda_x + \xi_y\lambda_y = h_{zz}\lambda^*_{zz} + h_{z^*z^*}\lambda_{zz}, \tag{3.30}$$

where we define $\lambda_{zz} = \frac{1}{2}(\lambda_x + i\lambda_y)$. Then λ_{zz} is the complex Fourier variable corresponding to $h_{z^*z^*}$ and we likewise introduce λ_{zzz} and λ_{zzz^*}, which are conjugate to $h_{z^*z^*z^*}$ and $h_{zz^*z^*}$. We will define integrals with respect to the complex Fourier variables, e.g. with respect to d^2h_{zz}, as integrals over the real and imaginary parts of h_{zz}, and the inverse Fourier transform will be performed by integrating over the real and imaginary parts of the λ's.

The generating function is thus

$$\begin{aligned}\log\chi = &- C_2(h_{zz}, h_{z^*z^*})\lambda_{z^*z^*}\lambda_{zz} \\ &- C_2(h_{zzz}, h_{z^*z^*z^*})\lambda_{z^*z^*z^*}\lambda_{zzz} \\ &- C_2(h_{zzz^*}, h_{zz^*z^*})\lambda_{zz^*z^*}\lambda_{zzz^*} \\ &- iC_3(h_{zz}, h_{zzz^*}, h_{z^*z^*z^*})\lambda_{z^*z^*}\lambda_{zz^*z^*}\lambda_{zzz} \\ &- iC_3(h_{zz}, h_{zzz^*}, h_{z^*z^*z^*})\lambda_{zz}\lambda_{zzz^*}\lambda_{z^*z^*z^*} \\ &+ \tfrac{1}{4}C_4(h_{zzz^*}, h_{zzz^*}, h_{zz^*z^*}, h_{zz^*z^*})\lambda^2_{zz^*z^*}\lambda^2_{zzz^*} \\ &+ \tfrac{1}{6}C_4(h_{zzz}, h_{zz^*z^*}, h_{zz^*z^*}, h_{zz^*z^*})\lambda_{z^*z^*z^*}\lambda^3_{zzz^*} \\ &+ \tfrac{1}{6}C_4(h_{zzz}, h_{zz^*z^*}, h_{zz^*z^*}, h_{zz^*z^*})\lambda_{zzz}\lambda^3_{zz^*z^*}. \end{aligned} \tag{3.31}$$

Upon entering the cumulants from eq. (3.24):

$$\begin{aligned}\log\chi = &-\tilde{\sigma}\lambda_{zz}\lambda_{z^*z^*} - \tilde{\tau}(\lambda_{zzz}\lambda_{z^*z^*z^*} + \lambda_{zzz^*}\lambda_{zz^*z^*}) \\ &+ 3i\sigma^2\langle f''(H)\rangle(\lambda_{zz}\lambda_{zzz^*}\lambda_{z^*z^*z^*} + \lambda_{z^*z^*}\lambda_{zz^*z^*}\lambda_{zzz}) \\ &- \sigma^3\langle f'''(H)\rangle(2\lambda^2_{zzz^*}\lambda^2_{zz^*z^*} + \lambda_{zzz}\lambda^3_{zz^*z^*} \\ &\qquad + \lambda_{z^*z^*z^*}\lambda^3_{zzz^*}). \end{aligned} \tag{3.32}$$

Here $\tilde{\sigma} = \sigma(1 + 2\langle f'(H)\rangle)$ and $\tilde{\tau} = \tau(1 + 2\langle f'(H)\rangle)$ have been introduced. Note that some cumulants appear multiple times in eq. (3.3) since the λ's can be permuted (if they are not all the same). The factors in front of the cumulants are the factor $i^k/k!$ in eq. (3.3) multiplied by the number of distinct permutations of the λ's.

To obtain the probability distribution, we take the exponential and perform the inverse Fourier transformation (see eq. (3.1)). This gives an integral over the exponential of a polynomial of degree 4. However, all terms of degree three and four are of order f, so we can expand the exponential and be left with only square terms in the exponent. The result is

$$\begin{aligned}\chi = \exp\Big(&-\tilde{\sigma}\lambda_{zz}\lambda_{z^*z^*} - \tilde{\tau}(\lambda_{zzz}\lambda_{z^*z^*z^*} + \lambda_{zzz^*}\lambda_{zz^*z^*})\Big)\\ &\times\Big(1 + 3i\sigma^2\langle f''(H)\rangle(\lambda_{zz}\lambda_{zzz^*}\lambda_{z^*z^*z^*} + \lambda_{z^*z^*}\lambda_{zz^*z^*}\lambda_{zzz})\\ &\quad - \sigma^3\langle f'''(H)\rangle(2\lambda^2_{zzz^*}\lambda^2_{zz^*z^*} + \lambda_{zzz}\lambda^3_{zz^*z^*}\\ &\qquad + \lambda_{z^*z^*z^*}\lambda^3_{zzz^*})\Big).\end{aligned} \tag{3.33}$$

Now we can take the inverse Fourier transform. Note that λ_{zz} and $\lambda_{z^*z^*}$ are each other's conjugate. Upon integrating the real and imaginary parts of λ_{zz} and imposing $\lambda_{z^*z^*} = \lambda^*_{zz}$ (the same procedure applies to the other two pairs of λ's), one obtains

$$\begin{aligned}&p(h_{zz}, h_{z^*z^*}, h_{zzz}, h_{z^*z^*z^*}, h_{zzz^*}, h_{zz^*z^*})\\ &\quad= \int \frac{\mathrm{d}^2\lambda_{zz}\mathrm{d}^2\lambda_{zzz}\mathrm{d}^2\lambda_{zzz^*}}{\pi^6}\,\chi\\ &\qquad\times e^{-i(\lambda_{zz}h_{zz} + \lambda_{zzz}h_{zzz} + \lambda_{zzz^*}h_{zzz^*} + \text{conj.})}.\end{aligned} \tag{3.34}$$

Note that the denominator is π^6 rather than $(2\pi)^6$ because of the factor of $\frac{1}{2}$ in the definitions of the λ's (see eq. (3.30)).

The Fourier transform of a Gaussian function multiplied by a polynomial is easy to perform by noting that multiplying by λ in Fourier space is equivalent to taking a derivative in normal space:

$$\int \mathrm{d}\lambda\, \lambda^n f(\lambda) e^{-i\lambda h} = \left(i\frac{\partial}{\partial h}\right)^n \int \mathrm{d}\lambda\, f(\lambda) e^{-i\lambda h}. \tag{3.35}$$

The inverse Fourier transform of the Gaussian part of the generating function is

$$\int \frac{\mathrm{d}^2\lambda_{zz}\mathrm{d}^2\lambda_{zzz}\mathrm{d}^2\lambda_{zzz^*}}{\pi^6} e^{-\tilde{\sigma}|\lambda_{zz}|^2-\tilde{\tau}(|\lambda_{zzz}|^2+|\lambda_{zzz^*}|^2)} e^{-i(\ldots)}$$
$$= \frac{1}{\pi^3\tilde{\sigma}\tilde{\tau}^2}\exp\left(-\frac{1}{\tilde{\sigma}}|h_{zz}|^2 - \frac{1}{\tilde{\tau}}(|h_{zzz}|^2+|h_{zzz^*}|^2)\right), \tag{3.36}$$

and the final result reads

$$p(h_{zz}, h_{z^*z^*}, h_{zzz}, h_{z^*z^*z^*}, h_{zzz^*}, h_{zz^*z^*})$$
$$= \left[1 - 3\sigma^2\langle f''(H)\rangle\frac{1}{\tilde{\sigma}\tilde{\tau}^2}\Big(2\Re(h_{z^*z^*}h_{zz^*z^*}h_{zzz})\Big)\right.$$
$$\left. - \sigma^3\langle f'''(H)\rangle\left(\frac{4}{\tilde{\tau}^2} - \frac{8|h_{zzz^*}|^2}{\tilde{\tau}^3} + \frac{2|h_{zzz^*}|^4 + 2\Re(h_{zzz}h^3_{zz^*z^*})}{\tilde{\tau}^4}\right)\right]$$
$$\times \frac{1}{\pi^3\tilde{\sigma}\tilde{\tau}^2}\exp\left(-\frac{|h_{zz}|^2}{\tilde{\sigma}} - \frac{|h_{zzz}|^2+|h_{zzz^*}|^2}{\tilde{\tau}}\right). \tag{3.37}$$

3.5 MONSTAR FRACTION

Once the joint probability distribution of the relevant derivatives is obtained, we can set $h_{zz} = h_{z^*z^*} = 0$, which defines an umbilical point. However, as we also saw in section 2.3, we still need another ingredient: The joint probability distribution states how likely it is that h_{zz} and $h_{z^*z^*}$ are *close* to zero for a *certain* point $\boldsymbol{r}$. What we need however is for h_{zz} and $h_{z^*z^*}$ to be *exactly* zero for a point *close* to $\boldsymbol{r}$, since we are looking for a density with respect to the (x, y)-plane. For this, we need to go from a probability density with respect to h_{zz} and $h_{z^*z^*}$ to one with respect to z and z^*. This is accomplished by multiplying p by the Jacobian

$$J = \left|\frac{\partial(h_{zz}, h_{z^*z^*})}{\partial(z, z^*)}\right| = \Big||h_{zzz}|^2 - |h_{zzz^*}|^2\Big|. \tag{3.38}$$

The last step is to integrate this product over h_{zzz} and h_{zzz^*}, either over all possible values, or just over those satisfying eq. (3.11), to get the density of umbilical points and the density of monstars respectively:

$$n = \int_R \mathrm{d}^2h_{zzz}\mathrm{d}^2h_{zzz^*}\, p(h_{zz}=0, h_{zzz}, h_{zzz^*})J(h_{zzz}, h_{zzz^*}), \tag{3.39}$$

where R represents the range of integration: the entire space to get the density of all umbilical points, or eq. (3.11) for just the monstars.

First we simplify by introducing polar coordinates,

$$h_{zzz} = |h_{zzz}|e^{i\phi}, \qquad h_{zzz^*} = |h_{zzz^*}|e^{i\theta}. \tag{3.40}$$

Next, we introduce

$$u \equiv \frac{|h_{zzz}|}{|h_{zzz^*}|}, \qquad \delta \equiv \frac{3\theta - \phi}{2}. \tag{3.41}$$

We find that we can rewrite the two conditions for monstars, eq. (3.11), in terms of u and δ only: The first one is simply $u > 1$, while the other is

$$\begin{aligned} 0 < 27 - u^4 - 18u^2 - 8u^3\cos 2\delta &= (3-u)^3(1+u) - 16u^3\cos^2\delta \\ \Leftrightarrow \quad \cos^2\delta &< \frac{(3-u)^3(1+u)}{16u^3}. \end{aligned} \tag{3.42}$$

Since the fraction on the right-hand side is negative for $u > 3$, we can extend the first condition to $1 < u < 3$.

The fact that the monstar conditions depend only on u and δ can be understood as follows: The type of umbilic should not be affected by rescaling and/or rotating the plane. Rescaling would add the same (real) factor to h_{zzz} and h_{zzz^*}, hence the type of umbilic should, as far as the moduli are concerned, depend only on the ratio $|h_{zzz}|/|h_{zzz^*}|$. A rotation introduces phase factors as given by eq. (3.12). We see that a rotation over an angle α causes h_{zzz} to pick up a factor $e^{-3i\alpha}$ while h_{zzz^*} picks up $e^{-i\alpha}$. Therefore, the only combination of ϕ and θ that is invariant under rotations is $3\theta - \phi$.

Now we return our attention to the probability distribution. First we rescale h_{zzz} and h_{zzz^*},

$$v \equiv \frac{h_{zzz}}{\sqrt{\tilde{\tau}}}, \qquad w \equiv \frac{h_{zzz^*}}{\sqrt{\tilde{\tau}}}. \tag{3.43}$$

This leads to

$$\begin{aligned} p(h_{zz} = 0, v, w)J \\ \propto \left(1 - \frac{\sigma^3}{\tilde{\tau}^2}\langle f'''(H)\rangle(4 - 8|w|^2 + 2|w|^4 + vw^{*3} + v^*w^3)\right) \\ \times e^{-|v|^2-|w|^2}\Big||v|^2 - |w|^2\Big|. \end{aligned} \tag{3.44}$$

Here we dropped an overall coefficient, which is of no importance since we are only interested in the ratio of the densities of monstars and all umbilical

points. Note that $\tilde{\tau}$ now only appears in the term proportional to f. Since we are not interested in higher orders of f, we need only consider the leading order of $\tilde{\tau}$, which is τ. For convenience, let us define

$$\tilde{\varepsilon} \equiv \frac{\sigma^3}{\tau^2}\langle f'''(H)\rangle. \tag{3.45}$$

Furthermore, note that multiplying p by the constant $1 + 4\tilde{\varepsilon}$—which we may do since we are only interested in the density of the ratios—causes the 4 inside the parentheses to be canceled out (up to first order).

Next, we move to polar coordinates, as we did before:[1]

$$v \equiv \rho e^{i\phi}, \qquad w \equiv re^{i\theta}, \tag{3.46}$$

and then substitute $r = u\rho$ and $\phi = 3\theta - 2\delta$. With these transformations we have

$$\begin{aligned} n \propto \int_R \rho^3 u \,\mathrm{d}\rho\mathrm{d}u\mathrm{d}\theta\mathrm{d}\delta\, e^{-\rho^2(u^2+1)}\rho^2|u^2-1| \\ \times \Big(1 - \tilde{\varepsilon}(-8\rho^2u^2 + 2\rho^4(u^4 + u^3\cos 2\delta)\Big). \end{aligned} \tag{3.47}$$

Finally, we integrate over ρ and θ to find the probability distribution $p(u, \delta)$. The integration over θ simply gives a factor of 2π, while the integral over ρ has the form of a polynomial times a Gaussian. For this we can use

$$\int_0^\infty \mathrm{d}\rho\, \rho^{2n+1} e^{-\rho^2(u^2+1)} = \frac{n!}{2(u^2+1)^{n+1}}. \tag{3.48}$$

The result is

$$p(u, \delta) \propto \frac{u|u^2-1|}{(u^2+1)^3}\left(1 + 24\tilde{\varepsilon}\frac{u^2(1 - u\cos 2\delta)}{(u^2+1)^2}\right). \tag{3.49}$$

The monstar density is proportional to the integral of $p(u, \delta)$ over the range

$$1 < u < 3, \qquad \cos^{-1}\left(\sqrt{\frac{(3-u)^3(1+u)}{16u^3}}\right) < \delta < \tfrac{1}{2}\pi, \tag{3.50}$$

while the total density of umbilical points is proportional (with the same prefactor) to the integral over the range $0 < u < \infty$, $0 < \delta < \frac{1}{2}\pi$ (extending

1 Apart from the sign of ϕ and a numerical factor, the variables r, ρ, ϕ and θ match their respective counterparts in [4].

the integration range of δ from $\frac{1}{2}\pi$ to 2π would just add a factor of 4 to both integrals). The latter can be done analytically: The integration over δ is trivial, while the remaining integral over ρ can be split into two parts which, apart from a factor $\mathrm{sgn}(u^2-1)$, are both of the form

$$\int \mathrm{d}u\, \frac{u^2-1}{(u^2+1)^2}\left(\frac{u}{u^2+1}\right)^n = -\frac{1}{n+1}\left(\frac{u}{u^2+1}\right)^{n+1}. \tag{3.51}$$

With this we find

$$\begin{aligned} n_{\mathrm{tot}} &\propto \tfrac{1}{2}\pi\left[\tfrac{1}{2}\frac{u^2}{(u^2+1)^2} + 24\tilde{\varepsilon}\tfrac{1}{4}\frac{u^4}{(u^2+1)^4}\right]_{u=0}^{1} \\ &\quad + \tfrac{1}{2}\pi\left[-\tfrac{1}{2}\frac{u^2}{(u^2+1)^2} - 24\tilde{\varepsilon}\tfrac{1}{4}\frac{u^4}{(u^2+1)^4}\right]_{u=1}^{\infty} \\ &= \tfrac{1}{8}\pi(1+3\tilde{\varepsilon}). \end{aligned} \tag{3.52}$$

For the monstar range, the integral over δ can be performed. The integral over the cosine gives

$$\int_{\cos^{-1}(\ldots)}^{\frac{1}{2}\pi} \mathrm{d}\delta\, \cos 2\delta = -\frac{1}{16u^3}\sqrt{(u^2-1)(9-u^2)^3}. \tag{3.53}$$

All together:

$$\begin{aligned} n_{\mathrm{M}} &\sim \int_1^3 \mathrm{d}u\, \frac{u(u^2-1)}{(u^2+1)^3}\sin^{-1}\left(\sqrt{\frac{(3-u)^3(1+u)}{16u^3}}\right) \\ &\quad + \tilde{\varepsilon}\int_1^3 \mathrm{d}u\, \frac{u(u^2-1)}{(u^2+1)^3}\left[\frac{24u^2}{(u^2+1)^2}\sin^{-1}\left(\sqrt{\frac{(3-u)^3(1+u)}{16u^3}}\right)\right. \\ &\qquad\qquad \left. + \frac{3\sqrt{(u^2-1)(9-u^2)^3}}{2(u^2+1)^2}\right] \\ &\equiv I_1 + \tilde{\varepsilon} I_2 \end{aligned} \tag{3.54}$$

The integrals can be done numerically. The monstar fraction is then

$$\begin{aligned} \alpha_M &= \frac{n_{\mathrm{M}}}{n_{\mathrm{tot}}} = \frac{I_1+\tilde{\varepsilon}I_2}{\frac{1}{8}\pi(1+3\tilde{\varepsilon})} = \frac{8}{\pi}(I_1 + \tilde{\varepsilon}(I_2 - 3I_1)) + O(\tilde{\varepsilon}^2) \\ &= 0.053 + 0.429\mu\langle f'''(H)\rangle + O(f^2), \end{aligned} \tag{3.55}$$

where

$$\mu \equiv \frac{\sigma^3}{\tau^2} = \frac{K_4^3}{K_6^2} \qquad (0 \le \mu \le 1). \tag{3.56}$$

Note that the zeroth order result matches the one in [4]. Remember that we set $K_0 = \langle H^2 \rangle = 1$ for convenience; if we drop this condition, then K_0 enters the denominator of the expression above.

There is an alternative expression for the term $\langle f'''(H) \rangle$ in eq. (3.55). Since H is Gaussian, with mean 0 and deviation $K_0 = 1$, we can write

$$\langle f'''(H) \rangle = \int \mathrm{d}z \, f'''(z) e^{-z^2/2}. \tag{3.57}$$

Repeated partial integration yields

$$\begin{aligned} \langle f'''(H) \rangle &= \int \mathrm{d}z \, z f''(z) e^{-z^2/2} = \int \mathrm{d}z \, (z^2 - 1) f'(z) e^{-z^2/2} \\ &= \int \mathrm{d}z \, (z^3 - 3z) f(z) e^{-z^2/2} = \langle (H^3 - 3H) f(H) \rangle. \end{aligned} \tag{3.58}$$

The *kurtosis* of a stochastic variable is defined as the fourth cumulant divided by the square of the second, which gives

$$\kappa \equiv \frac{\langle h^4 \rangle}{\langle h^2 \rangle^2} - 3. \tag{3.59}$$

If we enter $h = H + f(H)$, we find

$$\begin{aligned} \kappa &= \frac{\langle H^4 \rangle + 4 \langle H^3 f(H) \rangle}{\langle H^2 \rangle^2 + 4 \langle H^2 \rangle \langle H f(H) \rangle} - 3 + O(f^2) \\ &= \frac{4 \langle H^3 f(H) \rangle - 12 \langle H f(H) \rangle}{1 + 4 \langle H f(H) \rangle} + O(f^2) \\ &= 4 \langle H^3 f(H) \rangle - 12 \langle H f(H) \rangle + O(f^2). \end{aligned} \tag{3.60}$$

We see that $\langle f'''(H) \rangle = \kappa/4$ up to first order, which remains true if $K_0 \neq 1$. Hence an alternative form of eq. (3.55) is

$$\alpha_M = 0.053 + 0.107 \mu \kappa + O(f^2), \tag{3.61}$$

where κ is the kurtosis of h.

By comparing the fraction of monstars in a given field to the formula just found, we can determine one parameter of the deviation from a Gaussian distribution, $\langle f'''(H) \rangle$. This assumes that the field h is given by $h = H + f(H)$. To test this, one could, if possible, also measure the distribution $p(u, \delta)$ to test that it has the right form, eq. (3.49). Measuring $p(\delta)$ only could also suffice. For a Gaussian field H, all values of δ should be equally likely, whereas integrating eq. (3.49) shows that the distribution we expect for h is

$$p(\delta) = \frac{1}{\pi}(1 - 4\tilde{\varepsilon} \cos 2\delta), \tag{3.62}$$

where we define δ to lie between $-\pi/2$ and $\pi/2$.

3.6 COMPARISON WITH SIMULATIONS

The most basic example of a non-Gaussian variable for which eq. (3.55) can be tested is $h = H + \varepsilon H^3$, for which $\langle f'''(H)\rangle = 6\varepsilon$. Then we have

$$\alpha_M = 0.053 + 2.576\mu\varepsilon + O(\varepsilon^2). \tag{3.63}$$

Eq. (3.55) was compared to results from simulations, which were similar to the ones described in section 2.3 (see also appendix A). We chose the same two spectra for which the spectrum decays very quickly (or is zero) for large k: a disk spectrum,

$$A(k)^2 \sim \theta(k_0 - k), \qquad K_{2n} = \frac{k_0^{2n}}{n+1}, \qquad \mu = \frac{16}{27}, \tag{3.64}$$

and a Gaussian spectrum,

$$A(k)^2 \sim \exp(-k^2/2k_0^2), \qquad K_{2n} = 2^n n! k_0^{2n}, \qquad \mu = \frac{2}{9}. \tag{3.65}$$

A very good agreement between theory and simulation was found for both spectra (see fig. 3.1), for ε up to about 0.01. For larger values of ε, nonlinear terms start to dominate.

Another thing to note is the sensitivity: In eq. (3.63) we see that the prefactor of the perturbation term is very large compared to the leading order. As a result, even for small ε, the relative deviation from the universal 0.053 is quite large, as can be seen in the graphs. Therefore, measuring the monstar fraction of a given field proves to be a good method for detecting and quantifying small deviations from Gaussianity.

3.7 CONCLUSIONS

We have calculated how the density of monstars changes for a non-Gaussian field given by $h = H + f(H)$, where H is a Gaussian field. Comparing our formula to data allows to measure the parameter $\langle f'''(H)\rangle = \kappa/4$ of the non-Gaussian contribution. Furthermore, one can also measure the distribution of the parameters u and δ that define the type of umbilical point. The expected distribution is eq. (3.49), or eq. (3.62) for just the variable δ. Measuring these distributions further constrains the value of $\langle f'''(H)\rangle$, and more importantly, it gives a test that the non-Gaussianity really arises from a local nonlinear transformation of a Gaussian field.

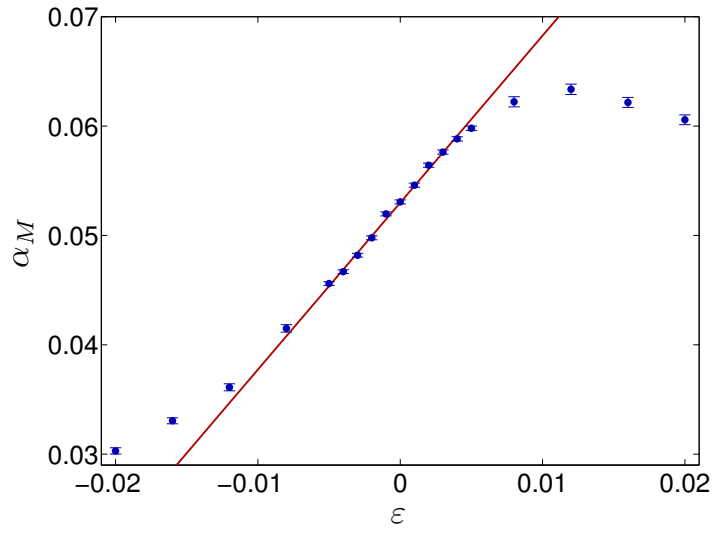

(a)

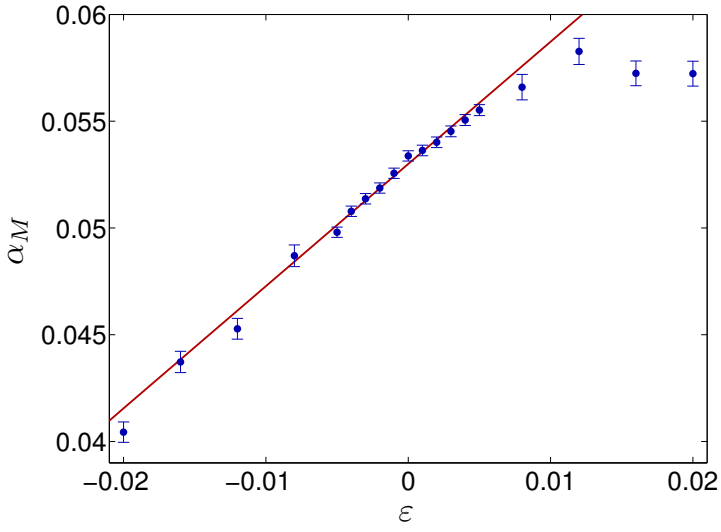

(b)

Figure 3.1: The monstar fraction α_M of $H + \varepsilon H^3$ as a function of ε, where H has (a) a disk spectrum ($\mu = \frac{16}{27}$); (b) a Gaussian spectrum ($\mu = \frac{2}{9}$). The data points stem from simulations, the solid line is eq. (3.63).

Even though in general the derivatives of h have an infinite number of nonzero cumulants up to first order in f, it turns out that the cumulants of the variables which are relevant for the umbilics (h_{zz}, h_{zzz} and h_{zzz^*} at a single point) vanish beyond the fourth order due to symmetry. As a result, we found the interesting result that (up to first order) α_M depends only on $\langle f'''(H)\rangle$.

For a more general type of non-Gaussian field there would be more independent variables and hence more nonzero cumulants. However, it often still holds that the higher order cumulants are of less importance. In this case, one can consider only the cumulants up to a specific order (e.g. fourth order), of which still many would be zero due to symmetry. Applying the same procedure as outlined here could then reveal the monstar fraction up to first order.

4

EXTREMA STATISTICS FOR NONLOCAL PERTURBATIONS

In this chapter we focus on non-Gaussianities of nonlocal origin, so that the field cannot be expressed as $h(\boldsymbol{r}) = f(H(\boldsymbol{r}))$ as before. Instead, $h(\boldsymbol{r})$ may also depend on e.g. ∇H, thereby introducing a mixing between the field values at different points.

Such a nonlocal non-Gaussianity may arise for instance as the result of a nonlinear diffusion equation. The non-Gaussianities that develop may provide clues about the details of the underlying microscopic mechanisms. Consider for example a gas-liquid phase transition. In the early stages, there are many small volumes in which all the molecules are in the same phase, distributed randomly. Over time, these volumes will grow and merge, thereby gradually replacing the Gaussian disorder with structure [5].

As a concrete example, let us consider a field that is Gaussian at $t = 0$ and evolves according to the heat equation:

$$\frac{\partial h(\boldsymbol{r}, t)}{\partial t} = D\nabla^2 h(\boldsymbol{r}, t). \tag{4.1}$$

The solution is then given by

$$\begin{aligned} h(\boldsymbol{r}, t) &= \sum_{\boldsymbol{k}} A_0(\boldsymbol{k}) e^{-k^2 Dt} \cos(\boldsymbol{k} \cdot \boldsymbol{r} + \phi_{\boldsymbol{k}}) \\ &= \sum_{\boldsymbol{k}} \tilde{A}(\boldsymbol{k}, t) \cos(\boldsymbol{k} \cdot \boldsymbol{r} + \phi_{\boldsymbol{k}}), \end{aligned} \tag{4.2}$$

where $A_0(\boldsymbol{k})$ is the amplitude spectrum of the initial field at $t = 0$. We see that the field remains Gaussian for $t > 0$, but the amplitude spectrum changes with time.

Now suppose that we add an extra term:

$$\frac{\partial h(\boldsymbol{r}, t)}{\partial t} = D\nabla^2 h(\boldsymbol{r}, t) + f_{NL}(h, \nabla h), \tag{4.3}$$

where f_{NL} is any nonlinear function. Now, even when h is a Gaussian field at $t = 0$, non-Gaussianities will emerge as a consequence of the last term.

A variety of known diffusion equations has the general form above. For instance, when f_{NL} takes the form $-h^2$ we get Fisher's equation, which can be used as a model to describe the growth and saturation of a population. Another example is the Cahn-Hilliard equation for the development of order after a phase transition [5]. Several models of structure formation, in both condensed matter [7] and cosmology [13], also belong to this class.

We return our focus to the relative difference between maxima and minima, as in chapter 2. We derive a general formula for this imbalance in the case of a general perturbation, up to first order.

To illustrate this result, we apply it to the case of a field obeying the deterministic KPZ equation [32], for which $f_{NL} = \frac{\lambda}{2}(\nabla h)^2$. This equation is often used to model the height profile of a growing surface. A field that starts out as a Gaussian field will acquire non-Gaussian characteristics as time progresses. We use our formula to quantify the effect of the gradient-squared term on the relative difference in densities of maxima and minima. We verify the analytical predictions by comparing them with results from computer simulations.

The outline of this chapter is as follows. In section 4.1 we determine a general expression for the imbalance between maxima and minima for a non-Gaussian field. This is applied to the KPZ equation in section 4.2. Finally, section 4.3 summarizes our conclusions.

4.1 NON-GAUSSIAN FIELDS

In what follows, we concentrate on homogeneous and isotropic fields $h(\boldsymbol{r})$, which we assume to be in the form of a Gaussian $H(\boldsymbol{r})$ with the addition of a perturbation. Unlike chapters 2 and 3, we will not restrict ourselves to a perturbation of the local kind, i.e. where the perturbation at any point $\boldsymbol{r}$ is a function of $H(\boldsymbol{r})$ only. We will now also accommodate perturbations which depend on $\boldsymbol{\nabla} H$ for instance, or evolve over time. Such perturbations introduce a mixing between the values of the field at different points, which we will designate as *nonlocal* perturbations.

We will investigate the effect of a perturbation on the densities of maxima and minima. As mentioned before, for a Gaussian field these are the same due to symmetry. For a non-Gaussian field, they can differ. It is noteworthy that the density of saddle points, the other type of critical points, is always

equal to the density of maxima and minima combined as a consequence of Morse theory [39] (see also chapter 1).

A maximum (minimum) $\boldsymbol{r_0}$ of h is defined by the condition $h_x(\boldsymbol{r_0}) = h_y(\boldsymbol{r_0}) = 0$, along with the inequalities $h_{xx}(\boldsymbol{r_0})h_{yy}(\boldsymbol{r_0}) - h_{xy}(\boldsymbol{r_0})^2 > 0$ (if this were negative, $\boldsymbol{r_0}$ would be a saddle point) and $h_{xx}(\boldsymbol{r_0})$, $h_{yy}(\boldsymbol{r_0})$ negative (positive); note that the first condition implies that $h_{xx}(\boldsymbol{r_0})$ and $h_{yy}(\boldsymbol{r_0})$ have the same sign. The x and y subscripts indicate derivatives with respect to the coordinates of the two-dimensional plane.

The general procedure that we use is very similar to the one in chapter 3 and is as follows: We consider a fixed point $\boldsymbol{r_0}$; due to the homogeneity of h, the analysis will not depend on this choice. We determine the joint probability distribution of h_x, h_y, h_{xx}, h_{yy} and h_{xy}, since these stochastic variables are the ingredients from which maxima and minima are defined, as outlined above. This distribution can be determined via the generating function, which in turn can be constructed by determining the relevant cumulants involving the five stochastic variables. Once the probability distribution is obtained, we set $h_x = h_y = 0$ and integrate the second derivatives over the region defining a minimum (maximum) in order to get the density of minima (maxima).

As we did in section 3.2, we transform to another coordinate system, based on the complex coordinates $z = x + iy$ and z^*, which will allow us to make full use of the homogeneity and isotropy of h later on. In this new basis, we have (see eq. (3.9))

$$\frac{\partial}{\partial z} = \tfrac{1}{2}\frac{\partial}{\partial x} - \tfrac{1}{2}i\frac{\partial}{\partial y}, \qquad \frac{\partial}{\partial z^*} = \tfrac{1}{2}\frac{\partial}{\partial x} + \tfrac{1}{2}i\frac{\partial}{\partial y}. \tag{4.4}$$

In this coordinate system, the definition of a maximum (minimum) becomes $h_z(\boldsymbol{r_0}) = 0$, $|h_{zz^*}(\boldsymbol{r_0})| > |h_{zz}(\boldsymbol{r_0})|$ and $h_{zz^*}(\boldsymbol{r_0})$ is negative (positive).[1]

We now need the cumulants. In the previous chapter we were able to argue that there is only a limited number of nonzero cumulants, based on the specific form of the variables we were dealing with, but this argument does not apply here. In principle, there are now infinitely many nonzero cumulants. However, a field that is generated by a nonlinear differential equation, like eq. (4.3), typically has small cumulants of high order. In particular, if f_{NL} is a quadratic function and the initial conditions are Gaussian, then the n-th order cumulants scale like f_{NL}^{n-2} (for $n > 2$) (see appendix D). Therefore we will only need to determine cumulants up to third order to get the correction to leading order.

1 Note that $h_{zz^*}(\boldsymbol{r_0})$ is real valued.

As in section 3.2, we can use symmetries to make our lives easier. From rotational symmetry it follows that each cumulant must have the same total number of z and z^* derivatives, otherwise it is zero. Translational invariance implies that any correlation should be constant with respect to $\boldsymbol{r}$, which leads to relations like

$$0 = \partial_{z^*}\langle h_z^2 h_{z^*}\rangle = \langle h_z^2 h_{z^*z^*}\rangle + 2\langle h_z h_{z^*} h_{zz^*}\rangle, \tag{4.5}$$

which gives us the relation present in eq. (4.6c).

Therefore, there are only a few independent cumulants that are (potentially) nonzero:

$$\sigma = \langle |h_z|^2\rangle, \tag{4.6a}$$
$$\alpha = \langle |h_{zz}|^2\rangle = \langle h_{zz^*}^2\rangle, \tag{4.6b}$$
$$\beta = \langle |h_z^2| h_{zz^*}\rangle = -\tfrac{1}{2}\langle h_z^2 h_{z^*z^*}\rangle = -\tfrac{1}{2}\langle h_{z^*}^2 h_{zz}\rangle, \tag{4.6c}$$
$$\gamma = \langle h_{zz^*}^3\rangle, \tag{4.6d}$$
$$\delta = \langle |h_{zz}|^2 h_{zz^*}\rangle. \tag{4.6e}$$

Here we introduced the shorthand notation $|h_z|^2 = h_z h_z^* = h_z h_{z^*}$ and similarly for $|h_{zz}|^2$. Note also that the third-order cumulants, β, γ and δ are close to zero when h is close to being Gaussian, which we assume. On the other hand, σ and α are nonzero in general.

Note that it is not generally true that correlations and cumulants are identical. It is true though in this special case of correlations / cumulants up to third order between derivatives of a homogeneous field, as shall be demonstrated with γ as an example. Expressing the cumulant in correlations gives

$$\gamma = C_3(h_{zz^*}, h_{zz^*}, h_{zz^*}) = \langle h_{zz^*}^3\rangle - 3\langle h_{zz^*}\rangle\langle h_{zz^*}^2\rangle + 2\langle h_{zz^*}\rangle^3. \tag{4.7}$$

Note that, with the exception of the first, all terms carry a factor $\langle h_{zz^*}\rangle$, which can be expressed as

$$\langle h_{zz^*}\rangle = \partial_{z_1}\partial_{z_1^*}\langle h(\boldsymbol{r})\rangle. \tag{4.8}$$

Since we consider h to be homogeneous, $\langle h(\boldsymbol{r})\rangle$ is constant and thus we have $\langle h_{zz^*}\rangle = 0$. This trick applies not only to γ, but to all five correlations in eq. (4.6).

We can now construct the logarithm of the generating function as prescribed by eq. (3.3),

$$\begin{aligned}\log\chi = &-\sigma|\lambda_z|^2 - \alpha|\lambda_{zz}|^2 - \tfrac{1}{2}\alpha\lambda_{zz^*}^2 \\ &- i\beta|\lambda_z|^2\lambda_{zz^*} + i\beta(\lambda_z^2\lambda_{z^*z^*} + \lambda_{z^*}^2\lambda_{zz}) \\ &- \tfrac{i}{6}\gamma\lambda_{zz^*}^3 - i\delta|\lambda_{zz}|^2\lambda_{zz^*}. \end{aligned} \tag{4.9}$$

Recall that the number of permutations of the λ's needs to be accounted for, as per eq. (3.3); this explains why for instance the term $\lambda_{zz^*}^3$ has a prefactor $i/6$ whereas the prefactor of $|\lambda_{zz}|^2\lambda_{zz^*} = \lambda_{zz}\lambda_{z^*z^*}\lambda_{zz^*}$ is i (due to the 6 distinct permutations of the λ's).

We see that χ features an exponential of a third-degree polynomial, making the inverse Fourier transform (to be performed in order to get the probability distribution) nontrivial. Remember however that the cubic terms are small owing to the near-Gaussianity of h, allowing us to make the expansion

$$\begin{aligned}\chi = &\Big(1 - i\beta|\lambda_z|^2\lambda_{zz^*} + i\beta(\lambda_z^2\lambda_{z^*z^*} + \lambda_{z^*}^2\lambda_{zz}) \\ &- \tfrac{i}{6}\gamma\lambda_{zz^*}^3 - i\delta|\lambda_{zz}|^2\lambda_{zz^*}\Big) \\ &\times \exp\Big(-\sigma|\lambda_z|^2 - \alpha|\lambda_{zz}|^2 - \tfrac{1}{2}\alpha\lambda_{zz^*}^2\Big). \end{aligned} \tag{4.10}$$

The inverse Fourier transform of this gives[2]

$$\begin{aligned}p(h_z, h_{zz}, h_{zz^*}) = &\Big(1 + \frac{\beta}{\alpha\sigma^2}h_{zz^*}(|h_z|^2 - \sigma) - \frac{\beta}{\alpha\sigma^2}(h_z^2 h_{z^*z^*} + h_{z^*}^2 h_{zz}) \\ &+ \frac{\gamma}{6\alpha^3}(h_{zz^*}^3 - 3\alpha h_{zz^*}) + \frac{\delta}{\alpha^3}h_{zz^*}(|h_{zz}|^2 - \alpha)\Big) \\ &\times \frac{1}{\pi^2\sqrt{2\pi}\sigma\alpha^{3/2}}e^{-|h_z|^2/\sigma - |h_{zz}|^2/\alpha - h_{zz^*}^2/2\alpha}. \end{aligned} \tag{4.11}$$

Now that the joint probability distribution of the relevant derivatives is obtained, we can set $h_z = h_{z^*} = 0$; this condition defines a critical point. As we have seen before in both chapter 2 and 3, we need to multiply p by the Jacobian

$$J = \left|\frac{\partial(h_z, h_{z^*})}{\partial(z, z^*)}\right| = \Big||h_{zz}|^2 - h_{zz^*}^2\Big|, \tag{4.12}$$

in order to get the appropriate probability distribution with respect to z and z^* (representing x and y).

2 A factor of π^2 rather than $(2\pi)^2$ is associated with the complex variables h_z and h_{zz} in the Fourier transform due to our normalization; see also eq. (3.34).

Now we are ready to set $h_z = h_{z^*} = 0$ and integrate pJ over h_{zz} and h_{zz^*}. The range is determined by the type of critical point of interest; focus on the minima first. For these we must have $|h_{zz}| < |h_{zz^*}|$ and $h_{zz^*} > 0$. The integration over h_{zz} is done by integrating over its real and imaginary part. Since the integrand depends only on the modulus of h_{zz}, we move to polar coordinates. Let us define $r = |h_{zz}|$ and $s = h_{zz^*}$. The integration range is then $0 < r < s$, and with eq. (4.11) we get

$$\begin{aligned} n_{min} = {} & \frac{1}{\pi^2\sqrt{2\pi}\sigma\alpha^{3/2}} \\ & \times \int_0^\infty \mathrm{d}s \int_0^s 2\pi r \,\mathrm{d}r \,(s^2 - r^2) e^{-r^2/\alpha - s^2/2\alpha} \\ & \times \left(1 - \frac{\beta}{\alpha\sigma}s + \frac{\gamma}{6\alpha^3}(s^3 - 3\alpha s) + \frac{\delta}{\alpha^3}s(r^2 - \alpha)\right). \end{aligned} \tag{4.13}$$

This integration is pretty straightforward: Although the range of r is finite, the integrand is a Gaussian multiplied by a polynomial that has only odd degrees of r, hence it does not give rise to error functions. The resulting integral over s is also standard. The final result reads

$$n_{min} = \frac{\alpha}{2\sqrt{3}\pi\sigma} - \frac{1}{\pi\sigma}\sqrt{\frac{\alpha}{2\pi}}\left(\frac{4}{3}\frac{\beta}{\sigma} + \frac{4}{9}\frac{\delta}{\alpha} - \frac{10}{27}\frac{\gamma}{\alpha}\right). \tag{4.14}$$

For a Gaussian field, we would have $\beta = \gamma = \delta = 0$, $\sigma = \frac{1}{4}K_2$ and $\alpha = \frac{1}{16}K_4$. This would give us $n_{min} = K_4/(8\sqrt{3}\pi K_2)$, exactly as noted before (eqs. (1.40) and (2.34)).

To get the density of maxima, the same integrand as in eq. (4.13) needs to be integrated over the range $s < 0$ and $0 < r < -s$. However, note that if we make the transformation $s \to -s$, the range of integration is the same as in eq. (4.13). Furthermore, note that the transformation $s \to -s$ in the integrand is equivalent to $\beta \to -\beta$, $\gamma \to -\gamma$ and $\delta \to -\delta$. With this insight, we easily find that the expression for n_{max} is the same as the above, except with a plus in place of the first minus.

With this result, the imbalance between maxima and minima is found to be

$$\Delta n \equiv \frac{n_{max} - n_{min}}{n_{max} + n_{min}} = \sqrt{\frac{6}{\pi\alpha}}\left(\frac{4}{3}\frac{\beta}{\sigma} + \frac{4}{9}\frac{\delta}{\alpha} - \frac{10}{27}\frac{\gamma}{\alpha}\right). \tag{4.15}$$

This is the main result of this chapter. As an illustration, we shall now use this result to understand the evolution of maxima and minima in the context of a differential equation describing surface growth.

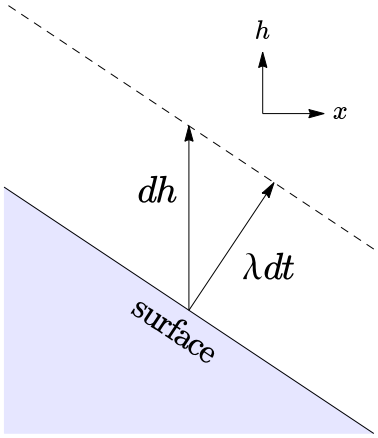

Figure 4.1: A two-dimensional (excluding the y direction) geometrical interpretation of the second term of the KPZ equation (eq. (4.16)) applied to a growing surface. The surface is assumed to grow perpendicularly at a constant rate λ. Measured vertically, the growth rate is $\mathrm{d}h/\mathrm{d}t = \lambda\sqrt{1+(\mathrm{d}h/\mathrm{d}x)^2}$. In three dimensions, the derivative is replaced by a gradient (see eq. (4.17)).

4.2 KPZ EQUATION

The deterministic Kardar-Parisi-Zhang (KPZ) equation [32] is given by

$$\frac{\partial h}{\partial t} = \nu\nabla^2 h + \frac{\lambda}{2}(\nabla h)^2. \tag{4.16}$$

This equation is often used to describe the height profile of a growing surface: The first term on the right-hand side describes the diffusion of particles along the surface, while the second term accounts for the assumption that the growth is perpendicular to the slope of the surface, while h describes the height along the universal up direction [1]. This leads to (see fig. 4.1)

$$\frac{\mathrm{d}h}{\mathrm{d}t} = \lambda\sqrt{1+(\nabla h)^2} = \lambda + \frac{\lambda}{2}(\nabla h)^2 + \dots \tag{4.17}$$

The leading term λ is ignored since it is just a constant that does not affect the profile of the surface.

Another interpretation of eq. (4.16) is obtained by taking the gradient on both sides, which yields

$$\frac{\partial \boldsymbol{v}}{\partial t} = \nu\nabla^2 \boldsymbol{v} + \lambda \boldsymbol{v}\boldsymbol{\nabla}\boldsymbol{v}, \tag{4.18}$$

where $\boldsymbol{v} = \boldsymbol{\nabla} h$ is a velocity field. This is a vector Burger's equation which arises in fluid mechanics. The maxima and minima of h correspond to sources and sinks of v.

We will take $h(\boldsymbol{r}, t)$ to be a Gaussian field at $t = 0$, and use our result eq. (4.15) to determine how the non-Gaussianities, which arise and evolve due to the KPZ equation, influence the densities of maxima and minima.

First note that if we would set $\lambda = 0$ in eq. (4.16), we retrieve the heat equation, which preserves the Gaussianity of a field: If we enter $h(\boldsymbol{r}, t = 0) = H(\boldsymbol{r})$, where $H(\boldsymbol{r})$ is a Gaussian field as given by eq. (1.9), we find that the solution is

$$h(\boldsymbol{r}, t) = \sum_{\boldsymbol{k}} A(k) e^{-k^2 \nu t} \cos(\boldsymbol{k} \cdot \boldsymbol{r} + \phi_k). \tag{4.19}$$

We find that the amplitudes pick up a factor $\exp(-k^2 \nu t)$, but the phases remain independent. Therefore, even though its amplitude spectrum changes, $h(\boldsymbol{r}, t)$ remains Gaussian at any time t and the density of maxima and minima remains the same, since this is a general property of Gaussian fields.

If we have $\lambda \neq 0$, $h(\boldsymbol{r}, t)$ no longer remains Gaussian. In fact, as we will see, the density of maxima and minima is no longer the same. We shall assume λ to be small in comparison to ν, and find out how these densities differ as a function of time, using eq. (4.15). For this, we need to determine the two- and three-point correlations σ, α, β, γ and δ.

First, we substitute $u = \exp((\lambda/2\nu)h)$. Note that, since this is a monotonically increasing function of h, the maxima and minima of u are exactly the same points as those of h. In terms of u, the KPZ equation becomes:

$$\frac{\partial u}{\partial t} = \nu \nabla^2 u, \tag{4.20}$$

which is simply the heat equation. However, $u(\boldsymbol{r}, t = 0) = \exp((\lambda/2\nu)h_0)$ is now not a Gaussian field. If we assume that $\lambda \ll \nu$, we have:

$$u_0 = 1 + \frac{\lambda}{2\nu} h_0 + \frac{\lambda^2}{8\nu^2} h_0^2 + O((\lambda/\nu)^3). \tag{4.21}$$

Since the leading term, equal to one, has no influence on either the maxima and minima or the heat equation, we can ignore it. The same applies to the prefactor $\frac{\lambda}{2\nu}$ of the second term. Hence we make a final transformation

$$v \equiv \frac{2\nu}{\lambda}(u - 1), \tag{4.22}$$

$$v_0 = h_0 + \frac{\lambda}{4\nu} h_0^2 + O((\lambda/\nu)^2). \tag{4.23}$$

Note that v still obeys the heat equation and also shares the same maxima and minima with h and u. Moreover, we now have $v(\boldsymbol{r}, t = 0)$ in the desired form of a Gaussian h_0 plus a perturbation. Since v obeys the heat equation, we can use the corresponding Green's function to write down the general solution

$$\begin{aligned} v(r,t) &= \int \mathrm{d}^2\tilde{\boldsymbol{r}}\, G(\boldsymbol{r}, \tilde{\boldsymbol{r}}, t) v_0(\tilde{\boldsymbol{r}}) \\ &= \int \mathrm{d}^2\tilde{\boldsymbol{r}}\, \frac{1}{4\pi\nu t} e^{-\frac{(\boldsymbol{r}-\tilde{\boldsymbol{r}})^2}{4\nu t}} \Big(h_0(\tilde{\boldsymbol{r}}) + \frac{\lambda}{4\nu} h_0(\tilde{\boldsymbol{r}})^2 \Big), \end{aligned} \tag{4.24}$$

where $v_0(\tilde{\boldsymbol{r}}) = v(\boldsymbol{r}, t = 0)$.

We can now calculate the five correlations needed to determine Δn. We will demonstrate the procedure using $\sigma = \langle v_z(\boldsymbol{r}, t) v_{z^*}(\boldsymbol{r}, t) \rangle$ as an example.

$$\begin{aligned} \sigma &= \langle v_z(r,t) v_{z^*}(r,t) \rangle \\ &= \iint \mathrm{d}^2\tilde{\boldsymbol{r}}_{\mathbf{1}} \mathrm{d}^2\tilde{\boldsymbol{r}}_{\mathbf{2}}\, \partial_{z_1} G(\boldsymbol{r}_{\mathbf{1}}, \tilde{\boldsymbol{r}}_{\mathbf{1}}, t) \partial_{z_2^*} G(\boldsymbol{r}_{\mathbf{2}}, \tilde{\boldsymbol{r}}_{\mathbf{2}}, t) \\ &\qquad \times \langle v_0(\tilde{\boldsymbol{r}}_{\mathbf{1}}) v_0(\tilde{\boldsymbol{r}}_{\mathbf{2}}) \rangle \Big|_{\boldsymbol{r}_{\mathbf{1}} = \boldsymbol{r}_{\mathbf{2}} = \boldsymbol{r}}. \end{aligned} \tag{4.25}$$

The brackets represent averaging over all $\phi_{\boldsymbol{k}}$ that define v_0, while the spatial derivatives act only on the respective Green's function. The latter gives

$$\begin{aligned} \partial_{z_1} G(\boldsymbol{r}_{\mathbf{1}}, \tilde{\boldsymbol{r}}_{\mathbf{1}}, t) &= \partial_{z_1} \left(\frac{1}{4\pi\nu t} e^{-\frac{(\boldsymbol{r}_{\mathbf{1}} - \tilde{\boldsymbol{r}}_{\mathbf{1}})^2}{4\nu t}} \right) \\ &= \frac{1}{\pi (4\nu t)^2} ((x_1 - \tilde{x}_1) - i(y - \tilde{y}_1)) e^{-\frac{(\boldsymbol{r}_{\mathbf{1}} - \tilde{\boldsymbol{r}}_{\mathbf{1}})^2}{4\nu t}}. \end{aligned} \tag{4.26}$$

The moment present in eq. (4.25) is

$$\begin{aligned} \langle v_0(\tilde{\boldsymbol{r}}_{\mathbf{1}}) v_0(\tilde{\boldsymbol{r}}_{\mathbf{2}}) \rangle &= \Big\langle \Big(h_0(\tilde{\boldsymbol{r}}_{\mathbf{1}}) + \frac{\lambda}{4\nu} h_0(\tilde{\boldsymbol{r}}_{\mathbf{1}})^2 \Big) \Big(h_0(\tilde{\boldsymbol{r}}_{\mathbf{2}}) + \frac{\lambda}{4\nu} h_0(\tilde{\boldsymbol{r}}_{\mathbf{2}})^2 \Big) \Big\rangle \\ &= \langle h_0(\tilde{\boldsymbol{r}}_{\mathbf{1}}) h_0(\tilde{\boldsymbol{r}}_{\mathbf{2}}) \rangle \\ &\quad + \frac{\lambda}{4\nu} \Big(\langle h_0(\tilde{\boldsymbol{r}}_{\mathbf{1}}) h_0(\tilde{\boldsymbol{r}}_{\mathbf{2}})^2 \rangle + \langle h_0(\tilde{\boldsymbol{r}}_{\mathbf{1}})^2 h_0(\tilde{\boldsymbol{r}}_{\mathbf{2}}) \rangle \Big) \\ &\quad + \left(\frac{\lambda}{4\nu} \right)^2 \langle h_0(\tilde{\boldsymbol{r}}_{\mathbf{1}})^2 h_0(\tilde{\boldsymbol{r}}_{\mathbf{2}})^2 \rangle. \end{aligned} \tag{4.27}$$

Note that the second term (the one linear in $\lambda/4\nu$) is a three-point correlation, and therefore zero due to the symmetry of the Gaussian field h_0.

We will ignore the last term since our analysis is restricted to first order in $\lambda/4\nu$. All that remains is the two-point correlation, which with the help of eq. (1.9) is seen to be

$$\begin{aligned}\langle v_0(\tilde{\boldsymbol{r}}_{\mathbf{1}})v_0(\tilde{\boldsymbol{r}}_{\mathbf{2}})\rangle &= \langle h_0(\tilde{\boldsymbol{r}}_{\mathbf{1}})h_0(\tilde{\boldsymbol{r}}_{\mathbf{2}})\rangle \\ &= \sum_{\boldsymbol{k}} \tfrac{1}{2}A(k)^2\cos(\boldsymbol{k}\cdot(\tilde{\boldsymbol{r}}_{\mathbf{1}}-\tilde{\boldsymbol{r}}_{\mathbf{2}})).\end{aligned} \tag{4.28}$$

We will now plug our intermediate results, eqs. (4.26) and (4.28), back into eq. (4.25). For convenience, we will set $\boldsymbol{r}=\mathbf{0}$, which we are allowed to do thanks to the homogeneity of v. We find

$$\begin{aligned}\sigma = \sum_{\boldsymbol{k}} \tfrac{1}{2}A(k)^2 \iint \mathrm{d}^2\tilde{\boldsymbol{r}}_{\mathbf{1}}\mathrm{d}^2\tilde{\boldsymbol{r}}_{\mathbf{2}}\,\pi^{-2}(4\nu t)^{-4}(\tilde{\boldsymbol{r}}_{\mathbf{1}}\cdot\tilde{\boldsymbol{r}}_{\mathbf{2}}) \\ \times e^{-(|\tilde{\boldsymbol{r}}_{\mathbf{1}}|^2+|\tilde{\boldsymbol{r}}_{\mathbf{2}}|^2)/(4\nu t)}\cos(\boldsymbol{k}\cdot(\tilde{\boldsymbol{r}}_{\mathbf{1}}-\tilde{\boldsymbol{r}}_{\mathbf{2}})).\end{aligned} \tag{4.29}$$

Note that based on eq. (4.26) we should have put $(\tilde{x}_1 - i\tilde{y}_1)(\tilde{x}_2 + i\tilde{y}_2)$ instead of $(\tilde{\boldsymbol{r}}_{\mathbf{1}}\cdot\tilde{\boldsymbol{r}}_{\mathbf{2}})$; the latter is merely the real part of the former. However, since we already know that the final answer is real (since $\sigma = \langle|v_z|^2\rangle$), we can conclude that the imaginary part would not give a contribution.

After performing the integrals in eq. (4.29) we get the result given below. The three-point correlations β, γ and δ give rise to six-dimensional integrals involving four-point correlations (which are first order in $\lambda/4\nu$). These correlations can be factorized into two two-point correlations by Wick's theorem, resulting in a sum over two wave vectors $\boldsymbol{k}_{\mathbf{1}}$ and $\boldsymbol{k}_{\mathbf{2}}$, as opposed to the one we had in the case of σ.

All the relevant correlations are

$$\sigma = \sum_{\boldsymbol{k}} \frac{1}{2} A(k)^2 \frac{1}{4} k^2 e^{-2k^2\nu t}, \tag{4.30a}$$

$$\alpha = \sum_{\boldsymbol{k}} \frac{1}{2} A(k)^2 \frac{1}{16} k^4 e^{-2k^2\nu t}, \tag{4.30b}$$

$$\beta = -\frac{\lambda}{4\nu} \sum_{\boldsymbol{k_1}} \sum_{\boldsymbol{k_2}} \frac{1}{4} A(k_1)^2 A(k_2)^2 \frac{1}{4} \Big(k_1^2 k_2^2 - (\boldsymbol{k_1} \cdot \boldsymbol{k_2})^2 \Big) \times e^{-2(k_1^2 + k_2^2 + \boldsymbol{k_1} \cdot \boldsymbol{k_2})\nu t}, \tag{4.30c}$$

$$\gamma = -\frac{\lambda}{4\nu} \sum_{\boldsymbol{k_1}} \sum_{\boldsymbol{k_2}} \frac{1}{4} A(k_1)^2 A(k_2)^2 \frac{3}{32} k_1^2 k_2^2 (\boldsymbol{k_1} + \boldsymbol{k_2})^2 \times e^{-2(k_1^2 + k_2^2 + \boldsymbol{k_1} \cdot \boldsymbol{k_2})\nu t}, \tag{4.30d}$$

$$\delta = -\frac{\lambda}{4\nu} \sum_{\boldsymbol{k_1}} \sum_{\boldsymbol{k_2}} \frac{1}{4} A(k_1)^2 A(k_2)^2 \frac{1}{32} \Big(-k_1^2 k_2^2 (k_1^2 + k_2^2) + ((\boldsymbol{k_1} + \boldsymbol{k_2})^4 - k_1^4 - k_2^4)(\boldsymbol{k_1} \cdot \boldsymbol{k_2}) \Big) \times e^{-2(k_1^2 + k_2^2 + \boldsymbol{k_1} \cdot \boldsymbol{k_2})\nu t}. \tag{4.30e}$$

For a continuous spectrum, the sums can be replaced by integrals.

We see that the parameters depend on the spectrum of h_0 in a nontrivial way. Especially the presence of $\boldsymbol{k_1} \cdot \boldsymbol{k_2}$ (which is also present in terms like $(\boldsymbol{k_1} + \boldsymbol{k_2})^2$) in the relations for β, γ and δ complicates matters, as it introduces a dependence on the angle between $\boldsymbol{k_1}$ and $\boldsymbol{k_2}$. An exact analytical evaluation is therefore only realizable for a few spectra of a convenient form. Even for the so-called ring spectrum, with $A(k) \propto \delta(k - k_0)$, arguably the simplest spectrum one can have, the angular dependence introduces nontrivial functions. In this case, eq. (4.15) reads

$$\Delta n = \frac{\lambda}{4\nu} \frac{8}{9} \sqrt{\frac{6}{\pi}} \frac{e^{-\tau}}{\tau} \Big(-(2 + \tau) I_0(2\tau) - 5\tau I_1(2\tau) + (2 + \tau + 6\tau^2)\, {}_0F_1(2; \tau^2) \Big), \tag{4.31}$$

where $\tau \equiv k_0^2 \nu t$; I_0 and I_1 are modified Bessel functions of the first kind and ${}_0F_1$ is the confluent hypergeometric function. Recall that we set $K_0 = \langle h_0^2 \rangle = 1$ for convenience; for the general case, a factor of $\sqrt{K_0}$ needs to be added.

Another, more elegant case in which an exact evaluation of eq. (4.15) is possible is the Gaussian spectrum $A(k) \propto \exp(-k^2/(4k_0^2))$, for which

$$\Delta n = \frac{\lambda}{4\nu} \frac{64\tau^3(1+4\tau)^{7/2}}{\sqrt{3\pi}(1+2\tau)^3(1+6\tau)^4}, \tag{4.32}$$

where again $\tau \equiv k_0^2 \nu t$ and a factor of $\sqrt{K_0}$ needs to be added for our result to apply in general.

Going back to the general case of an unspecified power spectrum, it is convenient to expand Δn in t. The result is

$$\Delta n = \frac{\lambda}{4\nu} \frac{4}{9} \sqrt{\frac{6}{\pi}} \frac{2K_2K_6 - 3K_4^2}{K_2\sqrt{K_4}} (\nu t)^2 + O(t^3), \tag{4.33}$$

for all K_0. One may note that for a Gaussian spectrum, there is no quadratic order in eq. (4.32), which is confirmed by the above formula, since $2K_2K_6 - 3K_4^2 = 0$ in this case.

The analytical results for Δn above are compared to results from numerical simulations (with $K_0 = 1$ and $\lambda/4\nu = 0.1$) in fig. 4.2. The general method is the same as seen in chapter 2 and appendix A. We start with a Gaussian field h_0 defined on a finite square grid with periodic boundary conditions. We then transform to v_0 and use the alternating direction implicit (ADI) method to simulate the heat equation, collecting statistics on the maxima and minima at every time step. The results are averaged over for tens of thousands of h_0's, each with the same spectrum but random phases.

In general, if a field evolves under a nonlinear equation for a long time, the non-Gaussianity can become large, even when the perturbation is small, because it will add up over time. Thus we may expect a breakdown of our predictions after some time, as in fig. 4.2b. However, the KPZ equation has a special mapping to a diffusion equation (eq. (4.20)), and this implies that the non-Gaussian perturbations never build up. Eq. (4.24) shows that the nonlinear correction diffuses outward but does not grow over time. Therefore, for the KPZ equation, our approximations should remain accurate for arbitrarily long times. This is indeed what we see in fig. 4.2a, where $h(t = 0)$ is Gaussian field with a Gaussian spectral function.

In fig. 4.2b however there is a breakdown for the ring spectrum. This spectrum is special because it has zero weight at $k = 0$. This implies that the leading Gaussian term in eq. (4.24) is suppressed exponentially, decaying as $\exp(-k_0^2\nu t)$ (see eq. (4.19)). Thus after a long time, the second term

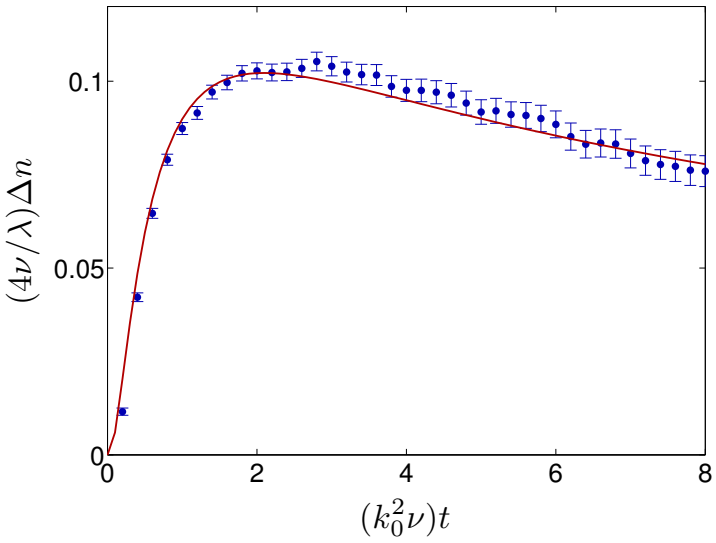

(a)

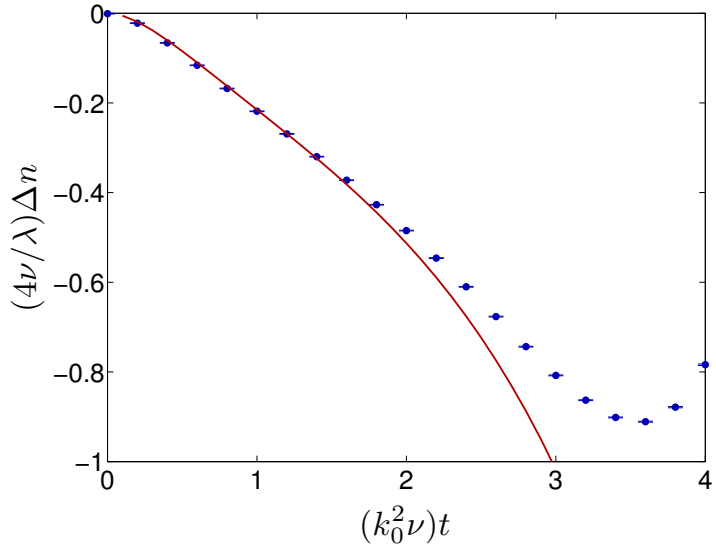

(b)

Figure 4.2: The imbalance between maxima and minima Δn of $h(\boldsymbol{r}, t)$, where h obeys the KPZ equation (with $\lambda/4\nu = 0.1$), as a function of time. At $t = 0$, $h(\boldsymbol{r})$ was taken to be a Gaussian field with (a) a Gaussian spectrum $A(k) \propto \exp(-k^2/(4k_0^2))$; (b) a ring spectrum $A(k) \propto \delta(k - k_0)$. Shown are our theoretical perturbative result (eq. (4.15)) and data from simulations.

dominates, and our approximation that v is close to a Gaussian no longer holds. Whenever the spectral function has a weight at $k = 0$ (as in fig. 4.2a), the approximation works for a longer time.

4.3 CONCLUSIONS

We have found a general perturbative formula, eq. (4.15), for determining the imbalance between maxima and minima of an isotropic random field that is almost Gaussian. It allows one to attack the reverse problem, namely, to determine the size of the phenomenon that causes the non-Gaussianity, by measuring the relative densities of maxima and minima. In the case of the deterministic KPZ equation for instance, the imbalance can reveal the size of the nonlinear parameter λ relative to the diffusion coefficient ν.

In chapter 2, we investigated the imbalance between maxima and minima as a result of non-Gaussianity. Although we arrived at an exact result, it applied only to the special case of a local perturbation, i.e. for a field given by $h(\boldsymbol{r}) = F_{NL}(H(\boldsymbol{r}))$ where H is a Gaussian field and F_{NL} any (nonlinear) function. The result in the present study, although perturbative, also accommodates *nonlocal* perturbations, provided that the resulting field is still homogeneous and isotropic.

For local perturbations, we found that the size of the imbalance is exponentially small in the size of the perturbation. Nonlocal perturbations however allow for a power-law relation. This is apparent in eq. (4.33), which shows that the KPZ equation can cause an imbalance that grows quadratically with time. As a result, the densities of maxima and minima can prove to be a sensitive test to not only detect non-Gaussianity, but also to distinguish local from nonlocal perturbations that induce non-Gaussian statistics.

5

NON-GAUSSIANITY AND COARSE-GRAINING

When a measurement is made, the resulting picture is usually not pixel perfect. A point source for instance may look like a blob of finite size. This is because, when slightly away from the point source, its presence still leaves its mark. In effect, a measured signal is typically a weighted average of the signal in a small neighborhood of the location in question. This process is known as coarse-graining.

One of the features of our geometric approach is that it does not require accurate measurements of the field in question, since the removal or addition of a singularity or topological defect typically requires a nontrivial operation. Having said that, it is natural to study the effect coarse-graining has on the statistics.

Coarse-graining is also interesting from another point of view: If the scale over which the field is coarse-grained is much larger than its correlation length, the coarse-graining effectively entails taking an average of a large number of independent regions. Therefore, the process of coarse-graining itself may, by virtue of the central limit theorem, give rise to near-Gaussian statistics.

An example in which coarse-graining plays a different but intriguing role is gravitational lensing tomography. Images from distant galaxies are sheared due to mass present between that galaxy and us. This phenomenon is called weak gravitational lensing. Measuring the shear offers a window on the distribution of mass in the universe [25]. The singularities of the shear field for instance correspond to the umbilics of the projected gravitational potential [45]. It is a two-dimensional window though, providing only information about the projected gravitational potential. If one however incorporates the redshift—which can be translated to distance—a three-dimensional picture can be constructed [26]. The entire range of redshifts is divided into bins that can be processed individually. Therefore each bin

yields an average of sources from a range of distances, rather than one specific distance. This can be interpreted as an effective source of coarse-graining.

The outline of this chapter is as follows. Section 5.1 sets up the mathematical framework for coarse-graining and discusses its effects. In section 5.2 we derive what the imbalance between maxima and minima looks like in the limit that one coarse-grains over a large scale. This is demonstrated in section 5.3, using a sample case that allows the imbalance to be determined analytically for arbitrary coarse-grain length scales. In section 5.4, the analytical result is compared to numerical simulations. Finally, section 5.5 summarizes our findings.

5.1 COARSE-GRAINING

In general, mathematically, coarse-graining a field $h(\boldsymbol{r})$ can be expressed as

$$\tilde{h}(\boldsymbol{r}) = \int \mathrm{d}^2\boldsymbol{u}\, K(\boldsymbol{u}) h(\boldsymbol{r}+\boldsymbol{u}), \tag{5.1}$$

with $\int \mathrm{d}^2\boldsymbol{u}\, K(\boldsymbol{u}) = 1$. It may be interpreted as a kind of averaging, with the function $K(\boldsymbol{u})$ corresponding to the weight. Coarse-graining may represent blurring as the result of an imprecise measurement of h, for example. Typically then, $K(\boldsymbol{u})$ is largest at $\boldsymbol{u} = \boldsymbol{0}$ and decreases for increasing $|\boldsymbol{u}|$. Ad extremum, $K(\boldsymbol{u}) = \delta(\boldsymbol{u})$ corresponds to no coarse-graining at all, or a perfectly accurate measurement.

When coarse-graining is applied to a Gaussian field $H(\boldsymbol{r})$, the result is (in complex notation):

$$\begin{aligned}\tilde{H}(\boldsymbol{r}) &= \int \mathrm{d}^2\boldsymbol{u}\, K(\boldsymbol{u}) \sum_{\boldsymbol{k}} A(k) e^{i(\boldsymbol{k}\cdot(\boldsymbol{r}+\boldsymbol{u})+\phi_{\boldsymbol{k}})} \\ &= \sum_{\boldsymbol{k}} A(k) \left(\int \mathrm{d}^2\boldsymbol{u}\, K(\boldsymbol{u}) e^{i\boldsymbol{k}\cdot\boldsymbol{u}} \right) e^{i(\boldsymbol{k}\cdot\boldsymbol{r}+\phi_{\boldsymbol{k}})}\end{aligned} \tag{5.2}$$

It is thus easily seen that coarse-graining only affects the amplitude spectrum of H, but not its Gaussianity.

Consider now what happens when applied to a non-Gaussian field h. Let us set $K(\boldsymbol{r}) = f(r/l)/l^2$, where l is a length scale that controls the size of the coarse-graining, while $f(x)$ is a dimensionless function that goes to zero for $x \gg 1$. Let ξ be (a measure of) the correlation length of h, so that $\langle h(\boldsymbol{r}) h(\boldsymbol{r}+\boldsymbol{R})\rangle$ vanishes when $|\boldsymbol{R}| \gg \xi$. If $l \gg \xi$, the coarse-

graining effectively entails taking the average over a large number (of the order of $(l/\xi)^2$) of independent regions, causing $\tilde{h}$ to acquire Gaussian characteristics on account of the central limit theorem.

There is a link between coarse-graining and the deterministic Kardar-Parisi-Zhang (KPZ) equation that was investigated in chapter 4. This equation is a diffusion equation that reads

$$\frac{\partial h}{\partial t} = \nu \nabla^2 h + \frac{\lambda}{2}(\nabla h)^2. \tag{5.3}$$

Following the substitution $u = \exp((\lambda/2\nu)h)$, this transforms into $\frac{\partial u}{\partial t} = \nu \nabla^2 u$, with the solution

$$u(\boldsymbol{r}, t) = \int \mathrm{d}^2 \tilde{\boldsymbol{r}} \, \frac{1}{4\pi\nu t} e^{-\frac{(\boldsymbol{r}-\tilde{\boldsymbol{r}})^2}{4\nu t}} u(\tilde{\boldsymbol{r}}, 0). \tag{5.4}$$

This relation has the same structure as that of the formula for coarse-graining: $u(\boldsymbol{r}, 0)$ can be identified as the original field and $l = \sqrt{\nu t}$ as the coarse-graining scale. The dimensionless coarse-graining function is therefore

$$f(\rho) = \frac{1}{4\pi} e^{-\rho^2/4}. \tag{5.5}$$

In summary, coarse-graining a non-Gaussian field over a large scale causes it to obtain Gaussian characteristics. A Gaussian field remains Gaussian, regardless of the scale over which it is coarse-grained.

5.2 LARGE SCALE LIMIT

In this section, the consequences of coarse-graining a non-Gaussian field h are investigated, in the limit that the coarse-graining scale becomes very large, as compared to the typical correlation length of the field. In particular, focus is put on the consequences for the densities of maxima and minima.

For a Gaussian field, the densities of maxima and minima are the same due to symmetry. For a non-Gaussian field, this is in general not the case. In chapter 4, a general expression was derived for the relative difference between the two densities for a perturbed Gaussian field, up to first order in the perturbation (see eq. (4.15)),

$$\Delta n \equiv \frac{n_{max} - n_{min}}{n_{max} + n_{min}} = \sqrt{\frac{6}{\pi\alpha}} \left(\frac{4}{3} \frac{\beta}{\sigma} + \frac{4}{9} \frac{\gamma}{\alpha} - \frac{10}{27} \frac{\delta}{\alpha} \right). \tag{5.6}$$

The parameters are second- and third-order correlations (see eq. (4.6)),

$$\sigma = \langle h_z h_{z^*} \rangle = C_2(h_z, h_{z^*}), \tag{5.7a}$$
$$\alpha = \langle h_{zz^*}^2 \rangle = C_2(h_{zz^*}, h_{zz^*}), \tag{5.7b}$$
$$\beta = \langle h_z h_{z^*} h_{zz^*} \rangle = C_3(h_z, h_{z^*}, h_{zz^*}), \tag{5.7c}$$
$$\gamma = \langle h_{zz^*}^3 \rangle = C_3(h_{zz^*}, h_{zz^*}, h_{zz^*}), \tag{5.7d}$$
$$\delta = \langle h_{zz} h_{z^*z^*} h_{zz^*} \rangle = C_3(h_{zz}, h_{z^*z^*}, h_{zz^*}). \tag{5.7e}$$

Here the subscripts denote partial differentiation, with $\partial_z = \frac{1}{2}(\partial_x - i\partial_y)$ and $\partial_{z^*} = \frac{1}{2}(\partial_x + i\partial_y)$, as before (eq. (3.9)). In each cumulant, the variables are all taken at the same point $\boldsymbol{r}$, e.g. $\sigma = C_2(h_z(\boldsymbol{r}) h_{z^*}(\boldsymbol{r}))$. Due to homogeneity, the choice of $\boldsymbol{r}$ is irrelevant.

Recall that, in general, correlations and cumulants are not the same; in an identity (see eqs. (3.4) and (3.5)), there would also be terms with correlations / cumulants of a single variable, but those are zero in this case (compare eq. (4.7)).

For the coarse-grained field $\tilde{h}$, the cumulants can be calculated in the following way (using β as an example):

$$\begin{aligned}\beta &= C_3(\tilde{h}_z, \tilde{h}_{z^*}, \tilde{h}_{zz^*}) \\ &= \partial_{z_1} \partial_{z_2^*} \partial_{z_3} \partial_{z_3^*} C_3(\tilde{h}(\boldsymbol{r_1}) \tilde{h}(\boldsymbol{r_2}) \tilde{h}(\boldsymbol{r_3})) \Big|_{\boldsymbol{r_1}=\boldsymbol{r_2}=\boldsymbol{r_3}} .\end{aligned} \tag{5.8}$$

Therefore, we see that the main ingredients for calculating the cumulants are $C_2(\tilde{h}(\boldsymbol{r_1}), \tilde{h}(\boldsymbol{r_2}))$ (for σ and α) and its third-order equivalent (for β, γ and δ).

Let ξ be a measure of the correlation length of h, in the sense that $h(\boldsymbol{r_1})$ and $h(\boldsymbol{r_2})$ can be said to be roughly uncorrelated when $|\boldsymbol{r_1} - \boldsymbol{r_2}| > \xi$. If $l \gg \xi$, then $\tilde{h}$ is nearly Gaussian (on account of the central limit theorem), so one can find the imbalance of maxima and minima using the approximation.

The second-order cumulant of $\tilde{h}$ can be expressed as

$$\begin{aligned}C_2(\tilde{h}(\boldsymbol{r_1}), \tilde{h}(\boldsymbol{r_2})) = \frac{1}{l^4} \iint \mathrm{d}^2\boldsymbol{R_1} \mathrm{d}^2\boldsymbol{R_2}\, C_2(h(\boldsymbol{R_1}), h(\boldsymbol{R_2})) \\ \times f\Big(\frac{\boldsymbol{R_1} - \boldsymbol{r_1}}{l}\Big) f\Big(\frac{\boldsymbol{R_2} - \boldsymbol{r_2}}{l}\Big).\end{aligned} \tag{5.9}$$

Since $C_2(h(\boldsymbol{R_1}), h(\boldsymbol{R_2}))$ is only appreciable when $|\boldsymbol{R_1} - \boldsymbol{R_2}| < \xi \ll l$, the approximation $f((\boldsymbol{R_2} - \boldsymbol{r_2})/l) \approx f((\boldsymbol{R_1} - \boldsymbol{r_2})/l)$ can be applied. This gives

$$C_2(\tilde{h}(\boldsymbol{r_1}), \tilde{h}(\boldsymbol{r_2})) = \frac{1}{l^4} \iint \mathrm{d}^2\boldsymbol{R_1}\mathrm{d}^2\boldsymbol{a}\, C_2(h(\boldsymbol{0}), h(\boldsymbol{a})) \times f\Big(\frac{\boldsymbol{R_1} - \boldsymbol{r_1}}{l}\Big) f\Big(\frac{\boldsymbol{R_1} - \boldsymbol{r_2}}{l}\Big), \tag{5.10}$$

where $\boldsymbol{a} = \boldsymbol{R_2} - \boldsymbol{R_1}$ and use was made of the homogeneity of h. This integration can now be split into two parts:

$$\begin{aligned} &C_2(\tilde{h}(\boldsymbol{r_1}), \tilde{h}(\boldsymbol{r_2})) \\ &\quad = \frac{1}{l^4} \int \mathrm{d}^2\boldsymbol{a}\, C_2(h(\boldsymbol{0}), h(\boldsymbol{a})) \int \mathrm{d}^2\boldsymbol{R_1} f\Big(\frac{\boldsymbol{R_1} - \boldsymbol{r_1}}{l}\Big) f\Big(\frac{\boldsymbol{R_1} - \boldsymbol{r_2}}{l}\Big) \\ &\quad = \frac{1}{l^2} I_2 K_2\Big(\frac{\boldsymbol{r_1}}{l}, \frac{\boldsymbol{r_2}}{l}\Big), \end{aligned} \tag{5.11}$$

where

$$I_2 \equiv \int \mathrm{d}^2\boldsymbol{a}\, C_2(h(\boldsymbol{0}), h(\boldsymbol{a})), \tag{5.12}$$

and

$$K_2(\boldsymbol{\rho_1}, \boldsymbol{\rho_2}) \equiv \int \mathrm{d}^2\boldsymbol{v}\, f(\boldsymbol{v} - \boldsymbol{\rho_1}) f(\boldsymbol{v} - \boldsymbol{\rho_2}). \tag{5.13}$$

For the third-order correlation an analogous derivation can be made. The result is

$$C_3(\tilde{h}(\boldsymbol{r_1}), \tilde{h}(\boldsymbol{r_2}), \tilde{h}(\boldsymbol{r_3})) = \frac{1}{l^4} I_3 K_3\Big(\frac{\boldsymbol{r_1}}{l}, \frac{\boldsymbol{r_2}}{l}, \frac{\boldsymbol{r_3}}{l}\Big), \tag{5.14}$$

with

$$I_3 \equiv \iint \mathrm{d}^2\boldsymbol{a}\mathrm{d}^2\boldsymbol{b}\, C_3(h(\boldsymbol{0}), h(\boldsymbol{a}), h(\boldsymbol{b})), \tag{5.15}$$

and

$$K_3(\boldsymbol{\rho_1}, \boldsymbol{\rho_2}, \boldsymbol{\rho_3}) \equiv \int \mathrm{d}^2\boldsymbol{v}\, f(\boldsymbol{v} - \boldsymbol{\rho_1}) f(\boldsymbol{v} - \boldsymbol{\rho_2}) f(\boldsymbol{v} - \boldsymbol{\rho_3}). \tag{5.16}$$

Note in particular that I_2 and I_3 depend on h only, whereas K_2 and K_3 depend only on f. Also note that none of these terms depends on l.

For the correlations, the z- and z^*-derivatives, as used in eq. (5.8), act only on $K_2(\frac{\boldsymbol{r_1}}{l}, \frac{\boldsymbol{r_2}}{l})$ and $K_3(\frac{\boldsymbol{r_1}}{l}, \frac{\boldsymbol{r_2}}{l}, \frac{\boldsymbol{r_3}}{l})$. Each derivative introduces a factor

$1/l$ as a result of the chain rule. It can therefore already be deduced how the relevant correlations scale with l:

$$\sigma \sim l^{-4}, \qquad \alpha \sim l^{-6}, \qquad \beta \sim l^{-8}, \qquad \gamma, \delta \sim l^{-10}, \tag{5.17}$$

and therefore $\Delta n \sim 1/l$. More precisely, we have the following:

$$\lim_{l/\xi \to \infty} \Delta n = \frac{c_h c_f}{l}, \tag{5.18}$$

where $c_h = I_3/I_2^{3/2}$ is a parameter that depends on the statistics of h only, and c_f is a parameter that depends on the coarse-graining function f only.

5.3 EXAMPLE

5.3.1 *Large scale limit*

As an example, let us consider the coarse-grain function from eq. (5.5). This gives

$$K_2(\boldsymbol{\rho_1}, \boldsymbol{\rho_2}) = \frac{1}{8\pi} e^{-\frac{1}{8}(\boldsymbol{\rho_1} - \boldsymbol{\rho_2})^2}, \tag{5.19a}$$

$$K_3(\boldsymbol{\rho_1}, \boldsymbol{\rho_2}, \boldsymbol{\rho_3}) = \frac{1}{48\pi^2} e^{-\frac{1}{4}\left(\rho_1^2 + \rho_2^2 + \rho_3^2 - \frac{1}{3}(\boldsymbol{\rho_1} + \boldsymbol{\rho_2} + \boldsymbol{\rho_3})^2\right)}. \tag{5.19b}$$

Applying the method as exemplified in eq. (5.8), we obtain

$$\beta = -\frac{I_3}{6912\pi l^8}. \tag{5.20}$$

Calculating all relevant cumulants ultimately leads to

$$\Delta n = \frac{2^{9/2}}{3^{11/2}\pi} \frac{I_3}{I_2^{3/2}} \frac{1}{l}, \tag{5.21}$$

for the KPZ-inspired Gaussian coarse-grain function eq. (5.5).

To get the parameter c_h, we use a non-Gaussian field of the form $h = H + \varepsilon H^2$, where H is a Gaussian field with a given two-point correlation function $\langle H(\boldsymbol{r_1}) H(\boldsymbol{r_2}) \rangle$, and ε is a small constant. The two-point correlation function of h differs from that of H only in second order of ε; this difference will be ignored.

The third-order cumulant of h is zero in leading order, since H is Gaussian, but in first order we find

$$\begin{aligned} C_3(h(\boldsymbol{r_1}),h(\boldsymbol{r_2}),h(\boldsymbol{r_3})) &= C_3(\varepsilon H(\boldsymbol{r_1})^2,H(\boldsymbol{r_2}),H(\boldsymbol{r_3})) \\ &\quad + C_3(H(\boldsymbol{r_1}),\varepsilon H(\boldsymbol{r_2})^2,H(\boldsymbol{r_3})) \\ &\quad + C_3(H(\boldsymbol{r_1}),H(\boldsymbol{r_2}),\varepsilon H(\boldsymbol{r_3})^2). \end{aligned} \tag{5.22}$$

This can be expanded with the help of Wick's theorem, e.g.

$$\begin{aligned} &C_3(H(\boldsymbol{r_1})^2,H(\boldsymbol{r_2}),H(\boldsymbol{r_3})) \\ &\quad = \langle H(\boldsymbol{r_1})^2 H(\boldsymbol{r_2})H(\boldsymbol{r_3})\rangle - \langle H(\boldsymbol{r_1})^2\rangle\langle H(\boldsymbol{r_2})H(\boldsymbol{r_3})\rangle \\ &\quad = 2\langle H(\boldsymbol{r_1})H(\boldsymbol{r_2})\rangle\langle H(\boldsymbol{r_1})H(\boldsymbol{r_3})\rangle, \end{aligned} \tag{5.23}$$

Therefore, the result is

$$\begin{aligned} &C_3(h(\boldsymbol{r_1}),h(\boldsymbol{r_2}),h(\boldsymbol{r_3})) \\ &\quad = 2\varepsilon\Big(\langle H(\boldsymbol{r_1})H(\boldsymbol{r_2})\rangle\langle H(\boldsymbol{r_1})H(\boldsymbol{r_3})\rangle \\ &\qquad + \langle H(\boldsymbol{r_2})H(\boldsymbol{r_3})\rangle\langle H(\boldsymbol{r_2})H(\boldsymbol{r_1})\rangle \\ &\qquad + \langle H(\boldsymbol{r_3})H(\boldsymbol{r_1})\rangle\langle H(\boldsymbol{r_3})H(\boldsymbol{r_2})\rangle\Big) \end{aligned} \tag{5.24}$$

If we consider the Gaussian two-point correlation function

$$\langle H(\boldsymbol{r_1})H(\boldsymbol{r_2})\rangle = e^{-\frac{1}{2}k_0^2(\boldsymbol{r_1}-\boldsymbol{r_2})^2}, \tag{5.25}$$

which corresponds to the spectrum $A(k)^2 \sim \exp(-k^2/(2k_0^2))$, we get

$$I_2 = \int \mathrm{d}^2\boldsymbol{a}\, C_2(0,\boldsymbol{a}) = \int \mathrm{d}^2\boldsymbol{a}\, \langle H(0)H(\boldsymbol{a})\rangle = \frac{2\pi}{k_0^2}, \tag{5.26}$$

and

$$\begin{aligned} I_3 &= \iint \mathrm{d}^2\boldsymbol{a}\mathrm{d}^2\boldsymbol{b}\, C_3(h(\boldsymbol{0}),h(\boldsymbol{a}),h(\boldsymbol{b})) \\ &= \iint \mathrm{d}^2\boldsymbol{a}\mathrm{d}^2\boldsymbol{b}\, 2\varepsilon\Big(e^{-\frac{1}{2}k_0^2(\boldsymbol{a}^2+\boldsymbol{b}^2)} + e^{-\frac{1}{2}k_0^2(\boldsymbol{a}^2+(\boldsymbol{a}-\boldsymbol{b})^2)} \\ &\qquad\qquad + e^{-\frac{1}{2}k_0^2(\boldsymbol{b}^2+(\boldsymbol{a}-\boldsymbol{b})^2)}\Big) \\ &= \frac{24\pi^2\varepsilon}{k_0^4}. \end{aligned} \tag{5.27}$$

This gives $c_h = I_3/I_2^{3/2} = 6\sqrt{2\pi}\varepsilon/k_0$.

Combined with the coarse-grain function as given above, we thus get

$$\Delta n \to \frac{c_f c_h}{l} = \frac{64}{81\sqrt{3\pi}k_0}\frac{\varepsilon}{l}. \tag{5.28}$$

5.3.2 *Analytic result*

The separation of the dependence on f and h, as displayed in eq. (5.18), is only valid in the limit of $l \gg \xi$. In general however, f and h can no longer be treated separately. Due to the complexity of the integrals involved, it is only in very specific cases possible to calculate Δn analytically, for arbitrary l. Not coincidentally, the f and h chosen in the previous section allow precisely this.

For example, the exact expression for β is

$$\begin{aligned}\beta &= \langle \tilde{h}_z \tilde{h}_{z^*} \tilde{h}_{zz^*} \rangle \\ &= \partial_{z_1} \partial_{z_2^*} \partial_{z_3} \partial_{z_3^*} \iiint \mathrm{d}^2\boldsymbol{u_1} \mathrm{d}^2\boldsymbol{u_2} \mathrm{d}^2\boldsymbol{u_3} \Big(K(\boldsymbol{u_1}) K(\boldsymbol{u_2}) K(\boldsymbol{u_3}) \\ &\qquad \times \langle h(\boldsymbol{r_1} + \boldsymbol{u_1}) h(\boldsymbol{r_2} + \boldsymbol{u_2}) h(\boldsymbol{r_3} + \boldsymbol{u_3}) \rangle \Big) \Big|_{\boldsymbol{r_1} = \boldsymbol{r_2} = \boldsymbol{r_3}} . \end{aligned} \tag{5.29}$$

The three-point correlation can be expanded in the same way as before (see eqs. (5.22) and (5.23)). The final result is

$$\beta = -\frac{k_0^4 \varepsilon}{2(1 + 2k_0^2 l^2)^2 (1 + 6k_0^2 l^2)^2}, \tag{5.30}$$

Determining and combining all the correlations gives the following result, which is exact with respect to l but still perturbative with respect to ε:

$$\Delta n = \frac{64 a^3 (1 + 4a)^{7/2} \varepsilon}{\sqrt{3\pi} (1 + 2a)^3 (1 + 6a)^4}, \tag{5.31}$$

where $a \equiv k_0^2 l^2$. In the limit of large l ($a \gg 1$) we find that it matches the perturbative result eq. (5.28).

One may also note that eq. (5.31) matches the result from the deterministic KPZ equation for the Gaussian spectrum (eq. (4.32)), following the substitution $\nu t \to l^2$.

5.4 NUMERICAL TESTS

5.4.1 *Setup*

The validity of eq. (5.31) was checked using computer simulations. The setup of the simulations and the identification of the extrema is similar to the process used in previous chapters and outlined in appendix A: For

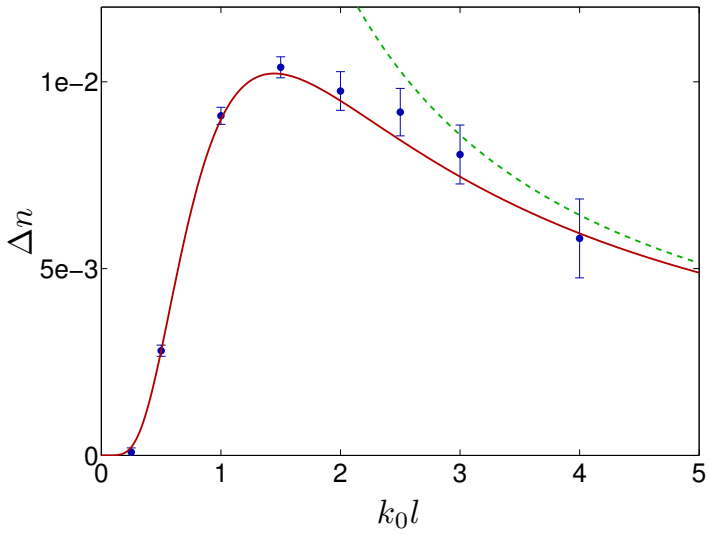

Figure 5.1: The imbalance between maxima and minima Δn for a field $h = H + \varepsilon H^2$, where H is a Gaussian field with a Gaussian power spectrum (with typical wavelength k_0^{-1}), coarse-grained with a Gaussian function $f(r) = \exp(r^2/(4l^2))$. The solid line is the exact result eq. (5.31) (perturbative in ε but not in l), while the data points stem from simulations. The dashed line is the theoretical result for large l, eq. (5.28).

each data point, corresponding to a particular value of l, thousands of Gaussian fields $H(\boldsymbol{r})$ were generated, following eq. (1.9). To each field, the perturbation εH^2 was added to it, with $\varepsilon = 0.1$. This new field h was then coarse-grained, after which the extrema were identified.

5.4.2 *Results*

Fig. 5.1 shows the theoretical result, as well as results from simulations at various values of l. As can be seen, there is an excellent agreement between the two. Also shown is the prediction of eq. (5.28), illustrating the large l limit, which matches well for $k_0 l \gg 1$.

An interesting point is that, for no coarse-graining at all, the imbalance is very close to zero. This general feature of local perturbations of the type $h = H + f(H)$ was already established in detail in chapter 2. Measuring the imbalance between maxima and minima thus does not reveal the non-Gaussianity of h. However, it is clear from fig. 5.1 that coarse-graining may

significantly increase the imbalance to measurable values, thereby not only granting the possibility of detecting non-Gaussianity, but also potentially identifying the size and type of the perturbation.

5.4.3 *Large scale coarse-graining*

It is difficult to test the formula for a large coarse-graining (eq. (5.18)) accurately in a numerical setting, since the size of the system is limited.

As explained in appendix A, the periodic boundary conditions are enforced by only using waves with wave vectors $\boldsymbol{k}$ for which the components are multiples of $\frac{2\pi}{L}$, where L is the system size. As long as L is large, this quantization has a high enough resolution to be of no significant source of error.

Now consider what happens when it is coarse-grained. We already saw in eq. (5.2) that, effectively, its amplitude spectrum changes:

$$\tilde{A}(k) = A(k)\left(\int \mathrm{d}^2\boldsymbol{u}\, K(\boldsymbol{u}) e^{i\boldsymbol{k}\cdot\boldsymbol{u}} \right) = A(k)\left(\int \mathrm{d}^2\boldsymbol{\rho}\, f(\rho) e^{il\boldsymbol{k}\cdot\boldsymbol{\rho}} \right). \quad (5.32)$$

In the limit that $lk \gg 1$, the phase factor causes the integral to vanish. Hence, for large l, only the waves with small wave vector k (in the order of $1/l$ or less) prevail. This is the technical justification of the statement that coarse-graining causes a field to become smoother, and thus dominated by long waves.

However, in combination with the periodic boundary conditions, this means that, in the case that l becomes comparable to L, there are only a few wave vectors left that are of importance from the coarse-graining point of view. The accuracy with which the simulated coarse-grained field represents an actual field thus becomes compromised. Therefore, L should be larger than l. Increasing L however naturally increases computation time. As a result, probing large coarse-grain scales indirectly requires a lot of computation time, making it difficult to properly explore the regime in which the imbalance Δn decays as $1/l$.

5.5 CONCLUSIONS

Coarse-graining a non-Gaussian field has the effect of giving it Gaussian characteristics, as the coarse-graining scale goes to infinity. More precisely, when this scale l is significantly larger than the correlation length of the

field, the imbalance between maxima and minima (which is zero for Gaussian fields) scales as $1/l$. The corresponding constant factor can be written as the product of two independent scalars: One depends on the field only, whereas the other depends on the coarse-graining function only.

Coarse-graining a signal on purpose can also be useful, because the imbalance between maxima and minima depends on the length scale of the coarse-graining for a non-Gaussian field. For example, locally perturbed fields, such as $h = H + \varepsilon H^2$, where H is Gaussian, do not show a significant imbalance between maxima and minima (if the resolution is perfect). However, coarse-graining—which would not produce an effect for Gaussian fields—creates an imbalance allowing ε to be measured. In general, coarse-graining by various amounts can give a multitude of data that can be used to shed light on some unknown parameters of the perturbation.

APPENDICES

A

COMPUTER SIMULATIONS

In order to verify our theoretical results, we use a large number of computer-generated realizations of the Gaussian field H (typically a few thousand), each with the same spectrum $A(k)$ but random phases $\phi_{\boldsymbol{k}}$. We then apply the desired transformation and extract the statistics of interest.

The fields are generated following the definition given in eq. (1.9),

$$H(\boldsymbol{r}) = \sum_{\boldsymbol{k}} A(k) \cos(\boldsymbol{k} \cdot \boldsymbol{r} + \phi_{\boldsymbol{k}}), \tag{A.1}$$

by adding together a large number of waves sampled from $\boldsymbol{k}$-space, each with the appropriate amplitude $A(k)$ and a random phase vector $\phi_{\boldsymbol{k}}$. The fields are defined on a square with double periodic boundary conditions, i.e. $H(x, y) = H(x + L, y) = H(x, y + L)$, in order to reduce finite-size effects. This is accomplished by only using waves with wave vectors $\boldsymbol{k}$ of which the x and y-components are multiples of $2\pi / L$.

The summation in eq. (A.1) is restricted to wave vectors with a magnitude below a certain threshold k_{max}. In order to minimize the potential effects of this cutoff, we choose spectra for which $A(k)$ decays very quickly or is zero for large k, such as the disk spectrum

$$A(k)^2 \propto \theta(k_0 - k), \tag{A.2}$$

and the Gaussian spectrum

$$A(k)^2 \propto \exp(-k^2 / 2k_0^2). \tag{A.3}$$

Finally, L is chosen in relation to k_{max} such that (1) the sum in eq. (A.1) features at least a few hundred waves (recall that L influences this number via the periodic boundary conditions) and that (2) L is at least a few times $2\pi / \sqrt{K_2}$, which is a measure of the typical wavelength of the spectrum. An example of a Gaussian field generated in this way is shown in fig. 1.1.

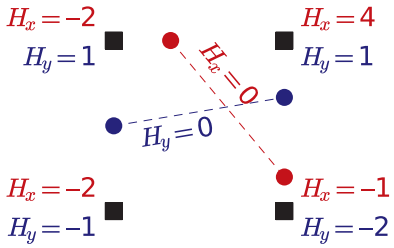

Figure A.1: Identifying a critical point. The four black squares are grid points at which H_x and H_y are known. At the red (blue) dots, $H_x = 0$ ($H_y = 0$) under the assumption that H_x (H_y) is linear between the two grid points. The two contour lines $H_x = 0$ and $H_y = 0$ then intersect inside the square, indicating the existence of a critical point.

The resulting formula for H is then evaluated at grid points only. The distance between neighboring grid points is taken to be much smaller (by a factor of 50 roughly) than the typical wavelength. Along with H itself, we also calculate its first, second and third derivatives (if required) at these grid points. The field H is then transformed into h using the perturbation of interest. The derivatives are transformed accordingly, or in the case of nonlocal perturbations, calculated numerically.

We use a very efficient approach to identifying critical (or umbilical) points and their type; we will use critical points as an example, but the case of umbilics is analogous.

Every square of four neighboring grid points is considered. If H_x or H_y has the same sign at all four points, we infer that it is not zero anywhere inside the square, which leads to the conclusion that the square does not contain a critical point. Otherwise, there would necessarily be at least two pairs of neighboring grid points with a different sign of H_x. For each pair, it is assumed that H_x changes linearly between the two points, which allows to pinpoint two points along the edges of the square where $H_x = 0$. The contour line $H_x = 0$ is then assumed to be a straight line between these two points. The same recipe is applied to H_y, after which it is determined whether the two contour lines crossed. The intersection (if present) is then a critical point. This idea is illustrated in fig. A.1.

It is also possible for all four neighboring points to have opposite signs of H_x (or H_y). This results in four points along the border of the square with $H_x = 0$, but without any information about which two pairs should be connected by a contour line. In combination with the two points with $H_y = 0$ it can however be established what the parity of the number of

intersections (i.e. critical points) is. We then simply assume this number to be 0 or 1. This case is sufficiently rare (provided that the grid is small enough) to not have a noticeable effect on the results.

Once established whether the square under consideration contains a critical point, the type is determined by averaging the values of H_{xx}, H_{yy} and H_{xy} at the four grid points and evaluating the signs of $H_{xx}H_{yy} - H_{xy}^2$ and $H_{xx} + H_{yy}$.

Although this method clearly does not always correctly determine the existence of a critical point or its type, it is not biased toward one outcome. Therefore, the mistakes that are made will get averaged out when statistics are taken over a large number of critical points. With regard to getting good statistics, the speed of this method is a big advantage.

This method, along with the proper values of k_{max}, L and the grid size, was thoroughly tested on Gaussian fields (for which the statistical outcomes are known from theory) to verify its validity, before applying it to the non-Gaussian fields under investigation.

B

ASYMPTOTES FOR A VERY SMALL NON-GAUSSIANITY

In the limit where z is very large and negative, $g(z)$ can be evaluated asymptotically. One can use the exact expression for $g(z)$ (eq. (2.35)), but returning to the original integral eq. (2.33) gives more insight (and makes the calculations shorter). The exponential weight in the integral is peaked at

$$s = \frac{1}{2}(H_{xx} + H_{yy}) = -\frac{1}{2}K_2 z. \tag{B.1}$$

Therefore, when $-z$ is large, the integrand is exponentially small unless s is large and positive, since the width of the distribution remains fixed. This allows us to extend the range of integration of s to include the negative reals and that of r to encompass all positive reals, since the additional parts of the range have a very small weight. Then the integral can be worked out exactly, giving

$$g(z) \approx \sqrt{\frac{6}{\pi}}\lambda z^2 e^{-z^2/2}, \tag{B.2}$$

apart from small corrections, when $-z$ is large and positive. We next substitute back in eq. (2.4). After noting that P dominates over Q we can use integration by parts to evaluate the integral asymptotically: For $A \to \infty$ we have

$$\int_A^\infty \mathrm{d}x\, z^2 e^{-z^2/2} \approx A e^{-A^2/2}. \tag{B.3}$$

This gives

$$\Delta n \approx \sqrt{\frac{3}{2\pi}}\frac{\lambda}{\varepsilon} e^{-1/(8\varepsilon^2)}. \tag{B.4}$$

C

PROOF OF CUMULANT IDENTITY

In this section we prove the identity

$$C_n(f(H_1), H_2, \ldots, H_n) = \langle f^{(n-1)}(H_1)\rangle \langle H_1 H_2\rangle \langle H_1 H_3\rangle \ldots \langle H_1 H_n\rangle, \tag{C.1}$$

for Gaussian variables H_i.

Recall the definition of a cumulant, eq. (3.3). The generating function χ is the Fourier transform of the probability distribution (see eq. (3.1)), which for Gaussian variables is eq. (2.8). This leads to the identity

$$C_n(f(H_1), H_2, \ldots, H_n) = (-i)^n \frac{\partial}{\partial\lambda_1} \ldots \frac{\partial}{\partial\lambda_n} \log \int \mathrm{d}h_1 \ldots \mathrm{d}h_n \left(e^{i(\lambda_1 f(h_1) + \lambda_2 h_2 + \ldots + \lambda_n h_n)} \times \frac{\exp\left(-\frac{1}{2}\sum_{ij} \sigma_{ij}^{-1} h_i h_j\right)}{(2\pi)^{n/2}\sqrt{\det\sigma}} \right) \Bigg|_{\lambda_1 = \ldots = \lambda_n = 0}. \tag{C.2}$$

First, the integration over h_2 through h_n is performed. This partial Fourier transform is not trivial. If h_1 were included, the answer would be

simply eq. (3.6). We can however use this result and take the inverse Fourier transform of it with respect to λ_1 to get the desired result:

$$\begin{aligned}
&\int \mathrm{d}h_2 \dots \mathrm{d}h_n \, e^{i(\lambda_2 h_2 + \dots + \lambda_n h_n)} \frac{\exp\left(-\frac{1}{2}\sum_{ij}\sigma_{ij}^{-1} h_i h_j\right)}{(2\pi)^{n/2}\sqrt{\det\sigma}} \\
&\quad = \int \frac{\mathrm{d}\lambda_1}{2\pi} e^{-i\lambda_1 h_1} \exp\left(-\tfrac{1}{2}\sum_{ij}\sigma_{ij}\lambda_i\lambda_j\right) \\
&\quad = \int \frac{\mathrm{d}\lambda_1}{2\pi} \exp\left(-\tfrac{1}{2}\sigma_{11}\lambda_1^2 - \Big(ih_1 + \sum_{j\geq 2}\sigma_{1j}\lambda_j\Big)\lambda_1 - \tfrac{1}{2}\sum_{i,j\geq 2}\sigma_{ij}\lambda_i\lambda_j\right) \\
&\quad = \frac{1}{\sqrt{2\pi\sigma_{11}}} \exp\left(\frac{1}{2\sigma_{11}}\Big(ih_1 + \sum_{j\geq 2}\sigma_{1j}\lambda_j\Big)^2 - \tfrac{1}{2}\sum_{i,j\geq 2}\sigma_{ij}\lambda_i\lambda_j\right). \qquad \text{(C.3)}
\end{aligned}$$

The integration was performed by completing the square. Now we do the Fourier transform with respect to h_1 and include the logarithm present in eq. (C.2), which leads to

$$\begin{aligned}
&\log \int \mathrm{d}h_1 \dots \mathrm{d}h_n e^{i(\lambda_1 f(h_1) + \lambda_2 h_2 + \dots + \lambda_n h_n)} \frac{\exp\left(-\frac{1}{2}\sum_{ij}\sigma_{ij}^{-1} h_i h_j\right)}{(2\pi)^{n/2}\sqrt{\det\sigma}} \\
&\quad = \log \int \mathrm{d}h_1 e^{i\lambda_1 f(h_1)} \frac{1}{\sqrt{2\pi\sigma_{11}}} e^{\frac{1}{2\sigma_{11}}[ih_1 + \sum_{j\geq 2}\sigma_{1j}\lambda_j]^2 - \frac{1}{2}\sum_{i,j\geq 2}\sigma_{ij}\lambda_i\lambda_j} \\
&\quad = -\tfrac{1}{2}\sum_{i,j\geq 2}\sigma_{ij}\lambda_i\lambda_j \\
&\qquad + \log \int \mathrm{d}h_1 e^{i\lambda_1 f(h_1)} \frac{1}{\sqrt{2\pi\sigma_{11}}} e^{\frac{1}{2\sigma_{11}}[ih_1 + \sum_{j\geq 2}\sigma_{1j}\lambda_j]^2}. \qquad \text{(C.4)}
\end{aligned}$$

In accordance with eq. (C.2), we must take the derivative of this equation with respect to the λ's and set them to zero. First the derivative with respect to λ_1 is taken. This causes the first term to vanish, since it does not depend on λ_1. This simplification can be regarded as the main reason why the final result depends on f in a rather simple way. What remains is

$$\begin{aligned}
&-i\frac{\partial}{\partial\lambda_1} \log \int \mathrm{d}h_1 e^{i\lambda_1 f(h_1)} \frac{1}{\sqrt{2\pi\sigma_{11}}} e^{\frac{1}{2\sigma_{11}}[ih_1 + \sum_{j\geq 2}\sigma_{1j}\lambda_j]^2}\Bigg|_{\lambda_1=0} \\
&\quad = \frac{\int \mathrm{d}h_1 \, f(h_1) \exp\left(\frac{1}{2\sigma_{11}}\Big(ih_1 + \sum_{j\geq 2}\sigma_{1j}\lambda_j\Big)^2\right)}{\int \mathrm{d}h_1 \, \exp\left(\frac{1}{2\sigma_{11}}\Big(ih_1 + \sum_{j\geq 2}\sigma_{1j}\lambda_j\Big)^2\right)} \\
&\quad = \frac{1}{\sqrt{2\pi\sigma_{11}}} \int \mathrm{d}h_1 \, f(h_1) e^{\frac{1}{2\sigma_{11}}[ih_1 + \sum_{j\geq 2}\sigma_{1j}\lambda_j]^2}. \qquad \text{(C.5)}
\end{aligned}$$

For each λ_k with $k \geq 2$ the derivative yields

$$-i\frac{\partial}{\partial\lambda_k}\, e^{\frac{1}{2\sigma_{11}}[ih_1+\sum_{j\geq 2}\sigma_{1j}\lambda_j]^2} = -i\frac{\sigma_{1k}}{\sigma_{11}}\Big(ih_1+\sum_{j\geq 2}\sigma_{1j}\lambda_j\Big)e^{\frac{1}{2\sigma_{11}}[ih_1+\sum_{j\geq 2}\sigma_{1j}\lambda_j]^2}. \tag{C.6}$$

Applying this for all k and subsequently setting all λ_k to zero then gives

$$(-i)^{n-1}\frac{\partial}{\partial\lambda_2}\cdots\frac{\partial}{\partial\lambda_n}\, e^{\frac{1}{2\sigma_{11}}[ih_1+\sum_{j\geq 2}\sigma_{1j}\lambda_j]^2} = \left(\frac{h_1}{\sigma_{11}}\right)^{n-1}\left(\prod_{j\geq 2}\sigma_{1j}\right)e^{-h_1^2/(2\sigma_{11})}. \tag{C.7}$$

This results in

$$C_n(f(H_1),H_2,\ldots,H_n) = \left(\prod_{j\geq 2}\sigma_{1j}\right)\frac{1}{\sqrt{2\pi\sigma_{11}}}\int \mathrm{d}h_1\, f(h_1)\left(\frac{h_1}{\sigma_{11}}\right)^{n-1} e^{-h_1^2/(2\sigma_{11})}. \tag{C.8}$$

Integrating by parts $n-1$ times leads to

$$C_n(f(H_1),H_2,\ldots,H_n) = \left(\prod_{j\geq 2}\sigma_{1j}\right)\frac{1}{\sqrt{2\pi\sigma_{11}}}\int \mathrm{d}h_1\, f^{(n-1)}(h_1)e^{-h_1^2/(2\sigma_{11})}. \tag{C.9}$$

Finally, we identify the integral (along with the prefactor) as the expectation value of $f^{(n-1)}$ and $\sigma_{1j} = \langle H_1 H_j\rangle$, which gives us

$$C_n(f(H_1),H_2,\ldots,H_n) = \langle f^{(n-1)}(H_1)\rangle\langle H_1H_2\rangle\langle H_1H_3\rangle\ldots\langle H_1H_n\rangle, \tag{C.10}$$

the equation we set out to prove.

D

HIGHER ORDER CUMULANTS

In this section it is demonstrated that, for an initially Gaussian field evolving according to a diffusion equation with a perturbative nonlinear term, the cumulants become smaller as the order increases (i.e. they are of higher order in the perturbation).

Consider the equation

$$\dot{h}_n = \sum_m A_{nm} + \varepsilon \sum_{p,q} B_{npq} h_p h_q, \tag{D.1}$$

with the initial condition

$$h_n(0) = H_n, \tag{D.2}$$

where the H_n's are a set of variables with a joint Gaussian distribution. These coupled differential equations are a simple model of a nonlinearity, with the lowest order (quadratic), and they also include the KPZ equation as a special case, if it is discretized. This differential equation illustrates the general principle that cumulants of a high order are very small if the nonlinear term in the differential equation is small (unless one waits long enough for these cumulants to build up).

For this family of equations the precise result is that, after a finite period of time, the k-th order cumulants of any of the h_n's are of order at most ε^{k-2} if $k > 2$ (for $k = 1$ or $k = 2$ they are bounded).

There are two steps in the proof: First, we find how h_n depends on the initial conditions, and show that it has the form of a power series in ε. The result is that

$$h_n(t) = F_n^{(0)}(\{H_j\}) + \varepsilon F_n^{(1)}(\{H_j\}) + \varepsilon^2 F_n^{(2)}(\{H_j\}) + \dots \tag{D.3}$$

where $F_n^{(0)}$ is a linear function, $F_n^{(1)}$ is quadratic, etc. So the dependence of a given term on the H_j's is polynomial; the dependence on t is all in the coefficients of these polynomials.

In other words, h_n can be expressed in the form of a nonlinear function of a Gaussian, the same type of function whose cumulants we calculated in chapter 3. We will see that many of the cumulants vanish; this is the second step of the proof. We calculate the cumulants,

$$C_k(h_{n_1},\ldots,h_{n_k}) = \sum_{r=0}^{\infty} \varepsilon^r \sum_{\substack{r_1,r_2,\ldots,r_k \\ \sum r_i = r}} C_k(F_{n_1}^{(r_1)},\ldots,F_{n_k}^{(r_k)}). \tag{D.4}$$

All the terms up to order $r = k-3$ vanish, so that the remaining terms are of order ε^{k-2} or smaller. This is a consequence of a general theorem: A cumulant of k polynomials in Gaussian variables is zero if

$$k > 1 + \frac{d}{2}, \tag{D.5}$$

where d is the sum of the degrees of the polynomials. In $C_k(F_{n_1}^{(r_1)},\ldots,F_{n_k}^{(r_k)})$ the sum of the degrees is $d = \sum_i r_i + 1 = r + k$. If $r \le k-3$, then eq. (D.5) follows, so the cumulant vanishes.

D.1 POWER SERIES SOLUTION

Expand $h_n(t) = \sum_r \varepsilon^r h_n^{(r)}(t)$ and substitute it into eq. (D.1), and then match the coefficients of ε^r. This gives the relation

$$\frac{\partial}{\partial t} h_n^{(r)}(t) - \sum_m A_{nm} h_m^{(r)}(t) = \sum_{p,q} \sum_{r_1=0}^{r-1} B_{npq} h_p^{(r_1)}(t) h_q^{(r-1-r_1)}(t). \tag{D.6}$$

Here, everything depending on $h^{(r)}$ is on the left-hand side; everything on the right-hand side depends on earlier terms in the series, $h^{(r_1)}$ with $r_1 < r$. This means that one can solve the equations recursively: First find the h's up to $r_1 = r-1$, then substitute it into the right-hand side of the equation and then solve for $h^{(r)}$, which is straightforward because it is a linear equation with a source. We only need to know the initial conditions, which are

$$h_n^{(0)} = H_n; \quad h_n^{(r)} = 0 \text{ for } r \ge 1. \tag{D.7}$$

The solutions to the equations are given as follows:

$$h_n^{(0)}(t) = \sum_m \left[e^{At}\right]_{nm} H_m, \tag{D.8}$$

$$h_n^{(r)}(t) = \int_0^t \mathrm{d}t' \sum_{m,p,q} \sum_{r_1=0}^{r-1} \left[e^{A(t-t')}\right]_{nm} B_{mpq} \times h_p^{(r_1)}(t') h_q^{(r-1-r_1)}(t'), \tag{D.9}$$

where e^{At} is the exponential of the matrix At, which is just a set of functions of t.

These functions are all polynomials in the H_j's. First, $h_n^{(0)}$ is obviously linear. Entering $r = 1$ in eq. (D.9) shows that $h_n^{(1)}$ is the sum and integral of $h_p^{(0)} h_q^{(0)}$, which is thus quadratic in the H_j's. Now we can find the general dependence inductively: Assume that it has already been shown that $h_n^{(r_1)}$ is a degree $r_1 + 1$ polynomial in the H_j's for $r_1 < r$. Then $h_p^{(r_1)}(t') h_q^{(r-1-r_1)}(t')$ is of degree $r + 1$, and thus $h^{(r)}$ is as well.

D.2 VANISHING CUMULANTS

We will calculate the cumulants of polynomials in the H_j's by reducing them to cumulants of the H_j's themselves, which are Gaussian. A helpful identity for this expresses $C(xy, z_1, \ldots, z_q)$ where x, y, z_i are any random variables in terms of simpler cumulants. The identity is

$$C(xy, z_1, \ldots, z_q) = C(x, y, z_1, \ldots, z_q) + \sum_{S \cup T = \{1,\ldots,q\}} C(x, z_S) C(y, z_T). \tag{D.10}$$

The sum is over all ways of partitioning the indices of the z's into two sets S and T. The symbol z_S is short for the list of all the z's corresponding to the indices S.

Here is an example:

$$C(xy, u, v) = C(x, y, u, v) + C(x)C(y, u, v) + C(x, u)C(y, v) + C(x, v)C(y, u) + C(x, u, v)C(y). \tag{D.11}$$

A proof of this relation can be obtained using induction. First note that it is trivially true for $q = 0$, since $C(x, y) = \langle xy \rangle - \langle x \rangle \langle y \rangle$. Now we assume the relation to hold for all $q' < q$. Consider the identity (see e.g. chapter 3 or [31])

$$\langle x_1 \ldots x_n \rangle = \sum C(x_{S_1}) C(x_{S_2}) \ldots C(x_{S_m}), \tag{D.12}$$

where the sum is taken over all the ways in which the set $\{1, \ldots, n\}$ can be partitioned into disjoint subsets S_i. If we apply this identity to the set

$\{x, y, z_1, \ldots, z_q\}$ and group together the terms for which x and y are in the same subset or in different ones, we find

$$\begin{aligned}\langle xyz_1 \ldots z_n\rangle &= \sum_{U,\{V_i\}} C(x, y, z_U)C(z_{V_1}) \ldots C(z_{V_m}) \\ &\quad + \sum_{S,T,\{V_i\}} C(x, z_S)C(y, z_T)C(z_{V_1}) \ldots C(z_{V_m}) \\ &= \sum_{U,\{V_i\}} C(z_{V_1}) \ldots C(z_{V_m}) \\ &\qquad \times \left(C(x, y, z_U) + \sum_{S\cup T=U} C(x, z_S)C(y, z_T)\right). \quad \text{(D.13)}\end{aligned}$$

We can also choose to expand $\langle xyz_1 \ldots z_n\rangle$ while treating xy as a single variable, which results in

$$\langle xyz_1 \ldots z_n\rangle = \sum_{U,\{V_i\}} C(xy, z_U)C(z_{V_1}) \ldots C(z_{V_m}). \quad \text{(D.14)}$$

The two decompositions into cumulants should be equal. By induction, we can pose

$$C(xy, z_U) = C(x, y, z_U) + \sum_{S\cup T=U} C(x, z_S)C(y, z_T), \quad \text{(D.15)}$$

for all $U \neq \{1, \ldots, q\}$. It then easily follows that the relation must also hold for $U = \{1, \ldots, q\}$.

We will use this identity to prove that if $p_1, \ldots p_k$ are degree $d_1, \ldots d_k$ polynomials in Gaussian variables and $d = \sum_i d_i$, then $C_k(p_1, \ldots, p_k)$ vanishes if eq. (D.5) is satisfied. We shall first demonstrate the procedure using a simple example: $C(H^2, H^2, H, H, H)$ where H is a Gaussian variable. We will reduce this to cumulants of H by using eq. (D.10); that will mean we have to apply the identity twice to split up both H^2's. After the first time, we have a sum featuring one term with a single cumulant, $C(H^2, H, H, H, H)$, while the other terms are products of two cumulants. Furthermore, there is only one H^2 left in each term. After applying eq. (D.10) a second time, we are left with products of at most three cumulants. Since there are 7 H's distributed among these cumulants, at least one of the cumulants in each product is of at least third order, and hence zero because the H's are Gaussian. Hence $C(H^2, H^2, H, H, H) = 0$.

In general, we first use the multilinear property of the cumulant function (i.e. $C(x + y, z, w, \ldots) = C(x, z, w, \ldots) + C(y, z, w, \ldots)$) to reduce each of

the variables to one term (which is a product of some of the H's). It takes $d-k$ applications of eq. (D.10) to split all the variables up into individual H's, because it takes $d_i - 1$ steps to factor the i-th variable, for a total of $\sum_i d_i - 1 = d - k$ steps. Since each application of eq. (D.10) adds at most one cumulant to each term, in the end each term has at most $d - k + 1$ factors of C. This is less than $\frac{d}{2}$ by eq. (D.5). But there are a total of d variables H's that are split among them. Hence one of the factors is a third-order cumulant or higher, which means that it has to be zero.

Now this result can be combined with eq. (D.3) to prove that the k-th order cumulants of the h_n's are of order ε^{k-2}, as we showed above.

BIBLIOGRAPHY

[1] A.-L. Barabási and H. E. Stanley. *Fractal Concepts in Surface Growth*. Cambridge: Cambridge University Press, 1995.

[2] N. B. Baranova, B. Ya. Zel'dovich, A. V. Mamaev, N. F. Pilipetskii, and V. V. Shkukov. "Dislocations of the wave-front of a speckle-inhomogeneous field (theory and experiment)." In: *JETP Lett.* 33 (1981), p. 195.

[3] M. V. Berry and M. R. Dennis. "Polarization singularities in isotropic random vector waves." In: *Proc. R. Soc. Lond. A* 457 (2001), pp. 141–155.

[4] M. V. Berry and J. H. Hannay. "Umbilic points on Gaussian random surfaces." In: *J. Phys. A: Math. Gen.* 10 (1977), p. 1809.

[5] A. J. Bray. "Theory of Phase Ordering Kinetics." In: *Adv. Phys.* 43 (1994), pp. 357–459.

[6] A. Cavagna, J. P. Garrahan, and I. Giardina. "Energy distribution of maxima and minima in a one-dimensional random system." In: *Phys. Rev. E* 59 (1999), pp. 2808–2811.

[7] P. M. Chaikin and T. C. Lubensky. *Principles of Condensed Matter Physics*. Cambridge: Cambride University Press, 2000.

[8] J. C. Dainty. "The statistics of speckle patterns." In: *Prog. Opt.* 14 (1976), pp. 1–46.

[9] G. Darboux. *Leçons sur la Théorie Générale des Surfaces*. Paris: Gauthier-Villars, 1896.

[10] M. R. Dennis. "Correlations and screening of topological charges in Gaussian random fields." In: *J. Phys. A: Math. Gen.* 36 (2003), pp. 6611–6628.

[11] M. R. Dennis. "Polarization singularity anisotropy: determining monstardom." In: *Optics Letters* 33 (2008), pp. 2572–2574.

[12] M. R. Dennis and K. Land. "Probability Density of the Multipole Vectors for a Gaussian Cosmic Microwave Background." In: *Mon. Not. R. Astron. Soc.* 383 (2008), pp. 424–434.

[13] S. Dodelson. *Modern Cosmology*. Amsterdam: Academic Press, 2003.

[14] I. E. Dzyaloshinskii. "Theory of disinclinations in liquid crystals." In: *Sov. Phys. JETP* 31 (1970), p. 773.

[15] F. Flossmann, K. O'Holleran, M. R. Dennis, and M. J. Padgett. "Polarization Singularities in 2D and 3D Speckle Fields." In: *Phys. Rev. Lett.* 100 (2008), p. 203902.

[16] G. Foltin. "Signed zeros of Gaussian vector fields–density, correlation function and curvature." In: *J. Phys. A: Math. Gen.* 36 (2003), pp. 1729–1741.

[17] G. Foltin. "The distribution of extremal points of Gaussian scalar fields." In: *J. Phys. A: Math. Gen.* 36 (2003), pp. 4561–4580.

[18] I. Freund. "Optical vortices in Gaussian random wave fields: statistical probability densities." In: *J. Opt. Soc. Am. A* 11 (1994), pp. 1644–1652.

[19] I. Freund and M. Wilkinson. "Critical-point screening in random wave fields." In: *J. Opt. Soc. Am. A* 15 (1998), pp. 2892–2902.

[20] J. W. Goodman. "Statistical properties of laser speckle patterns." In: *Laser Speckle and Related Phenomena*. Vol. 9. Topics in Applied Physics. Springer Berlin Heidelberg, 1975, pp. 9–75.

[21] Ilya A. Gruzberg. "Stochastic Geometry of Critical Curves, Schramm-Loewner Evolutions, and Conformal Field Theory." In: *J. Phys. A* 39 (2006), pp. 12601–12656.

[22] S. Gupta and A. F. Heavens. "Peaks in the CMB – sensitively testing the Gaussian hypothesis." In: *AIP Conf. Proc.* 555 (2001), pp. 337–340.

[23] B. I. Halperin. *Physics of Defects*. Les Houches XXXV NATO ASI, 1981.

[24] A. F. Heavens and R. K. Sheth. "The correlation of peaks in the microwave background." In: *Mon. Not. R. Astron. Soc.* 310 (1999), pp. 1062–1070.

[25] Henk Hoekstra and Bhuvnesh Jain. "Weak Gravitational Lensing and its Cosmological Applications." In: *Ann. Rev. Nucl. Part. Sci.* 58 (2008), pp. 99–123.

[26] W. Hu. "Power Spectrum Tomography with Weak Lensing." In: *ApJL* 522 (1999), p. L21.

[27] S. D. Hudson and E. L. Thomas. "Frank elastic-constant anisotropy measured from transmission-electron-microscope images of disclinations." In: *Phys. Rev. Lett.* 62 (1989), pp. 1993–1996.

[28] D. Huterer and T. Vachaspati. "Distribution of singularities in the cosmic microwave background polarization." In: *Phys. Rev. D* 72 (2005), pp. 043004–043010.

[29] B. Jain, U. Seljak, and S. D. M. White. "Ray-tracing Simulations of Weak Lensing by Large-Scale Structure." In: *Astrophys. J.* 530 (2000), pp. 547–577.

[30] R. Kamien. "The Geometry of Soft Materials: a Primer." In: *Rev. Mod. Phys.* 74 (2002), pp. 953–971.

[31] N. G. van Kampen. *Stochastic Processes in Physics and Chemistry*. Amsterdam: North-Holland Publishing company, 1981.

[32] M. Kardar, G. Parisi, and Y. C. Zhang. "Dynamic Scaling of Growing Interfaces." In: *Phys. Rev. Lett.* 56 (1986), pp. 889–892.

[33] F. Liu and G. F. Mazenko. "Defect-defect correlation in the dynamics of first-order phase transitions." In: *Phys. Rev. B* 46 (1992), p. 5963.

[34] M. S. Longuet-Higgins. "Statistical Properties of an Isotropic Random Surface." In: *Phil. Trans. R. Soc. Lond. A* 250 (1957), pp. 157–174.

[35] M. S. Longuet-Higgins. "The Statistical Analysis of a Random, Moving Surface." In: *Phil. Trans. R. Soc. Lond. A* 249 (1957), pp. 321–387.

[36] T. Lopez-Leon, V. Koning, K. B. S. Devaiah, V. Vitelli, and A. Fernandez-Nieves. "Frustrated nematic order in spherical geometries." In: *Nature Physics* 7 (2011), pp. 391–394.

[37] J. C. Mather, D. J. Fixsen, R. A. Shafer, C. Mosier, and D. T. Wilkinson. "Calibrator Design for the COBE Far Infrared Absolute Spectrophotometer (FIRAS)." In: *Astrophys. J.* 512 (1999), p. 511.

[38] N. D. Mermin. "The topological theory of defects in ordered media." In: *Rev. Mod. Phys.* 51 (1979), pp. 591–648.

[39] J. W. Milnor. *Morse Theory*. Princeton: Princeton University Press, 1963.

[40] J. W. Milnor. *Topology from the differentiable viewpoint*. Charlottesville: University Press of Virginia, 1965.

[41] P. D. Naselsky and D. I. Novikov. "General Statistical Properties of the Cosmic Microwave Background Polarization Field." In: *Ap. J.* 507 (1998), pp. 31–39.

[42] J. F. Nye. "Lines of Circular Polarization in Electromagnetic Wave Fields." In: *Proc. R. Soc. Lond. A* 389 (1983), pp. 279–290.

[43] J. F. Nye and J. V. Hajnal. "The Wave Structure of Monochromatic Electromagnetic Radiation." In: *Proc. R. Soc. Lond. A* 409 (1987), pp. 21–36.

[44] T. Vachaspati and A. Lue. "Topological properties of the cosmic microwave background polarization map." In: *Phys. Rev. D* 36 (2003), p. 121302.

[45] V. Vitelli, B. Jain, and R. D. Kamien. "Topological Defects in Gravitational Lensing Shear Fields." In: *JCAP* 09 (2009), p. 034.

[46] A. Weinrib and B. I. Halperin. "Distribution of maxima, minima, and saddle points of the intensity of laser speckle patterns." In: *Phys. Rev. B* 26 (1982), pp. 1362–1368.

[47] K. J. Worsley, S. Marrett, P. Neelin, A. C. Vandal, K. J. Friston, and A. C. Evans. "A Unified Statistical Approach for Determining Significant Signals in Location and Scale Space Images of Cerebral Activation." In: *Human Brain Mapping* 4 (1996), pp. 58–73.

SUMMARY

Gaussian random fields are ubiquitous in physics. The central limit theorem ensures that a lot of random fields are Gaussian—or approximately so—making them of special theoretical importance and practical interest. Examples in physics include optical speckle fields, the projected gravitational potential and the cosmic microwave background radiation.

Typically though it is the non-Gaussian contributions that are the target of investigation, since these can provide a window on the interesting nonlinear processes that give rise to them.

Gaussian fields have, regardless of their spectra, certain properties in common. Testing whether a given random field has them thus gives a possible way of detecting non-Gaussianity. The focus of this thesis is on quantities pertaining their stochastic geometry, which provide a very low-key and robust measuring tool. Specifically, this thesis is devoted to studying the exact amount in which some geometric quantities of a Gaussian field change when it is perturbed. This does not only provide a way of detecting non-Gaussianity in a given field, but also potentially to determine the type and/or size of the perturbation.

In chapters 2 and 3 we consider first local perturbations, which at each point, are a function only of the original value at that same point. In chapter 2 we look at the relative difference in densities of local maxima and minima. For Gaussian fields these are the same due to symmetry, but for a non-Gaussian field this may no longer be the case. The locality of the perturbation allows for an exact calculation of the imbalance, which does not require the perturbation to be small. One of the features of the result we find is that the imbalance is exponentially small for small perturbations, regardless of its precise form.

In chapter 3 we stick with the local perturbations, but turn to umbilical points. We find a formula for the monstar fraction, up to first order in the perturbation. The result depends on the spectrum of the original Gaussian field and the perturbation, but those contributions are separate. A comparison with the maxima and minima gives two interesting differences: While the maxima-minima imbalance is insensitive to odd perturbations, the mon-

star fraction does not change (up to first order) for even ones. Second, the monstar fraction may change dramatically for small perturbations.

In chapter 4 we go back to the maxima and minima, but this time in a more general setting. A recipe for determining the imbalance up to first order in the perturbation is presented. The method is tested explicitly by applying it to the case of a field that is initially Gaussian, but evolves according to the deterministic Kardar-Parisi-Zhang (KPZ) equation. This equation causes non-Gaussianities to develop which are nonlocal in nature. We find that indeed an imbalance between maxima and minima may result, which we can quantify. An interesting find is that in the case of small nonlocal perturbations, the imbalance need not be exponentially small, as we found for the local case. This means that a nonvanishing imbalance is indicative of either a large non-Gaussianity, or one of nonlocal origin.

In chapter 5 we consider the effects of coarse-graining. This process involves an averaging, which can be used to model an imprecise measurement. It is also a way in which a random field can become nearly Gaussian. In the limit of the coarse-graining scale going to infinity, an imbalance between maxima and minima will converge to zero, at a rate that is inversely proportional to the length scale of the coarse-graining. The precise imbalance depends on the details of both the original field and the coarse-graining function, but in the limit of the aforementioned length scale going to infinity, the contributions of these two can be separated. An interesting fact is that, even though coarse-graining can be seen as a convergence toward Gaussianity, it can actually help to reveal a non-Gaussianity by amplifying the imbalance, which is of particular interest for the case of a locally perturbed Gaussian field.

SAMENVATTING

Gaussische velden zijn alomtegenwoordig in de natuurkunde. De centrale limietstelling garandeert dat veel willekeurige velden Gaussisch zijn – of tenminste bij benadering – zodat ze van speciaal theoretisch belang en praktische interesse zijn. Optische "speckle fields", de geprojecteerde gravitatiepotentiaal en de kosmische achtergrondstraling zijn slechts enkele voorbeelden van (bijna-)Gaussische velden in de natuurkunde.

Over het algemeen zijn het echter de niet-Gaussische bijdragen die het richtpunt van onderzoek zijn, aangezien deze inzicht kunnen verschaffen in de onderliggende niet-lineaire processen waardoor ze veroorzaakt worden.

Gaussische velden hebben, ongeacht hun spectra, bepaalde eigenschappen gemeen. Testen of een gegeven willekeurig veld die heeft is dus een manier om niet-Gaussische signalen te detecteren. De focus in dit proefschrift ligt op grootheden die betrekking hebben op stochastische geometrie, die een betrekkelijk eenvoudige en robuuste meetmethode vormen. Dit proefschrift is in het bijzonder gewijd aan de vraag in welke exacte mate bepaalde geometrische eigenschappen veranderen als een Gaussisch veld een perturbatie ondergaat. Dit geeft niet alleen een manier om niet-Gaussische signalen te detecteren, maar ook om mogelijk de grootte en/of aard van de perturbatie vast te stellen.

In hoofdstukken 2 en 3 bekijken we eerst lokale perturbaties, die op elk punt een functie zijn van enkel de oorspronkelijke waarde op datzelfde punt. In hoofdstuk 2 beschouwen we het relatieve verschil in de dichtheden van lokale maxima en minima. Voor Gaussische velden zijn deze hetzelfde vanwege symmetrie, maar voor niet-Gaussische velden hoeft dit niet langer het geval te zijn. De lokaalheid van de perturbatie maakt het mogelijk het verschil exact te berekenen, waarbij de perturbatie niet klein hoeft te zijn. Een van de kenmerken van het resultaat is dat het relatieve verschil tussen maxima en minima exponentieel klein is voor kleine perturbaties, ongeacht de exacte vorm.

In hoofdstuk 3 blijven we bij lokale perturbaties, maar bekijken we "umbilische punten" (Eng: umbilical points). We vinden een formule voor de relatieve dichtheid van "monstars", tot eerste orde in de perturbatie. De formule hangt van zowel het spectrum van het oorspronkelijke Gaussische

veld als de perturbatie af, maar beide contributies kunnen gescheiden worden. Een vergelijking met de maxima en minima geeft twee interessante verschillen: Terwijl het verschil tussen maxima en minima ongevoelig is voor oneven perturbaties, verandert de monstarfractie niet (tot op eerste orde) voor even perturbaties. Ten tweede kan de monstarfractie drastisch veranderen voor kleine perturbaties.

In hoofdstuk 4 gaan we terug naar de maxima en minima, maar dan in een meer algemene context. Om te beginnen wordt een methode om het verschil tussen maxima en minima te bepalen tot op eerste orde gepresenteerd. Deze methode wordt expliciet getest door hem toe te passen op het geval van een veld dat aanvankelijk Gaussisch is, maar evolueert volgens de deterministische Kardar-Parisi-Zhang (KPZ) vergelijking. Deze vergelijking zorgt voor niet-Gaussische contributies die van niet-lokale aard zijn. We vinden dat er inderdaad een verschil tussen maxima en minima ontstaat dat we kunnen kwantificeren. Een interessante vondst is dat, in het geval van kleine niet-lokale perturbaties, het verschil niet noodzakelijkerwijs exponentieel klein is. Dit betekent dat een significant verschil duidt op een grote perturbatie danwel een perturbatie van niet-lokale origine.

In hoofdstuk 5 nemen we de effecten van “schuren” (Eng: coarse-graining) onder de loep. Bij dit proces wordt een signaal gemiddeld, wat model kan staan voor een niet-precieze meting. Het is tevens een manier waarop een veld bijna-Gaussisch kan worden. In de limiet dat de schaal waarover geschuurd wordt naar oneindig gaat convergeert het relatieve verschil tussen maxima en minima naar nul, omgekeerd evenredig met de lengtemaat van het schuren. De precieze waarde van het verschil hangt af van de details van zowel het oorspronkelijke veld als de schuurfunctie, maar in de hierboven genoemde limiet kunnen beide bijdragen gescheiden worden. Een interessant gegeven is dat, ook al kan schuren gezien worden als een convergentie richting een Gaussisch veld, het juist kan helpen om een niet-Gaussisch signaal te ontmaskeren door het verschil in maxima en minima te vergroten, wat van specifieke relevantie kan zijn voor Gaussische velden met een lokale perturbatie.

CURRICULUM VITAE

I was born on August 4th 1985, in Baarn (The Netherlands). I went to elementary school in Maastricht and high school in Bergen op Zoom. I developed a keen interest in mathematics and participated in a few contests for high school students. In 2002, I was one of six who managed to qualify for the Dutch national team for the International Mathematical Olympiad, held in Glasgow, Scotland.

I went to Leiden University to study mathematics and physics. I finished my physics Bachelor in 2009. I went on to do a Master in theoretical physics, still at Leiden University. Part of this track is a one-year project, which I did under supervision of dr. Vincenzo Vitelli (now professor) and in collaboration with dr. A.M. Turner, on the same topic as this thesis. In 2011, I got my Master's degree cum laude.

During my student days, I have represented Leiden in programming contests for student teams. Together with Johan de Ruiter and Misha Stassen I won the Benelux Algorithm Programming Contest (BAPC) in 2007 and 2008. In 2008, we got third place in the North West European Regional Contest (NWERC). In 2010 I again got third place, this time with Alexey Gritsenko and Eric Stansifer. With this result we qualified for the ICPC World Finals in 2011, held in Orlando, Florida. After my competing days, I assisted in a few contests as a member of the jury, which has the task of designing and creating problems. I did this for BAPC from 2011 to 2014 and for NWERC in 2011 and 2014.

After my Master, I got the opportunity to stay with dr. Vitelli to do a PhD, continuing what I had been working on. During this time I presented my work on several occasions, such as the APS March Meeting in 2012 (Boston, MA) and the GPSRS conference in 2013 (Freudenstadt, Germany). During my final year I worked on fracture in rigid and floppy networks, in collaboration with dr. B.G. Chen in Leiden and dr. M.M. Driscoll and prof.dr. S.R. Nagel in Chicago. This research is not included in this thesis.

During my PhD I have also worked on a C++ library for molecular dynamics simulations, together with B. van Zuiden and dr. J. Paulose. It is called "libmd" but has not yet been released. I have also assisted in under-

graduate courses: In my first year I was a teaching assistent for Classical Mechanics. In the following three years I assisted in Electrodynamics.

PUBLICATIONS

- T.H. Beuman, A.M. Turner and V. Vitelli (2012), *Stochastic geometry and topology of non-Gaussian fields*, PNAS 109: 19943-19948
- T.H. Beuman, A.M. Turner and V. Vitelli (2013), *Extrema statistics in the dynamics of a non-Gaussian random field*, Phys. Rev. E 87: 022142
- T.H. Beuman, A.M. Turner and V. Vitelli (2013), *Critical and umbilical points of a non-Gaussian random field*, Phys. Rev. E 88: 012115
- T.H. Beuman, A.M. Turner and V. Vitelli (2014), *Geometrical detection of weak non-Gaussianity upon coarse-graining*, J. Stat. Phys. 157 (3): 571-581
- M.M. Driscoll, B.G. Chen, T.H. Beuman, S. Ulrich, S.R. Nagel and V. Vitelli (2015), *Tunable failure in marginally rigid matter*, (submitted)

ACKNOWLEDGMENTS

A PhD is supposed to prove that the person holding the degree is able to do research independently, but this thesis could not have existed if it had not been for quite a few people, who deserve recognition.

I owe a great deal of thanks to Ari Turner, who is responsible for a lot of the pioneering mathematical work presented in this thesis, and who coauthored all papers that it is based on. I have always found him willing and able to help me whenever I had questions.

I also thank the research group, everyone who is part of it or has been during my time. Although they have not been directly involved in the research itself, they have been indispensable in providing a nice environment to work in.

I now turn my attention to Vincenzo, who has mastered the art of being both the leader of the group and part of the gang. Always in a "superposition", if you will, of being someone with whom you can share a joke and have a serious discussion, ready to "collapse" into the state you need him to be. The excellent guidance, assistance and encouragement made it a pleasure, in spite of the occasional biscuit raids. I can honestly say he is the greatest PhD supervisor I have ever had.

Finally, I thank my parents, not just for bringing me into existence and raising me, but also for continuing to serve as a solid foundation; a place I can always rely on to provide a warm bed, moral support and good advice.